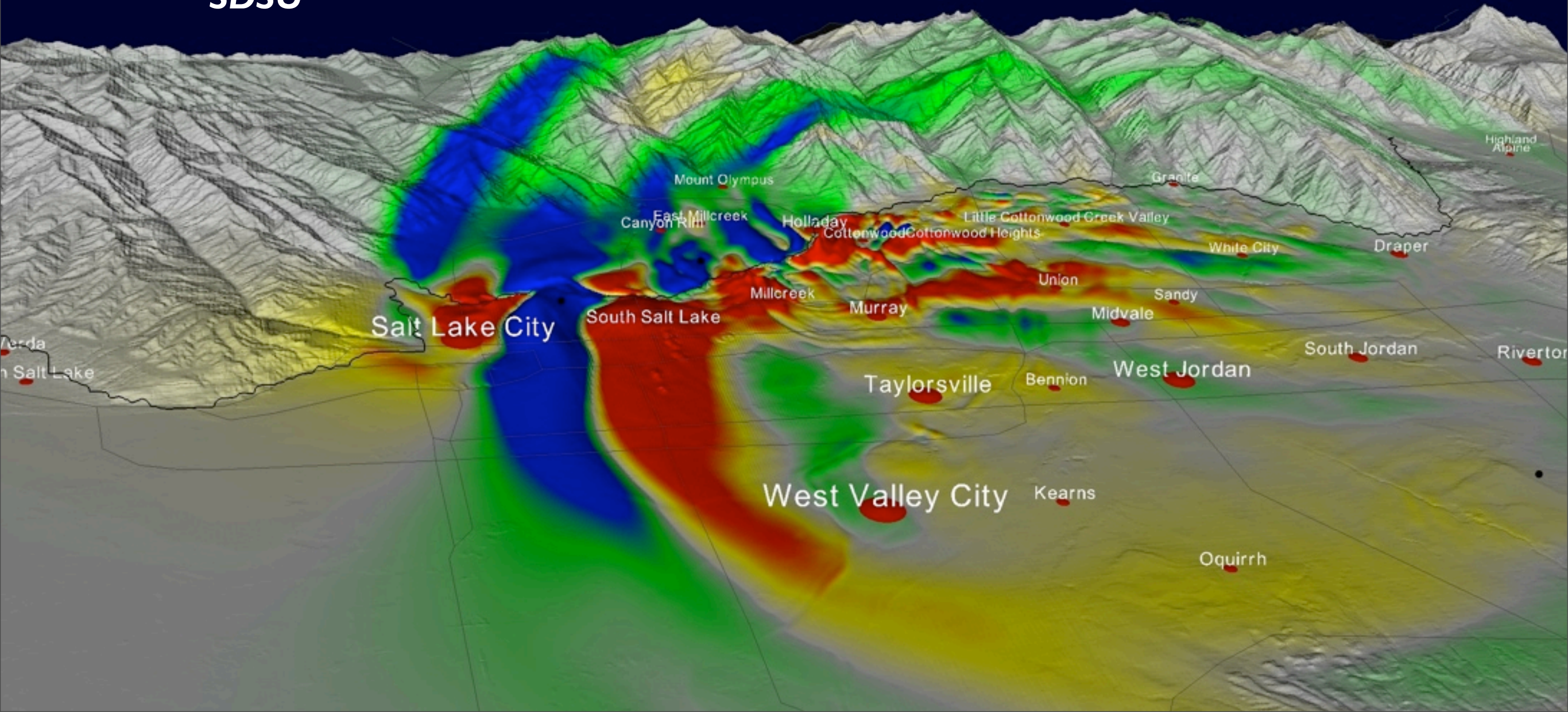


3D Nonlinear Broadband Ground Motion Predictions for M7 Earthquakes on the Salt Lake City Segment of the Wasatch Fault Using Dynamic Source Models

Daniel Roten
Kim B. Olsen
Harold W. Magistrale
SDSU

James C. Pechmann
University of Utah

Victor M. Cruz Atienza
UNAM



Outline

■ Revalidation of the WFCVM version 3c

■ Dynamic M7 rupture models

- depth-dependent normal stress (Dalguer & Mai, 2008)

■ Long-period (0-1 Hz) 3D FD simulations for 6 scenario EQs

- 2s-SAs obtained from individual scenarios
- importance of source directivity effects
- average 2s/1s-SAs compared to Solomon et al. (2004) and NGA models
- analysis of wave propagation effects causing large amplification

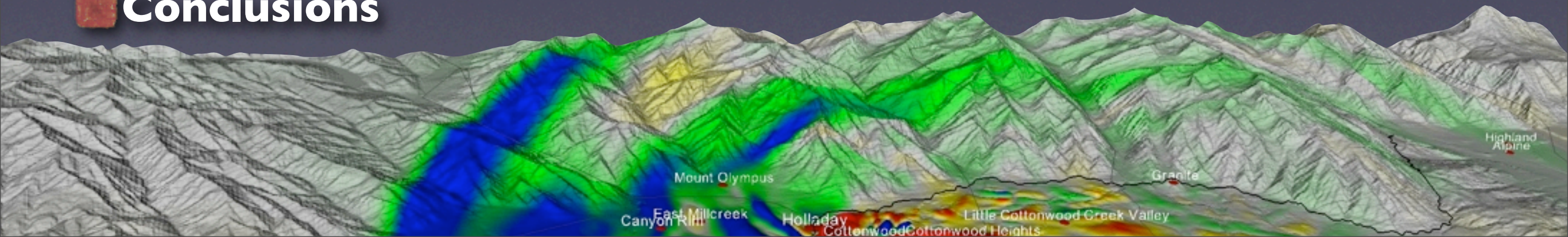
■ Broadband (BB) synthetics (0-10 Hz)

- maps of SAs and PGAs derived from BB time series
- comparison of BB SAs and PGAs along 3 profiles with NGA predictions

■ I-D simulations of nonlinear soil behavior

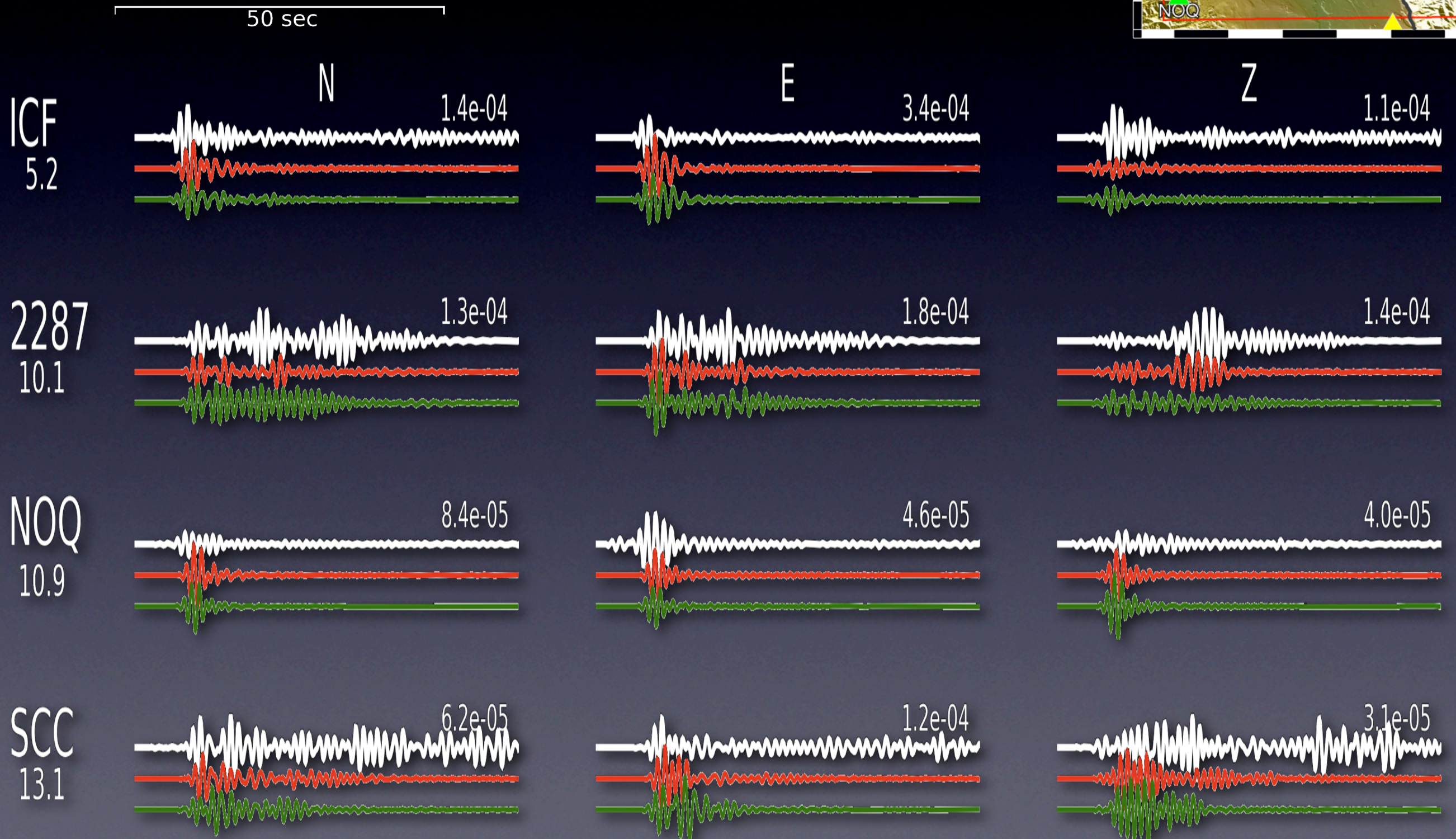
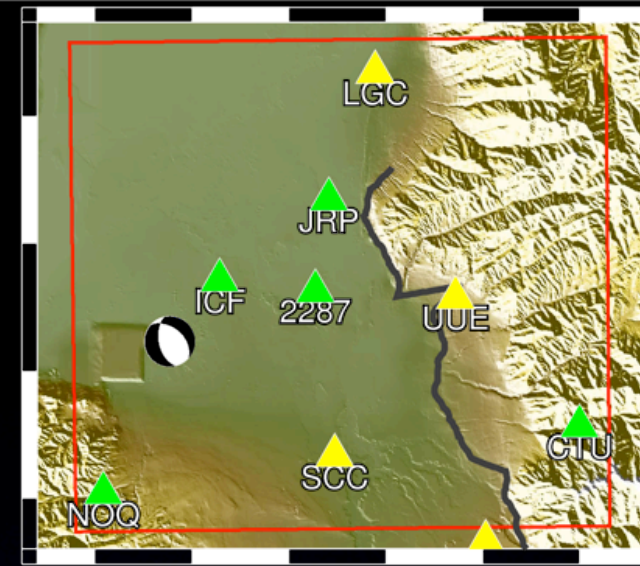
- estimation of nonlinear soil parameters
- impact of nonlinearity on PGAs and SAs, compared to NGA models

■ Conclusions



Validation of WFCVM (3c)

M_w 3.6 Magna 010708, depth = 12 km

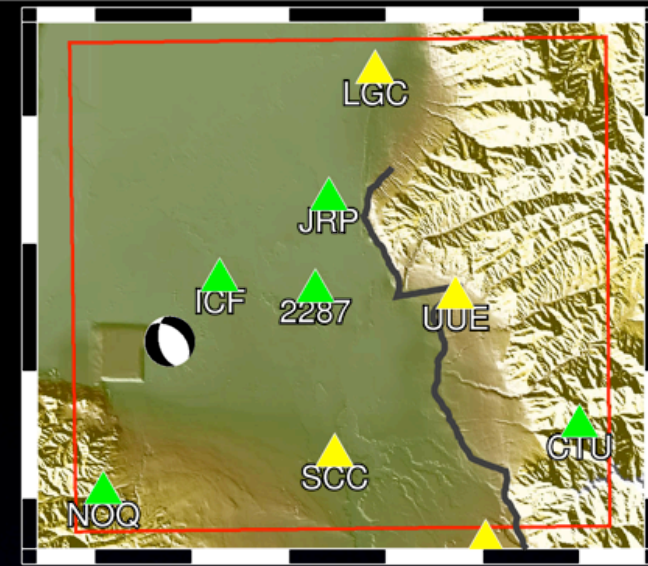


Validation of WFCVM (3c)

M_w 3.6 Magna 010708, depth = 12 km

50 sec

— recorded
— WFCVM 3c
— WFCVM 2c

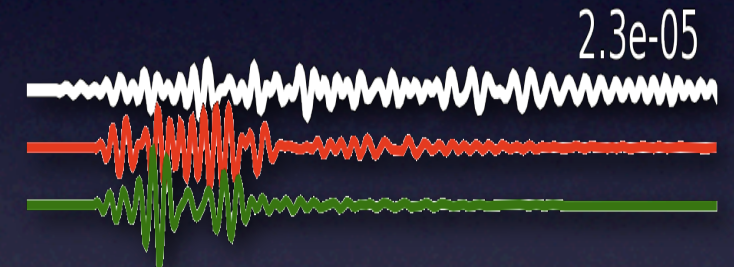
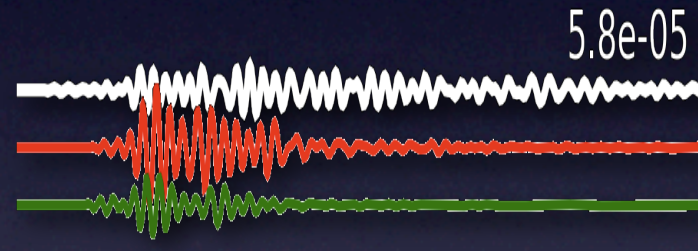
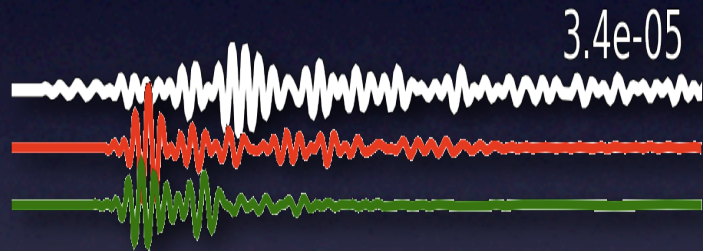


N

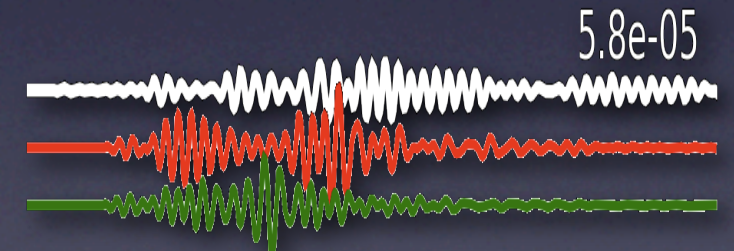
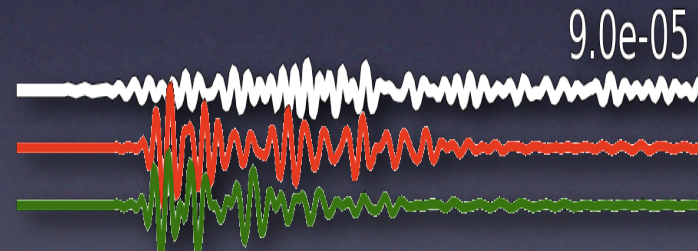
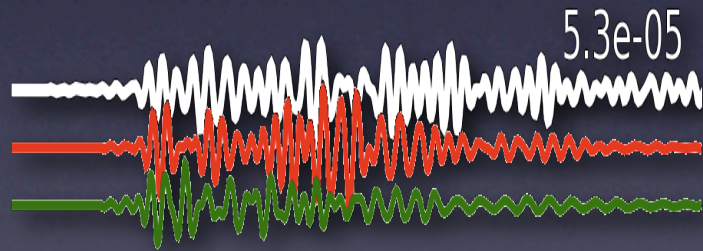
E

Z

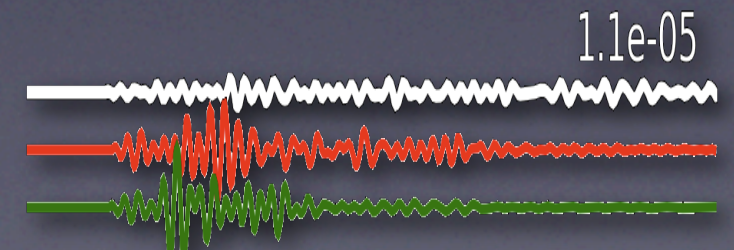
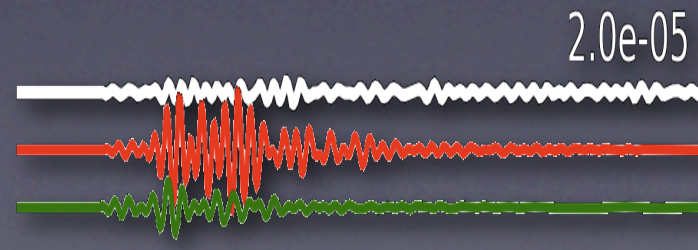
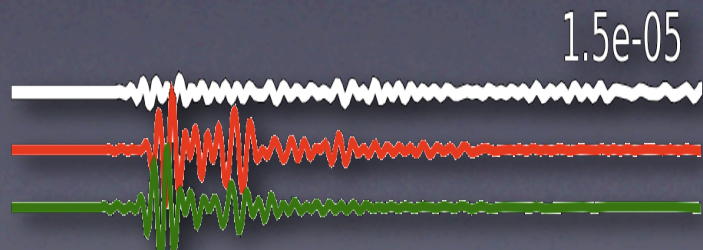
UUE
18.9



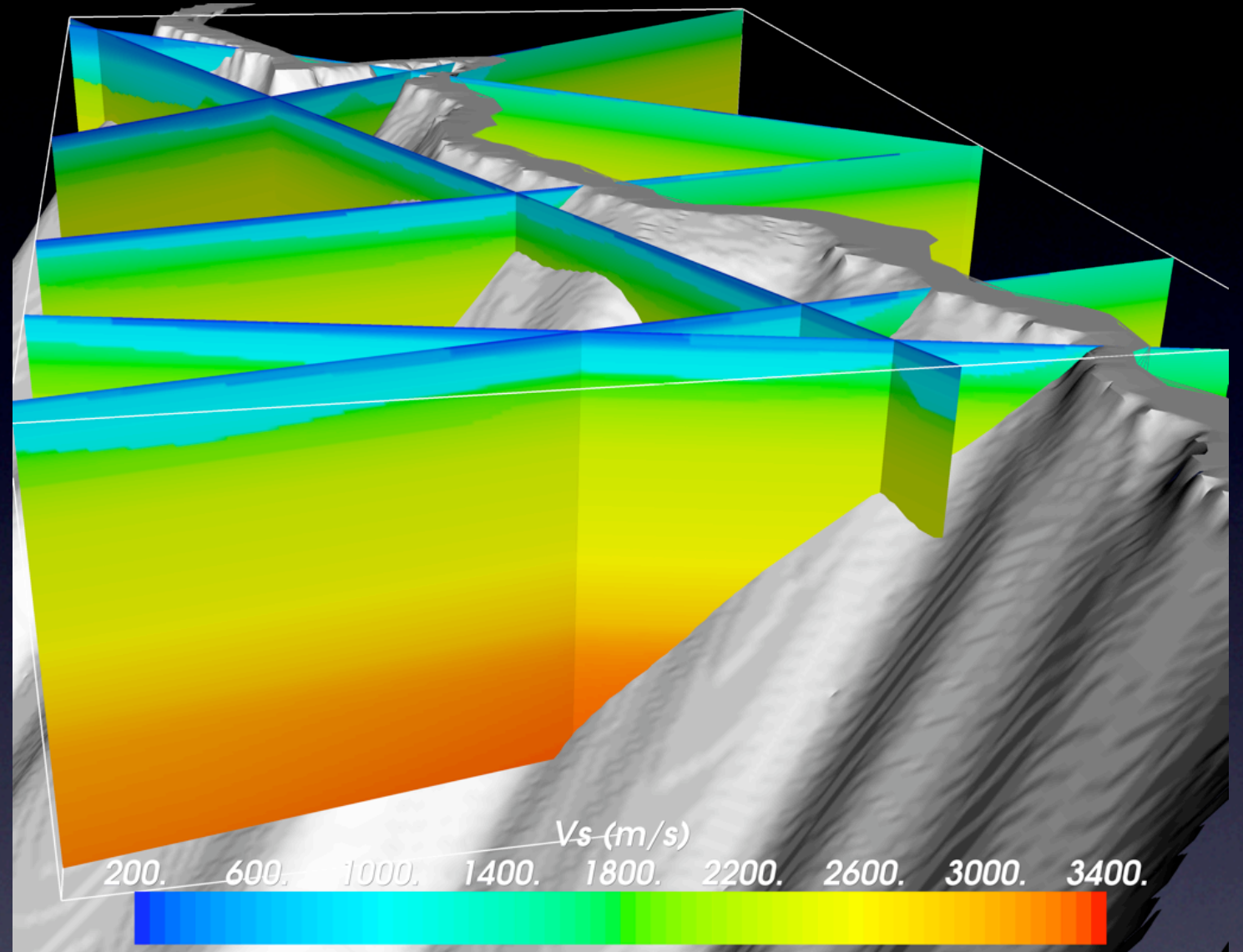
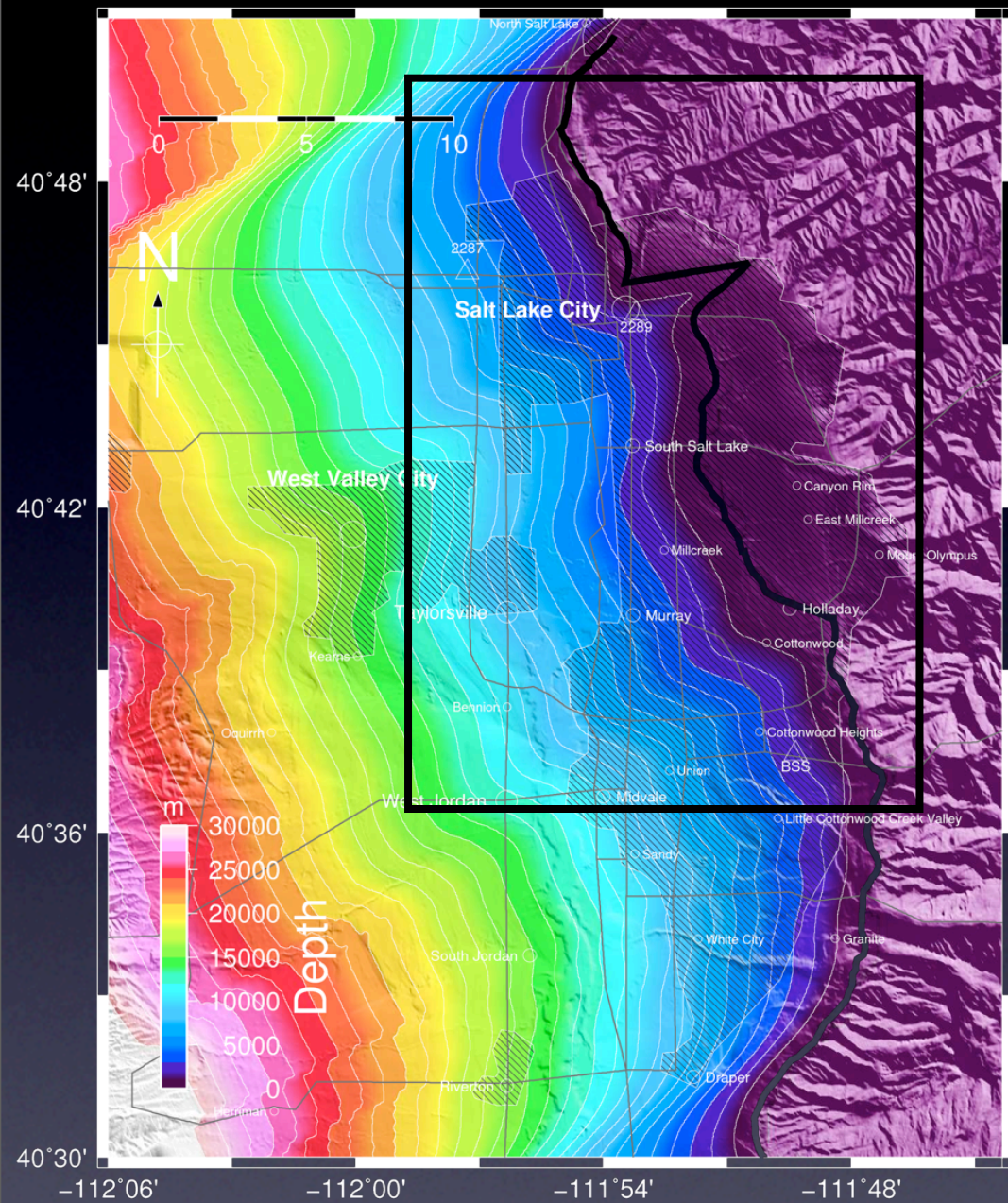
LGC
22.1



CTU
27.3



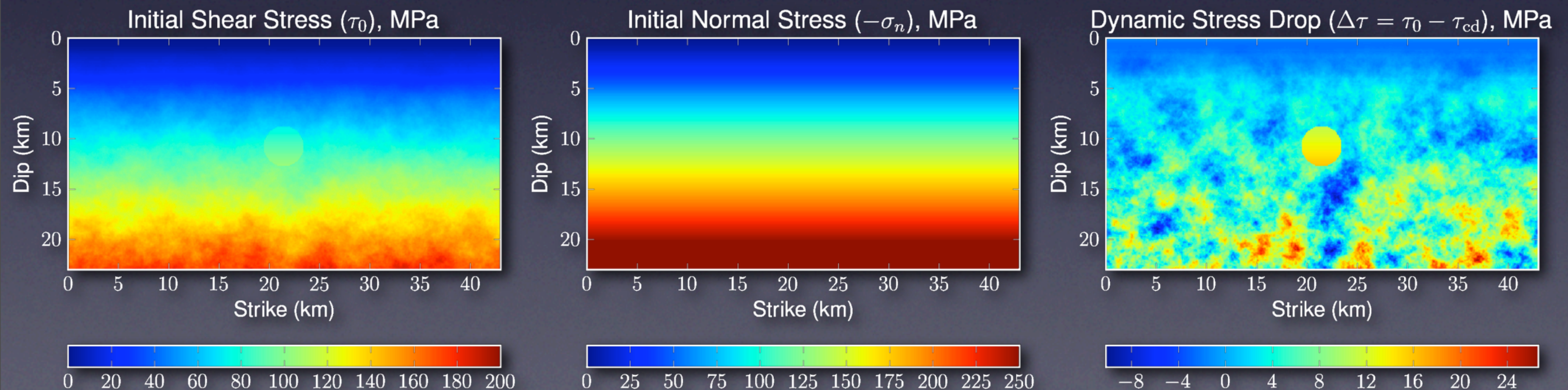
3D model of the WF SLC segment



- Final model of the SLC segment of the WF used for M7 scenario simulations
- Fault geometry mostly consistent with eastern boundaries of the Salt Lake Valley basin

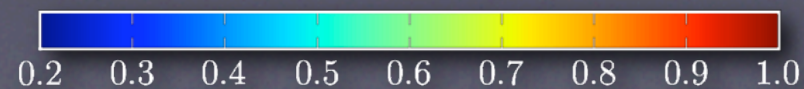
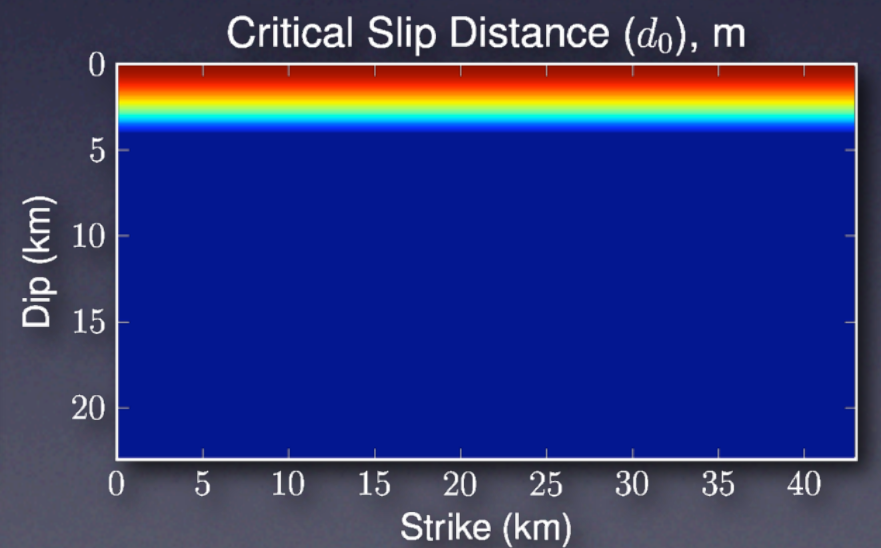
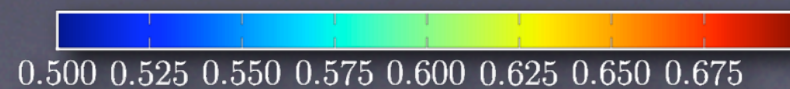
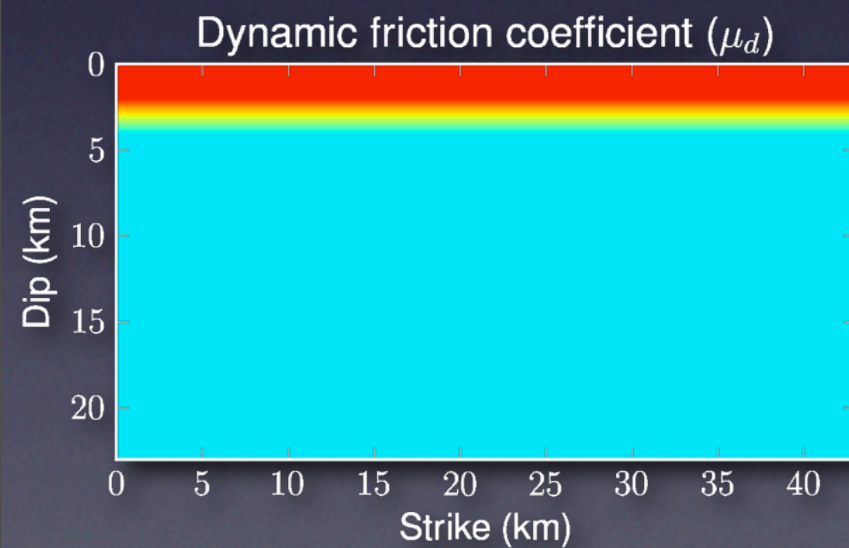
Spontaneous Rupture Models

- Simulation of dynamic rupture process on a planar vertical fault
- Staggered-grid split node finite difference method (Dalguer & Day, 2007)
- Depth-dependent normal stress (Dalguer & Mai, 2008)
- Simulated velocity strengthening near the free surface (reduce τ_0 , increase d_0 , $\mu_d > \mu_s$)
- Four rupture models with different hypocenter locations



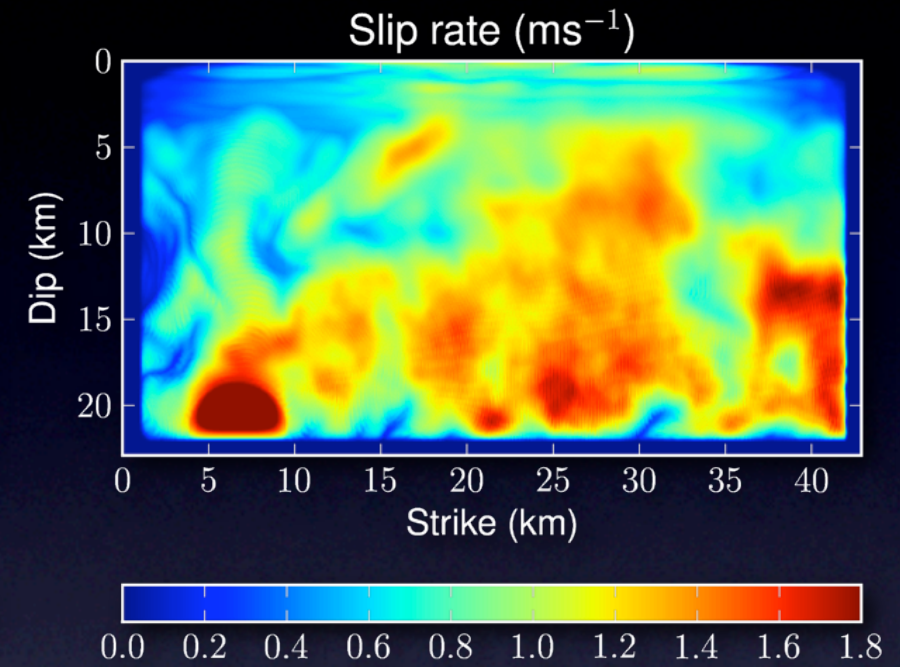
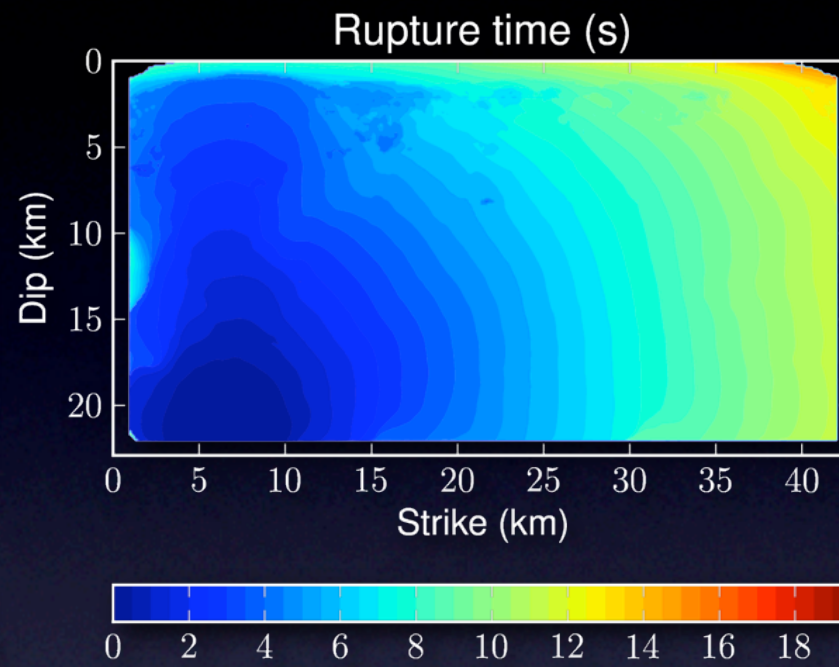
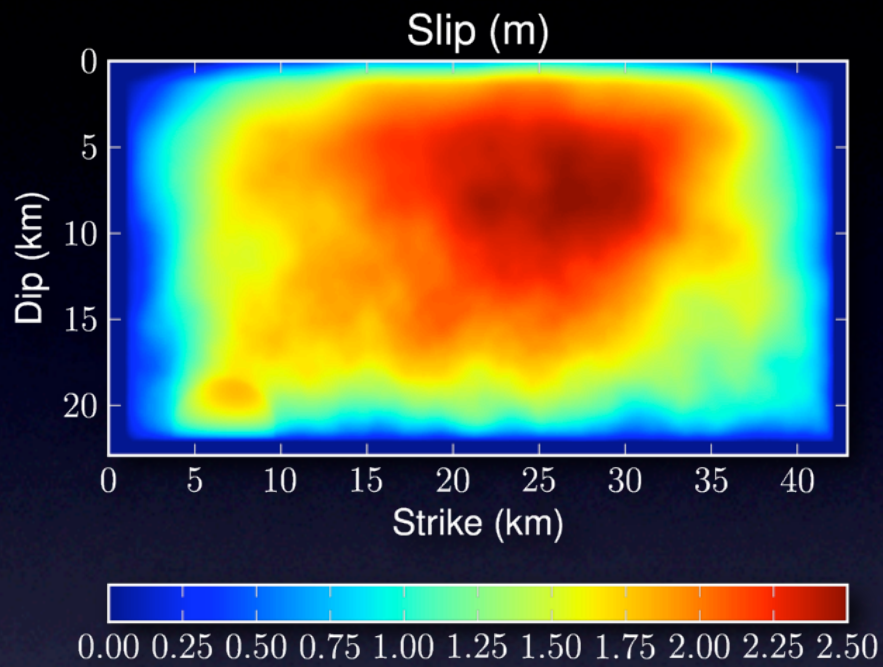
Spontaneous Rupture Models

- Simulation of dynamic rupture process on a planar vertical fault
- Staggered-grid split node finite difference method (Dalguer & Day, 2007)
- Depth-dependent normal stress (Dalguer & Mai, 2008)
- Simulated velocity strengthening near the free surface (reduce τ_0 , increase d_0 , $\mu_d > \mu_s$)
- Four rupture models with different hypocenter locations

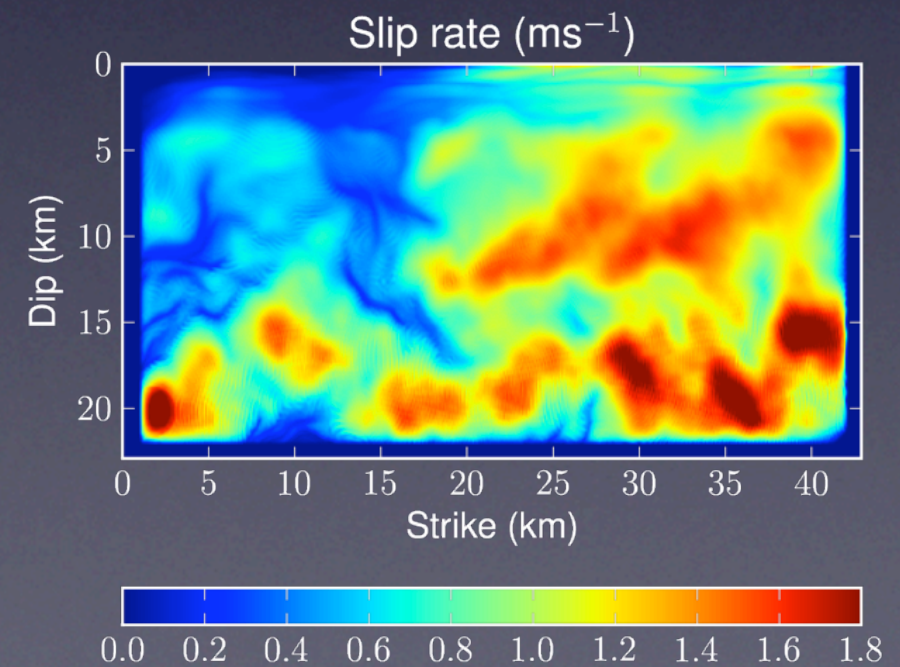
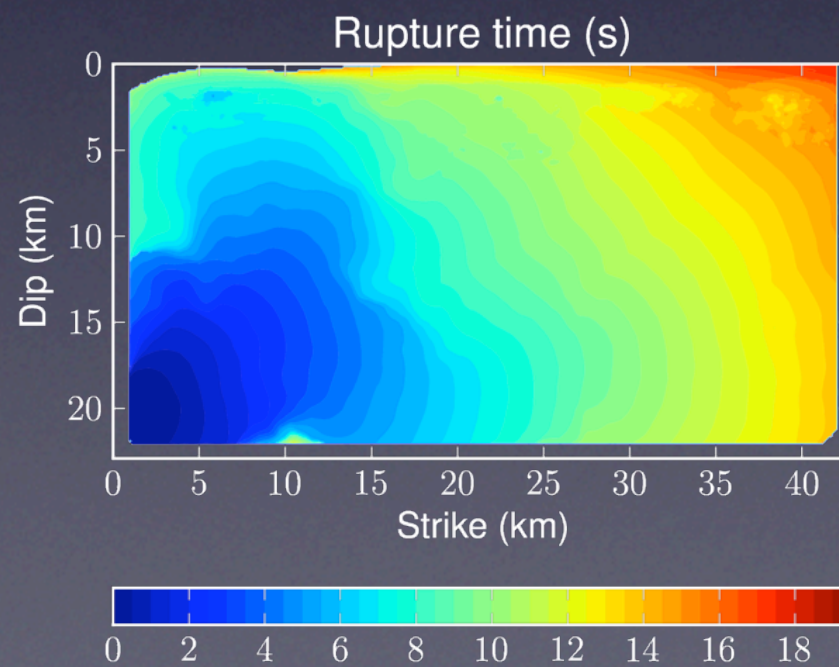
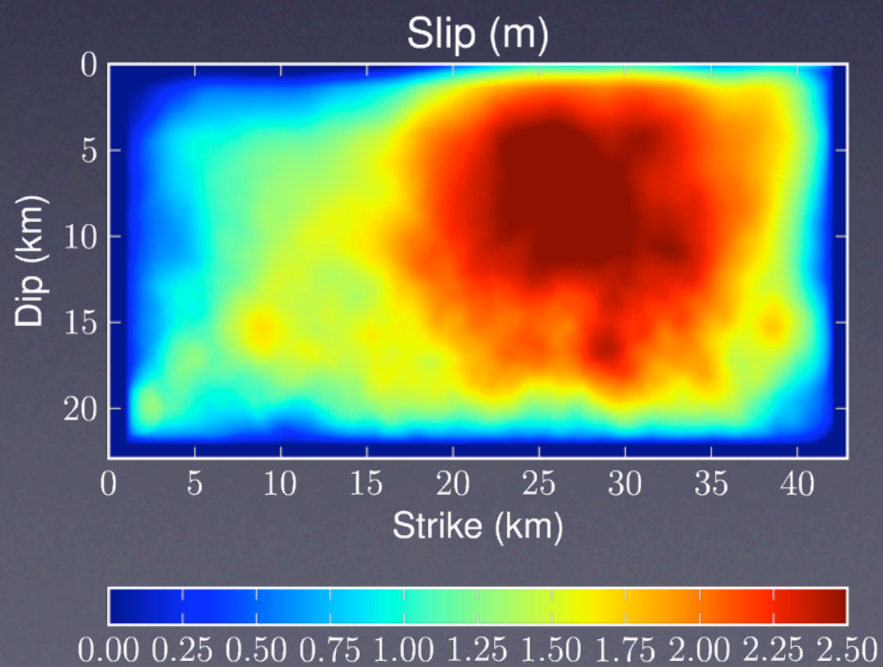


Spontaneous Rupture Models

Scenario 2a

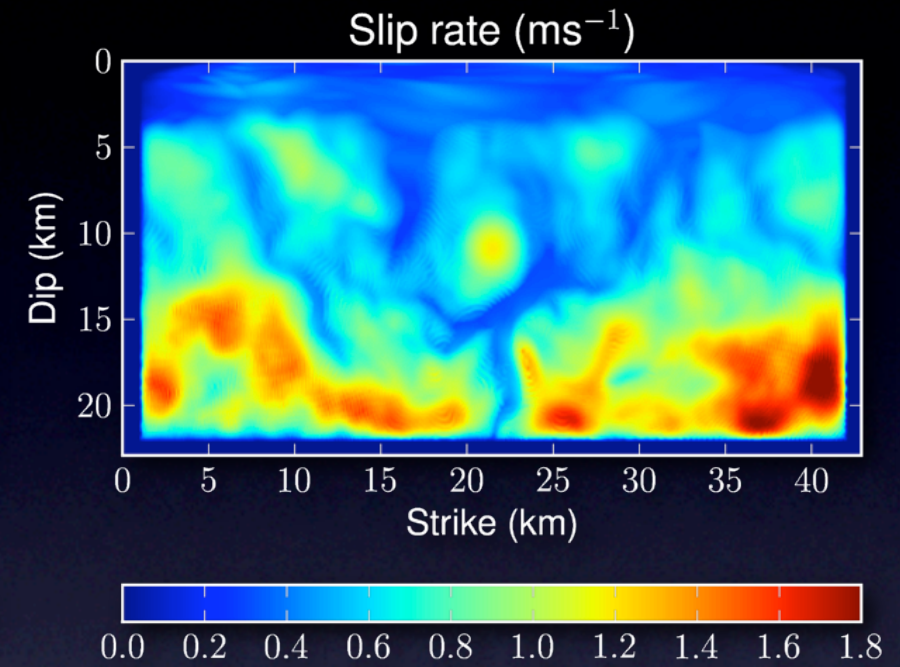
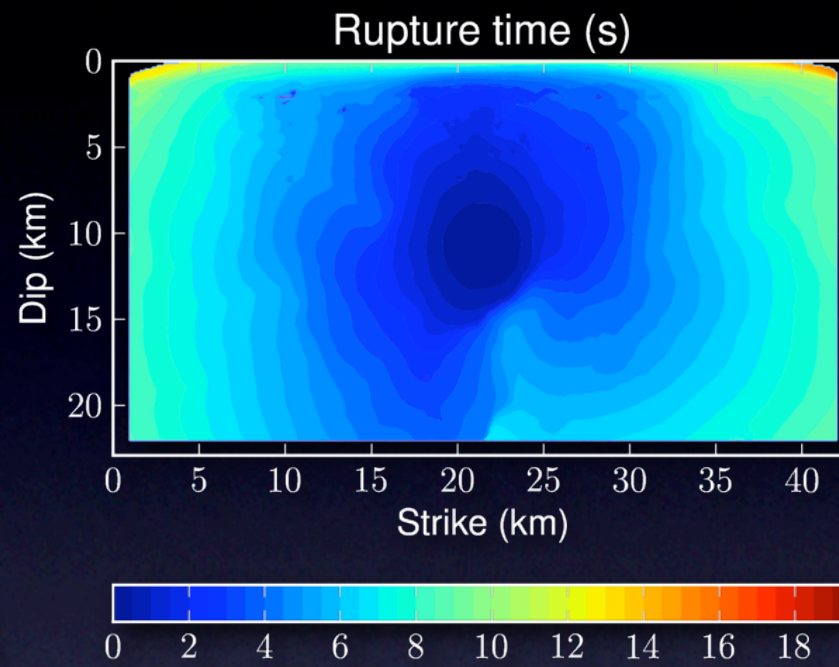
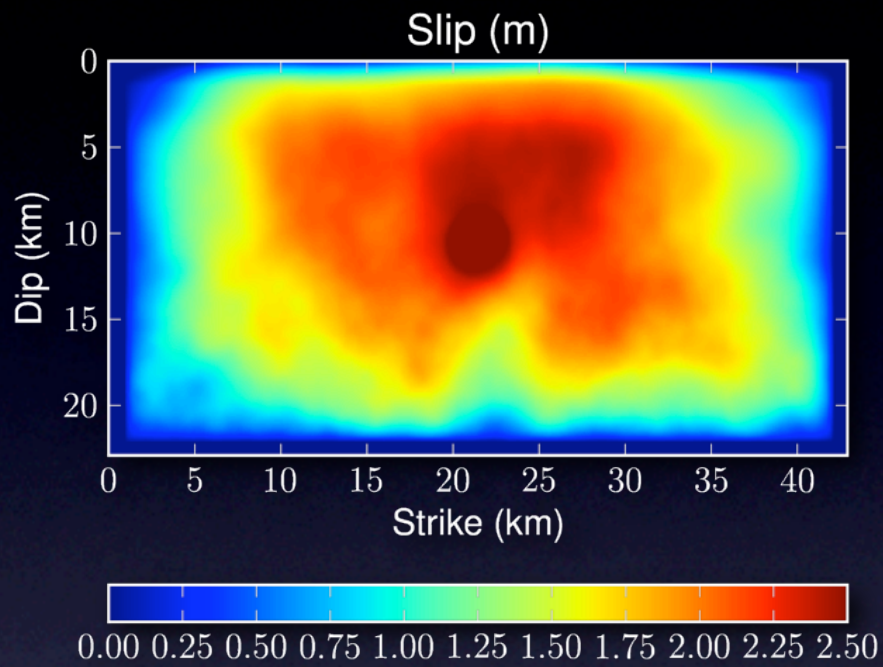


Scenario 5a

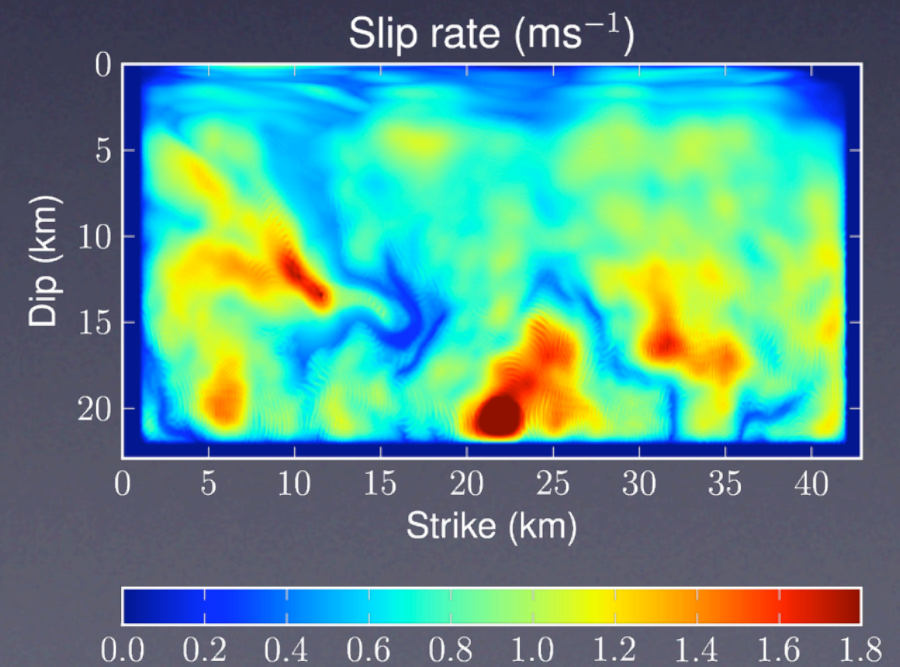
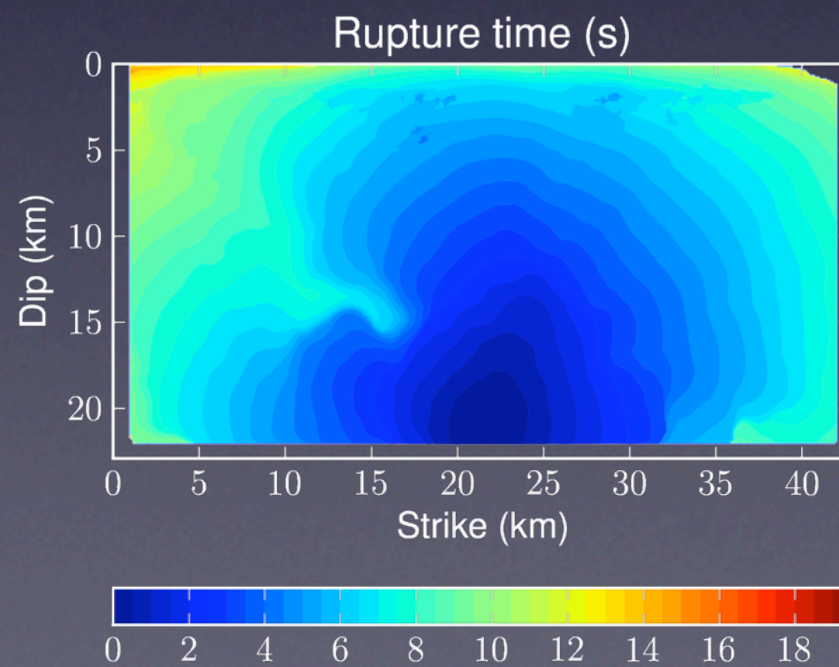
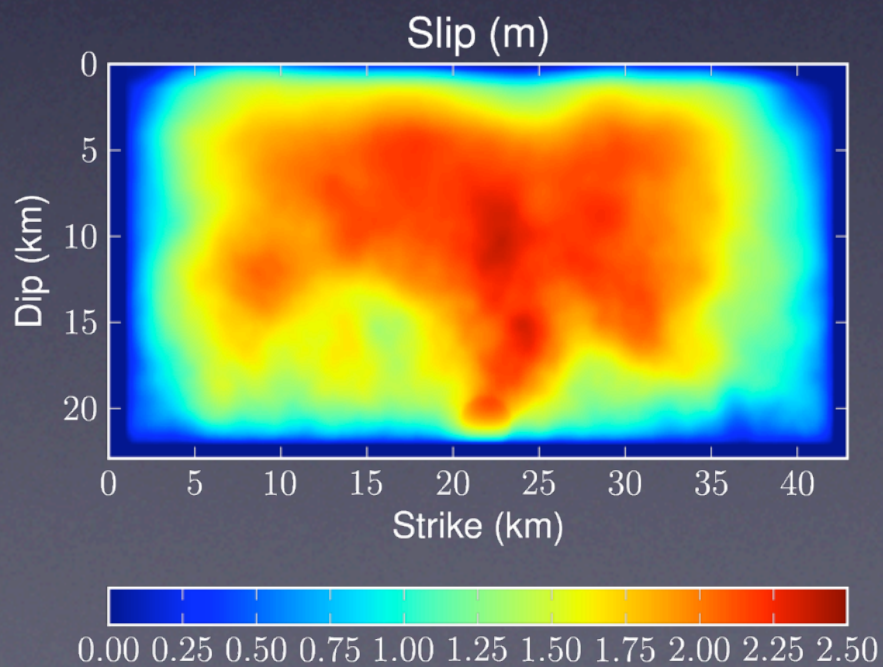


Spontaneous Rupture Models

Scenario 3a



Scenario 6c



Six scenario EQs

Representative distribution of hypocenter locations:

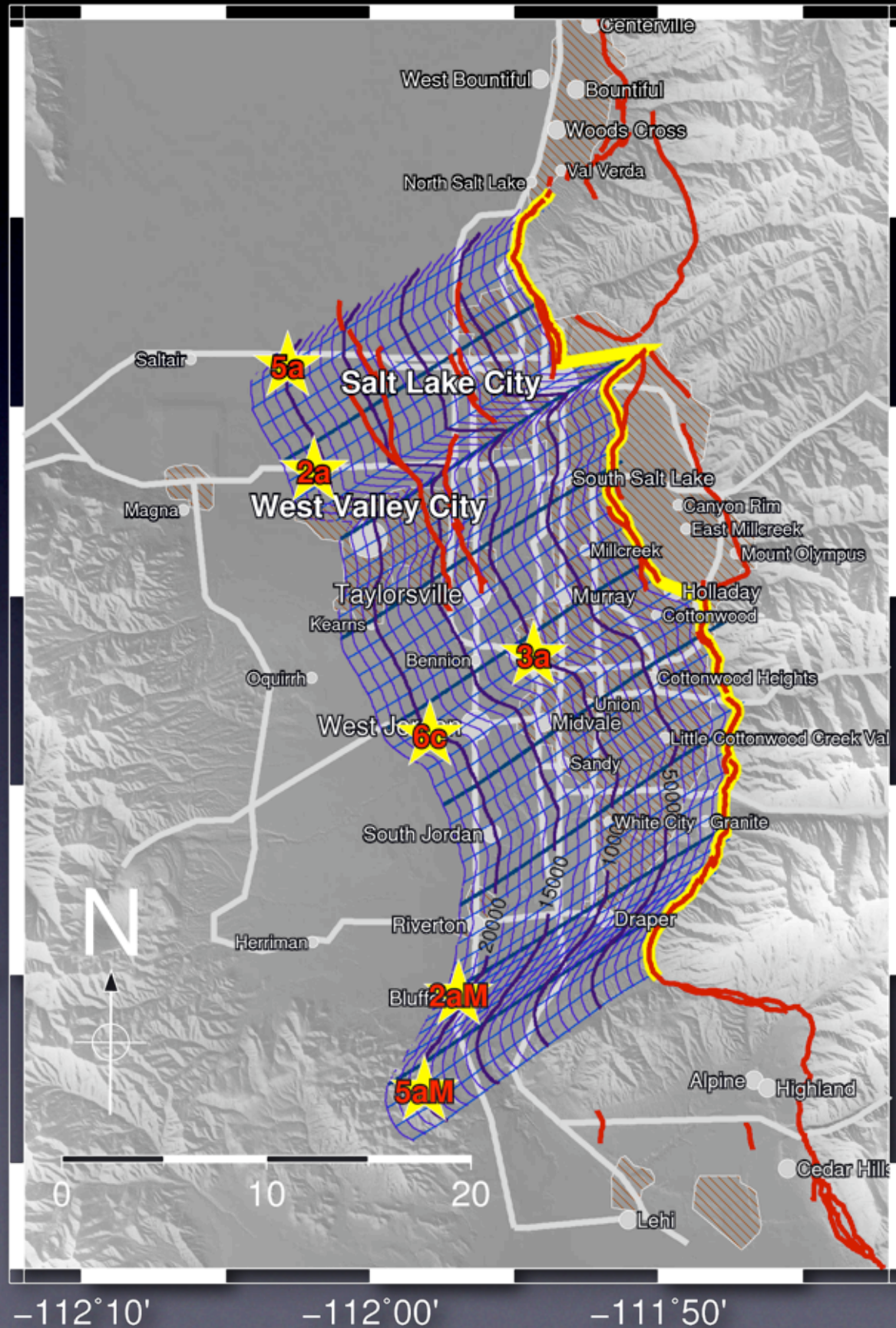
Normal faulting EQs tend to originate near brittle-ductile transition zone (~15 km depth):

- 5 deep hypocenters (20 km down-dip)
- 1 shallower hypocenter (10 km down-dip)

Rupture tends to start near non-conservative barriers:

- near northern end (2a, 5a)
- near southern end (2aM, 5aM)
- near bifurcation near Holladay stepover (3a, 6c)

(Bruhn et al., 1992)

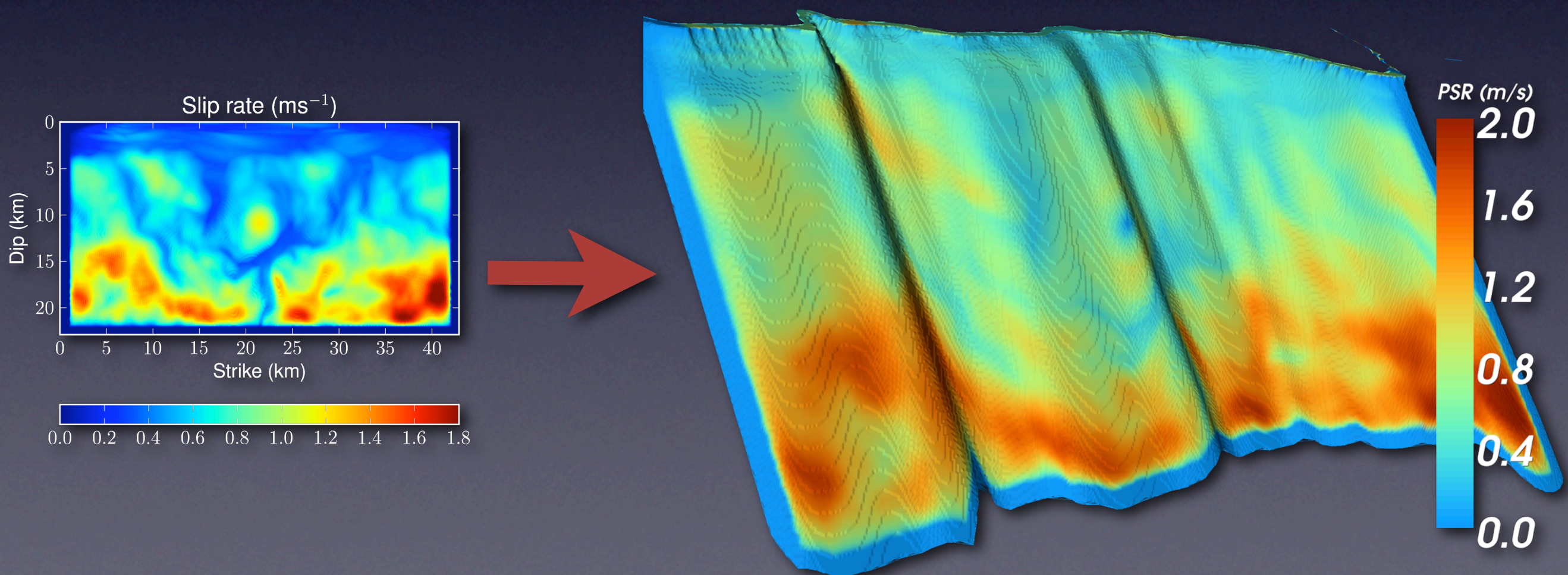


FD Simulation of Wave Propagation

Planar rupture model is projected onto irregular 3-D model of the WF and the moment rate time histories are inserted into grid nodes

Wave propagation of this source model is simulated with velocity-stress staggered-grid finite difference method (Olsen, 1994):

FD3D parameters	
Model dimensions	1500 × 1125 × 500
Simulation length	60s (24,000 iter.)
Discretization	40m / 0.0025 s
Minimum V_s	200 ms^{-1}
Highest frequency	1 Hz
# of CPU cores	1875
Wall-clock runtime	2.5 hrs (NICS Kraken)

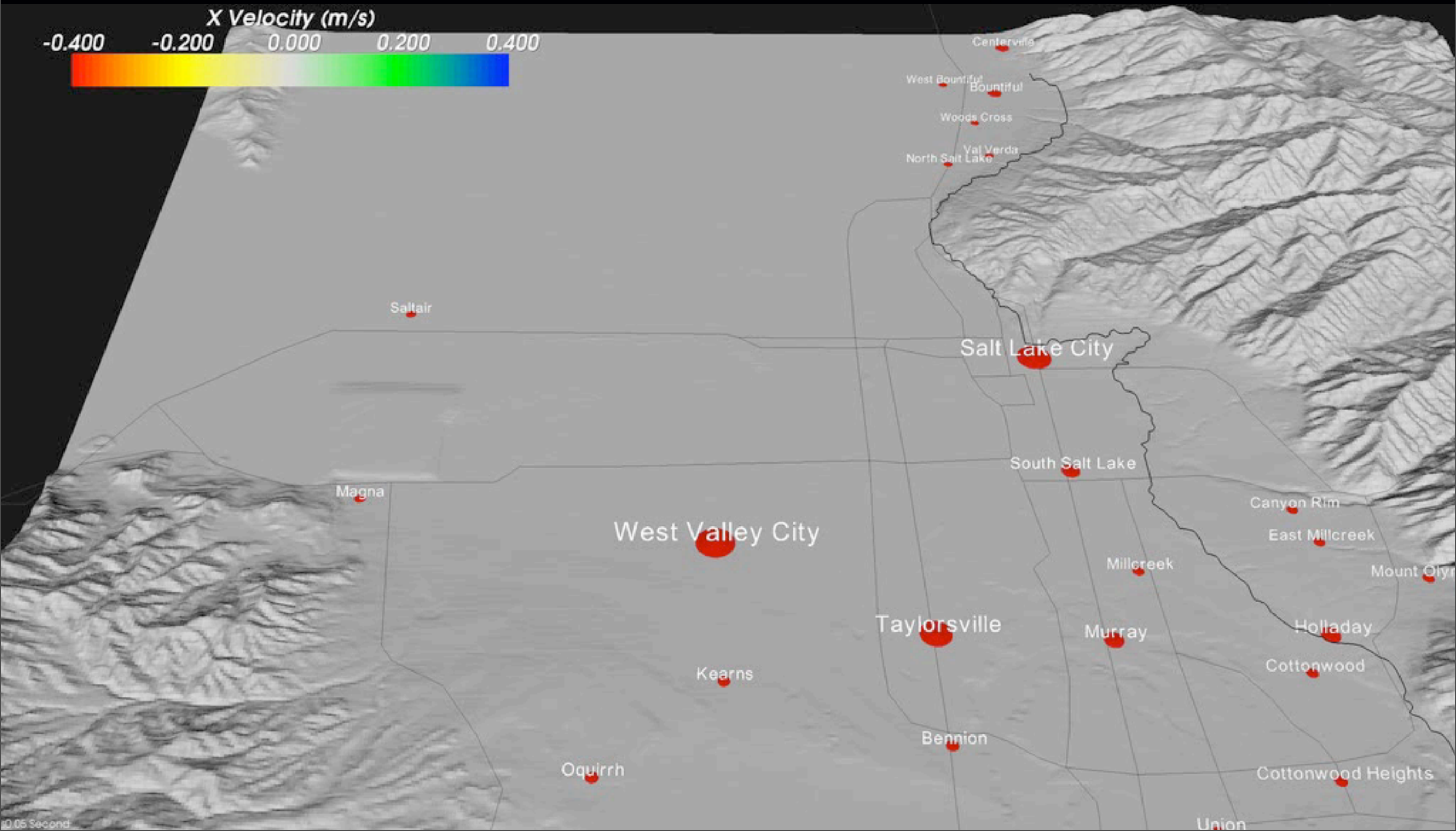


3-D Simulation of Wave Propagation

Scenario 2a

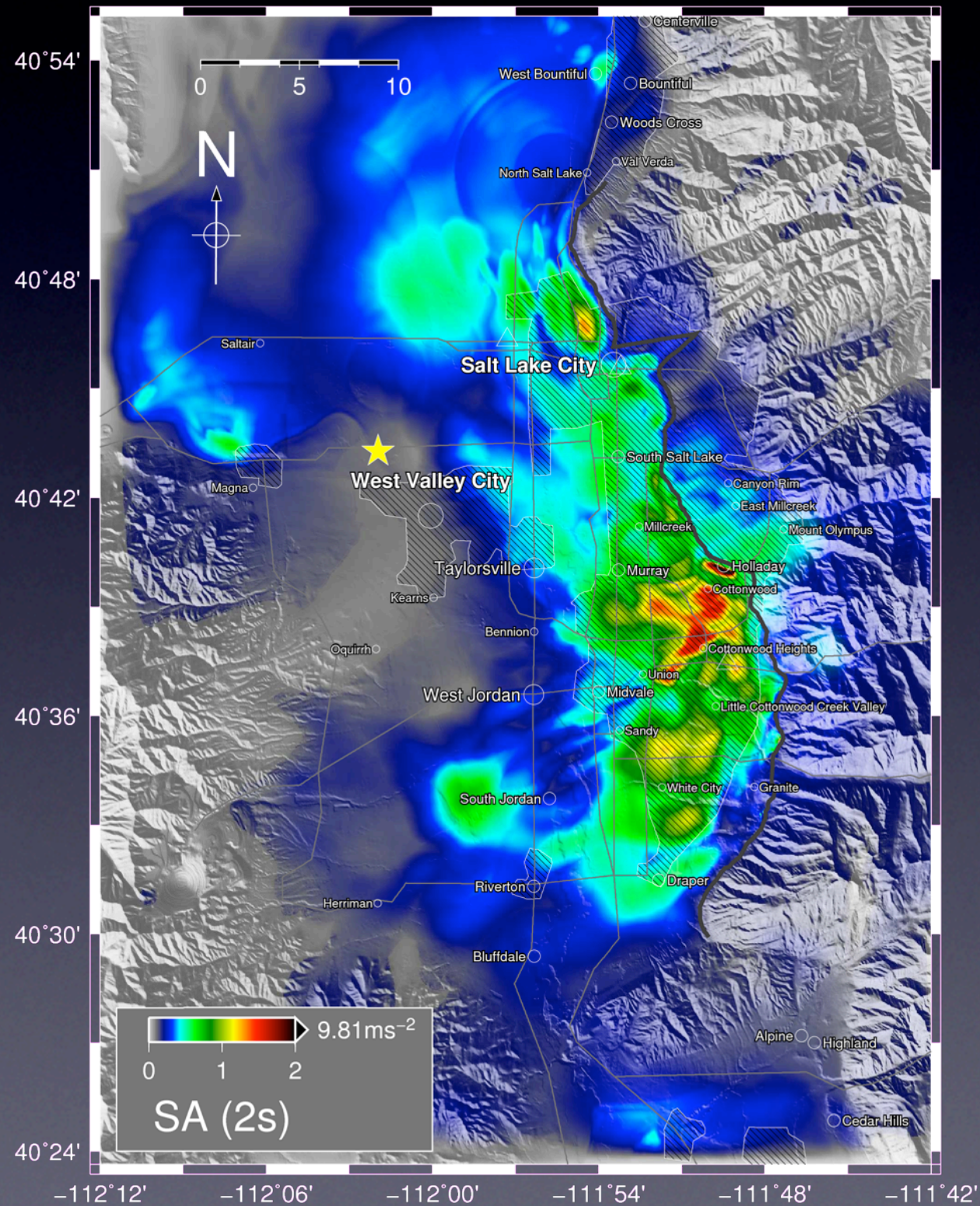
3-D Simulation of Wave Propagation

Scenario 2a

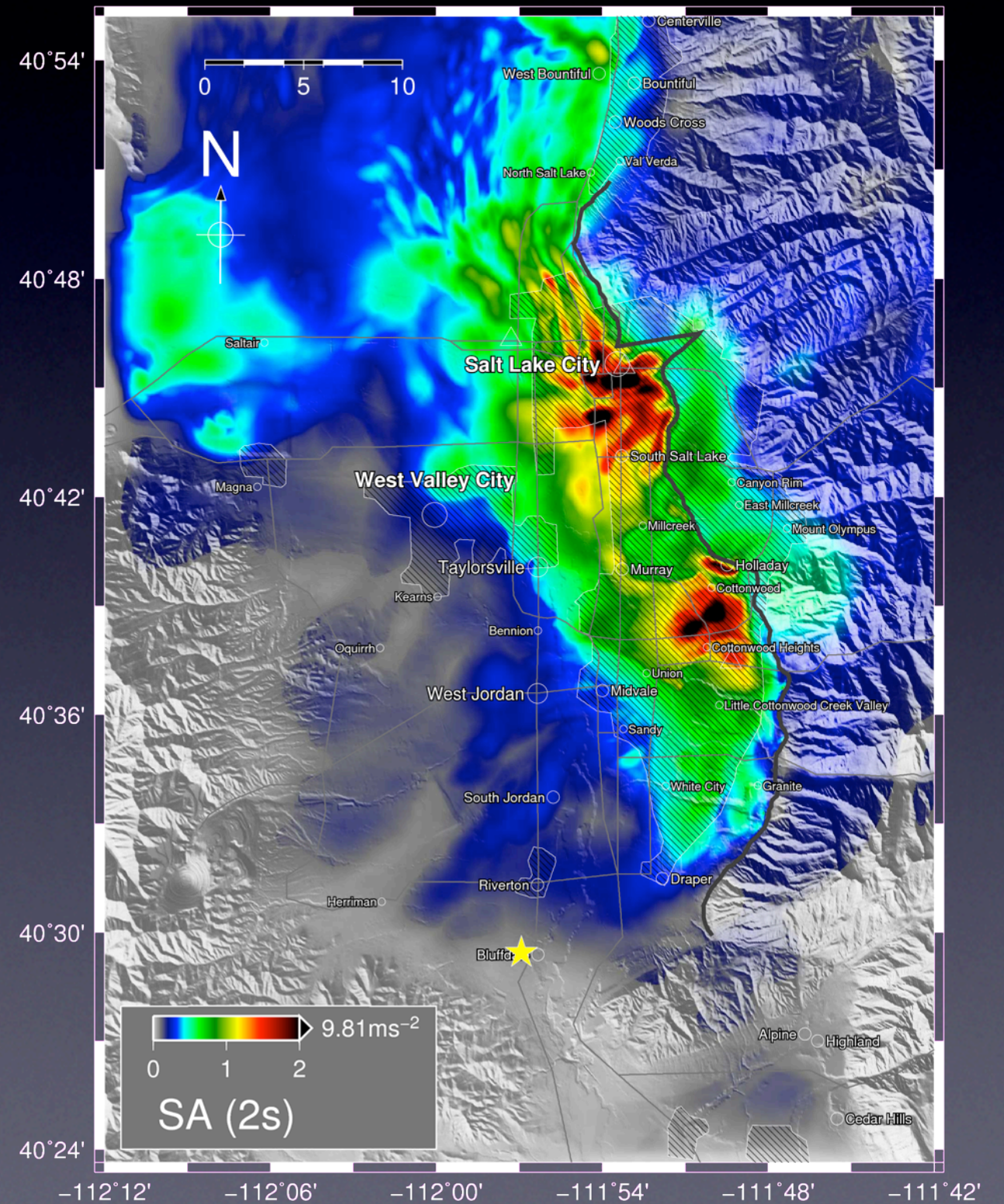


Spectral Accelerations at 2s (2s-SAs)

Scenario 2a

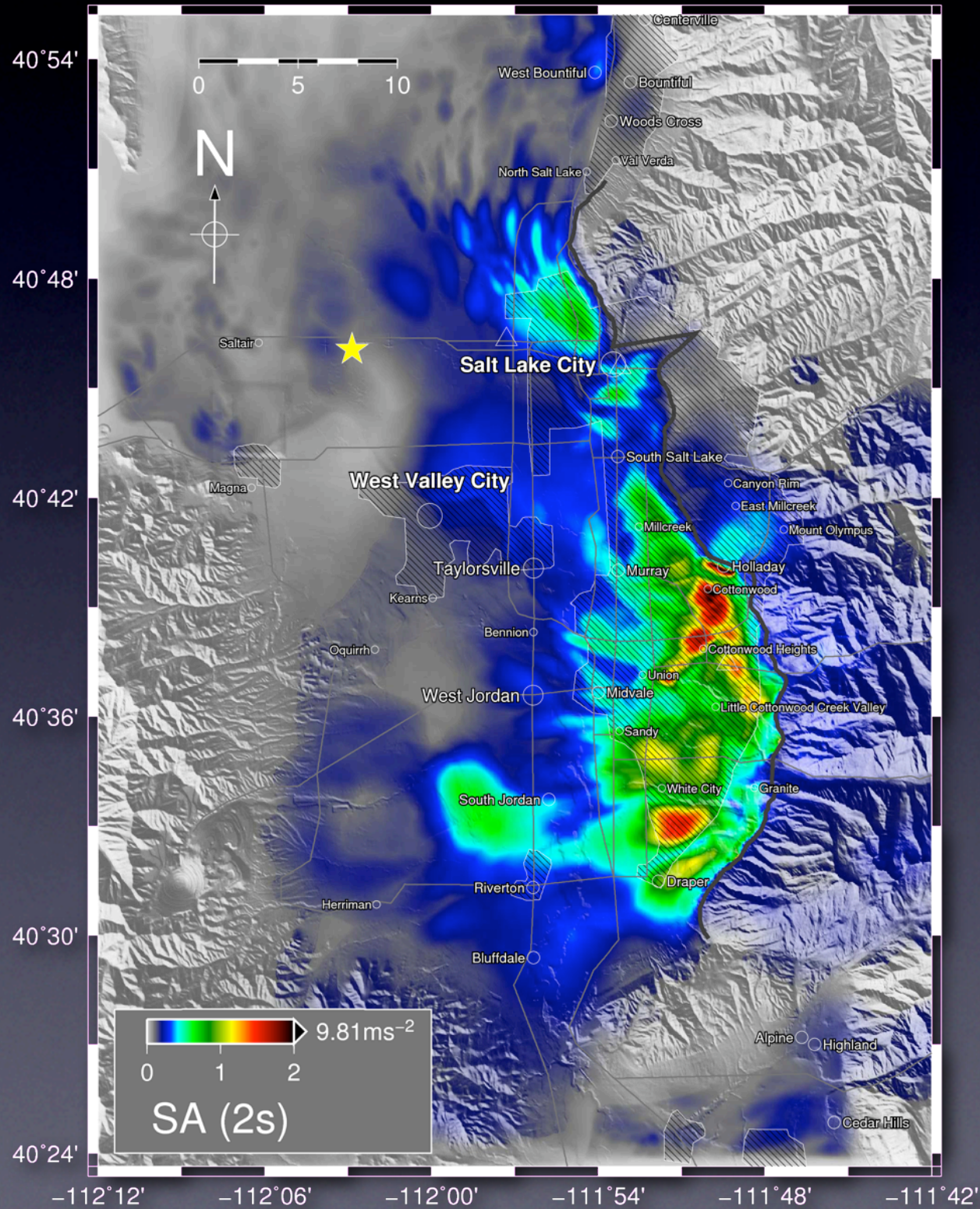


Scenario 2aM

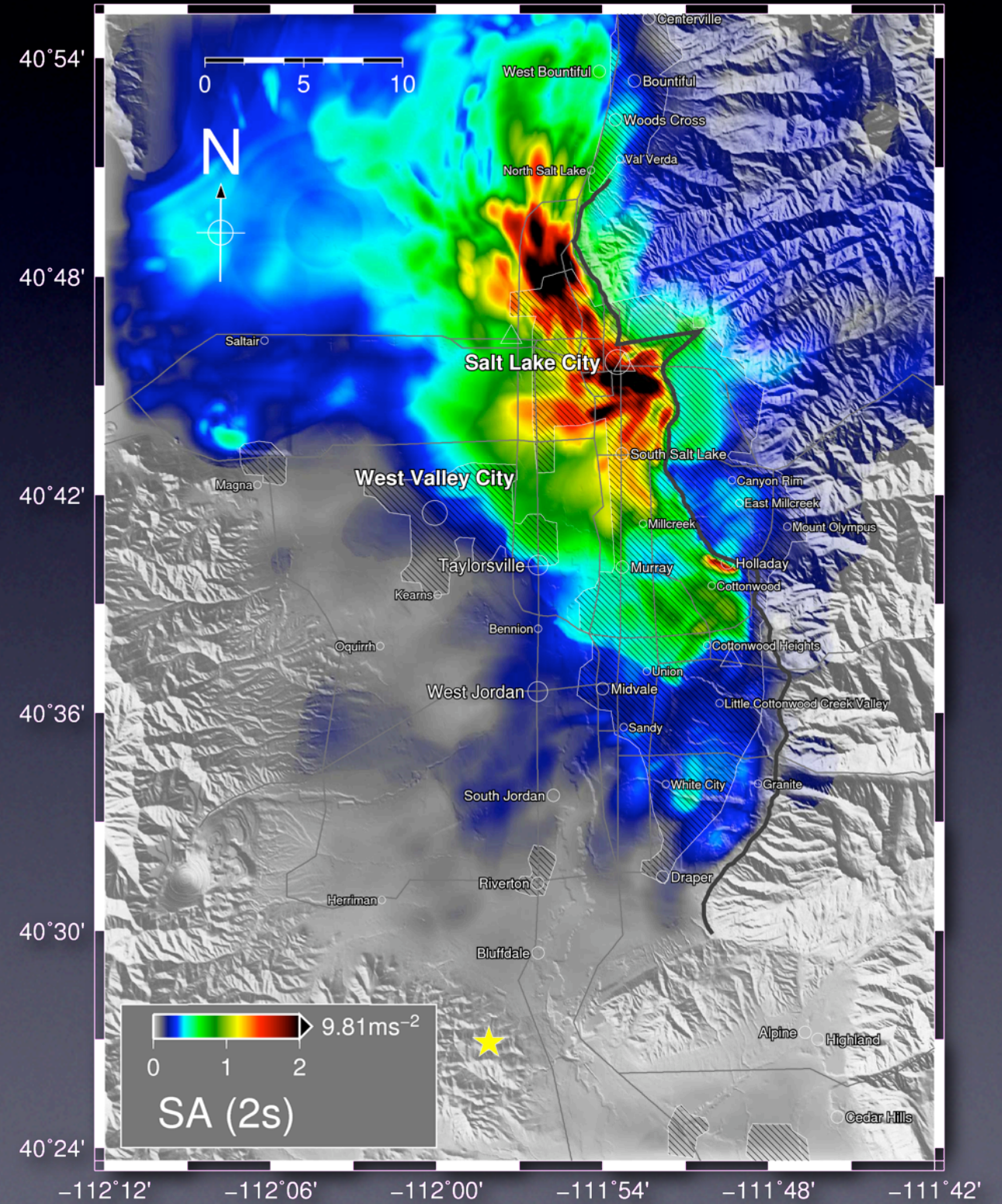


Spectral Accelerations at 2s (2s-SAs)

Scenario 5a



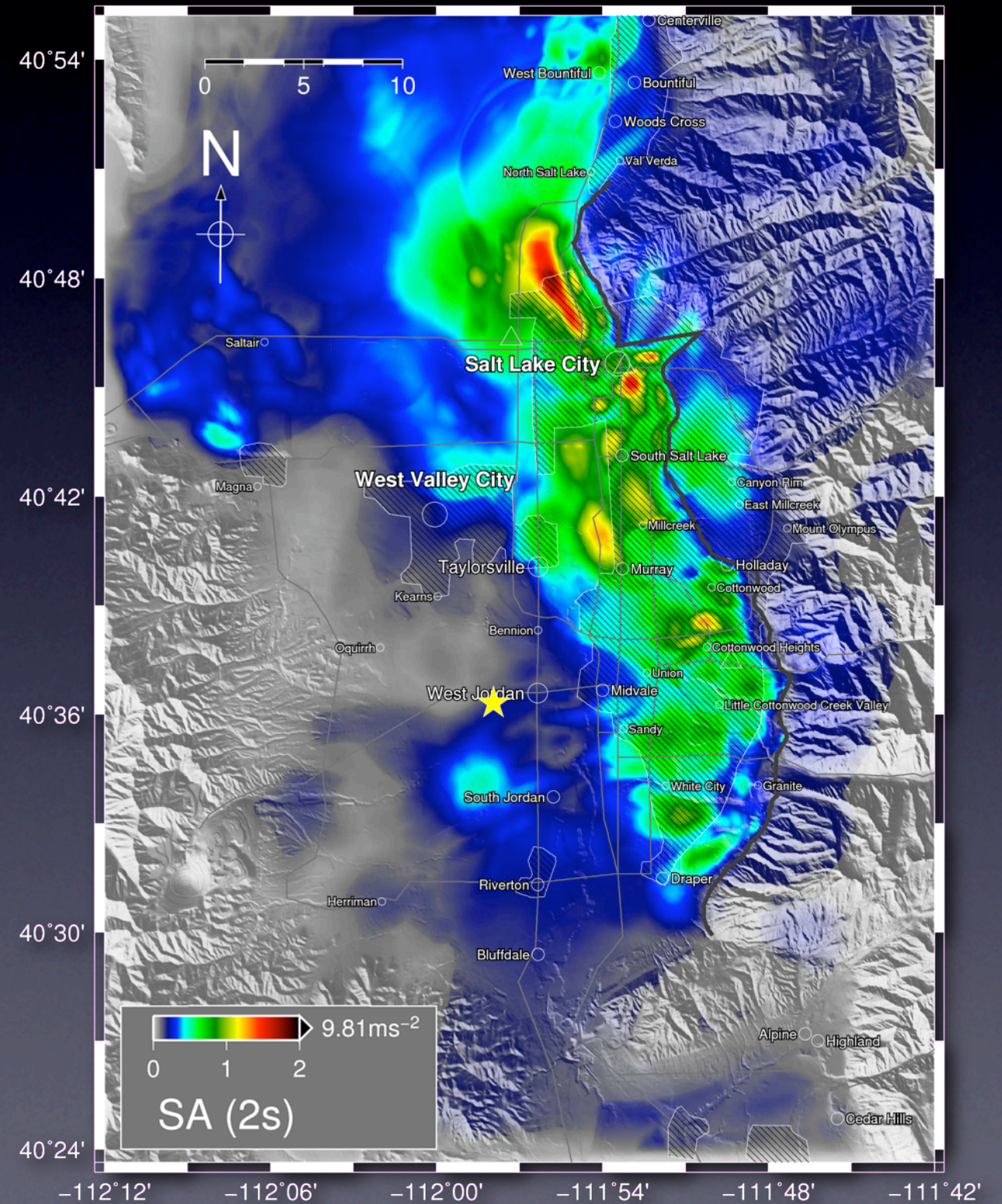
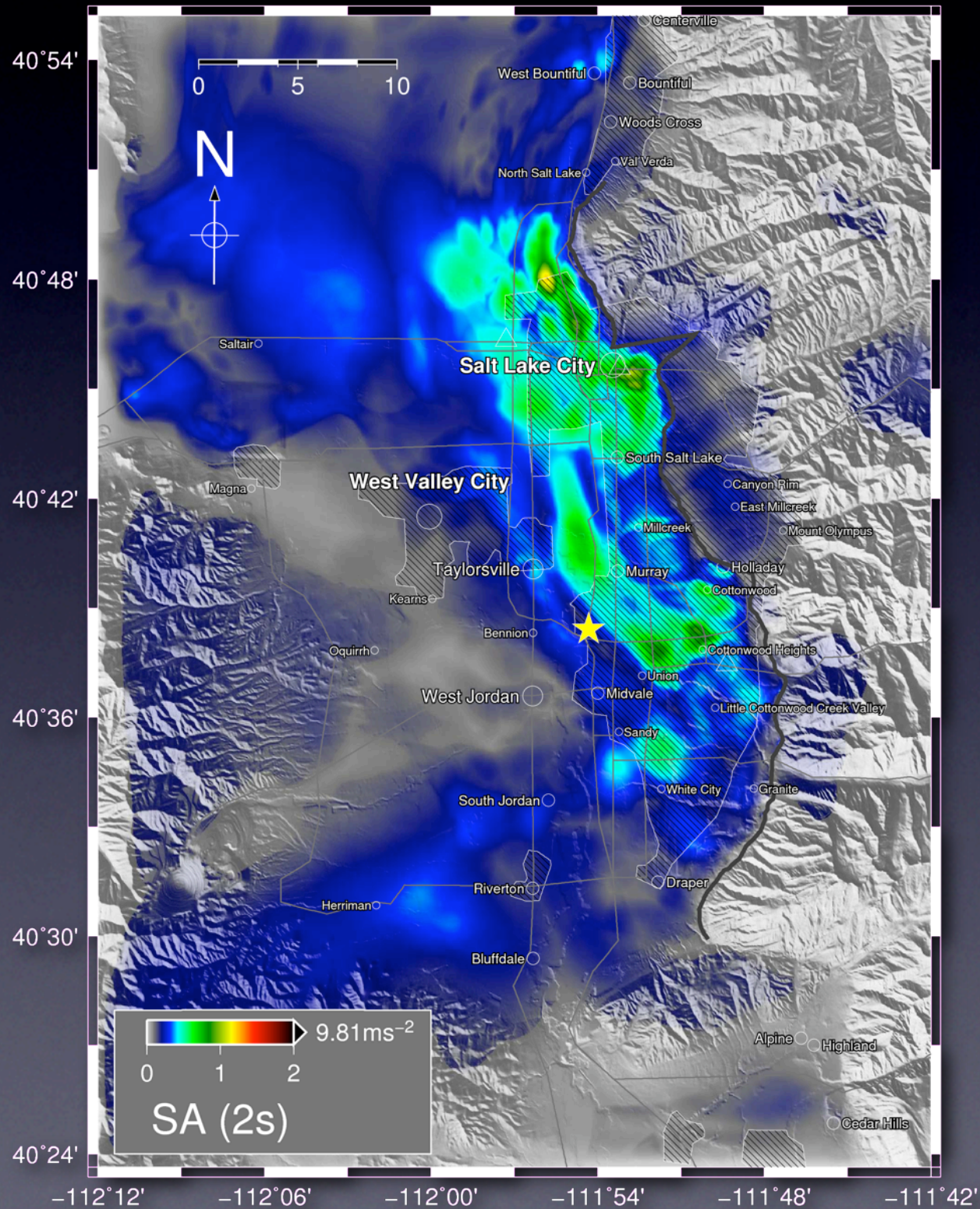
Scenario 5aM



Spectral Accelerations at 2s (2s-SAs)

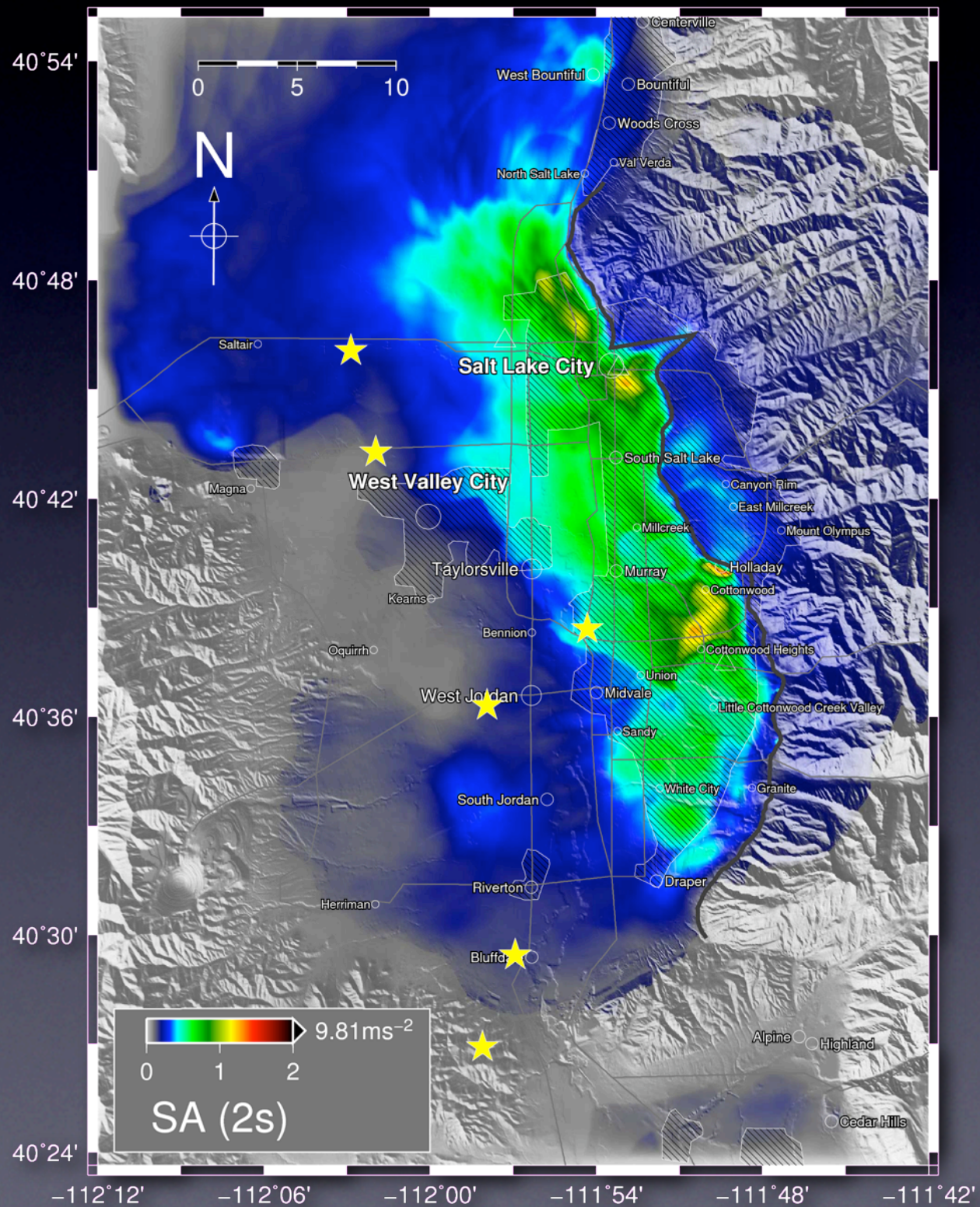
Scenario 3a

Scenario 6c



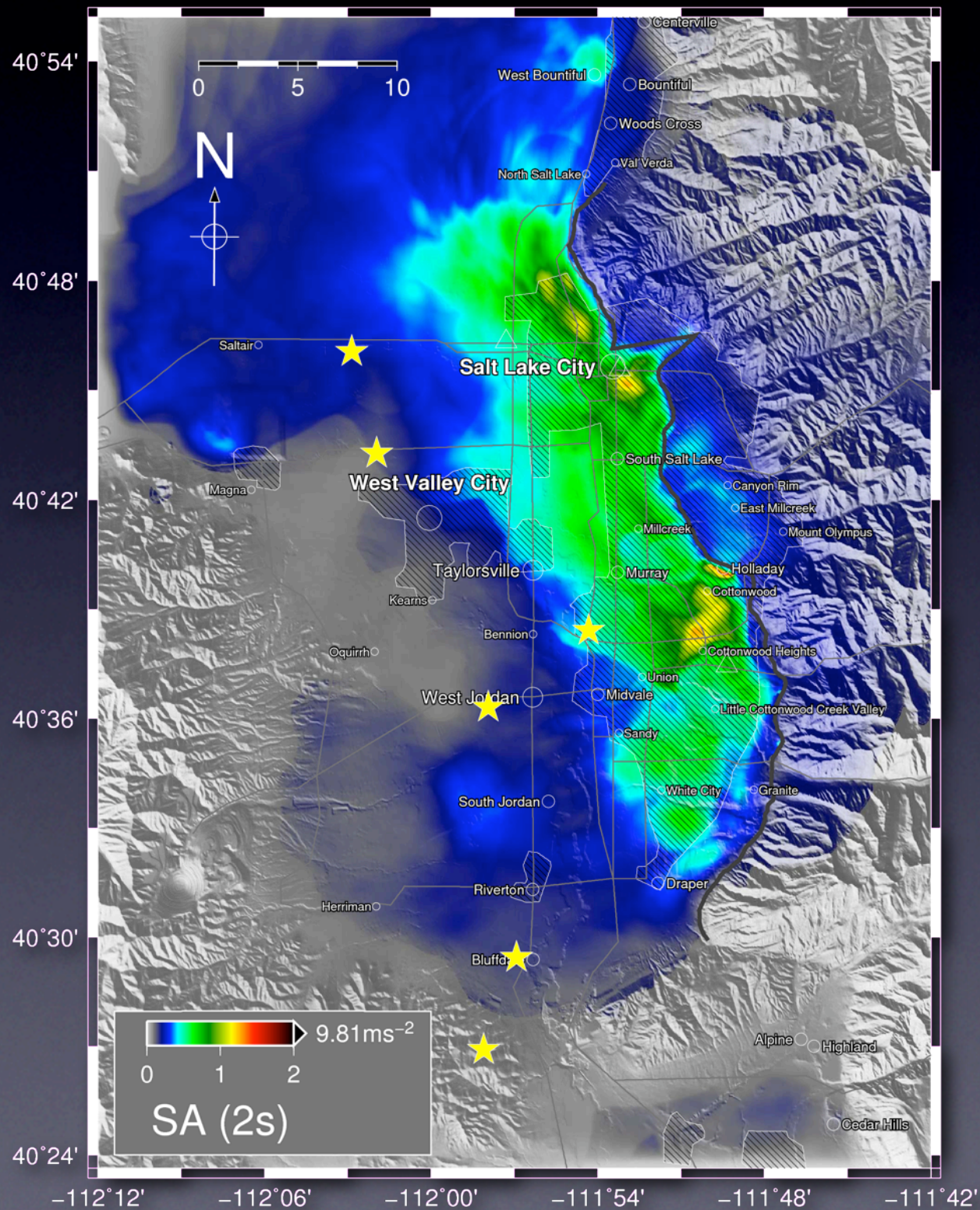
Average SAs

Average 2s-SAs

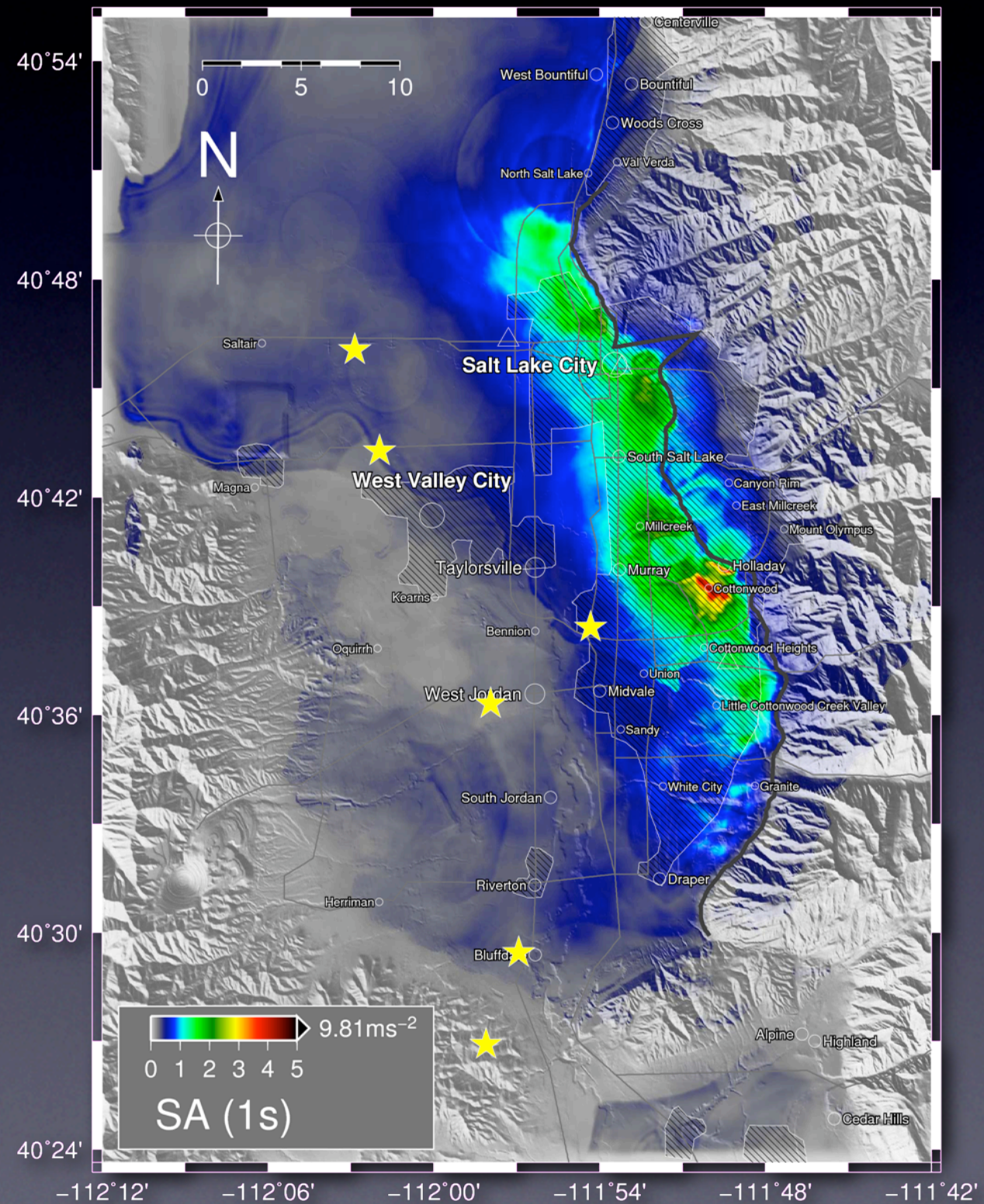


Average SAs

Average 2s-SAs



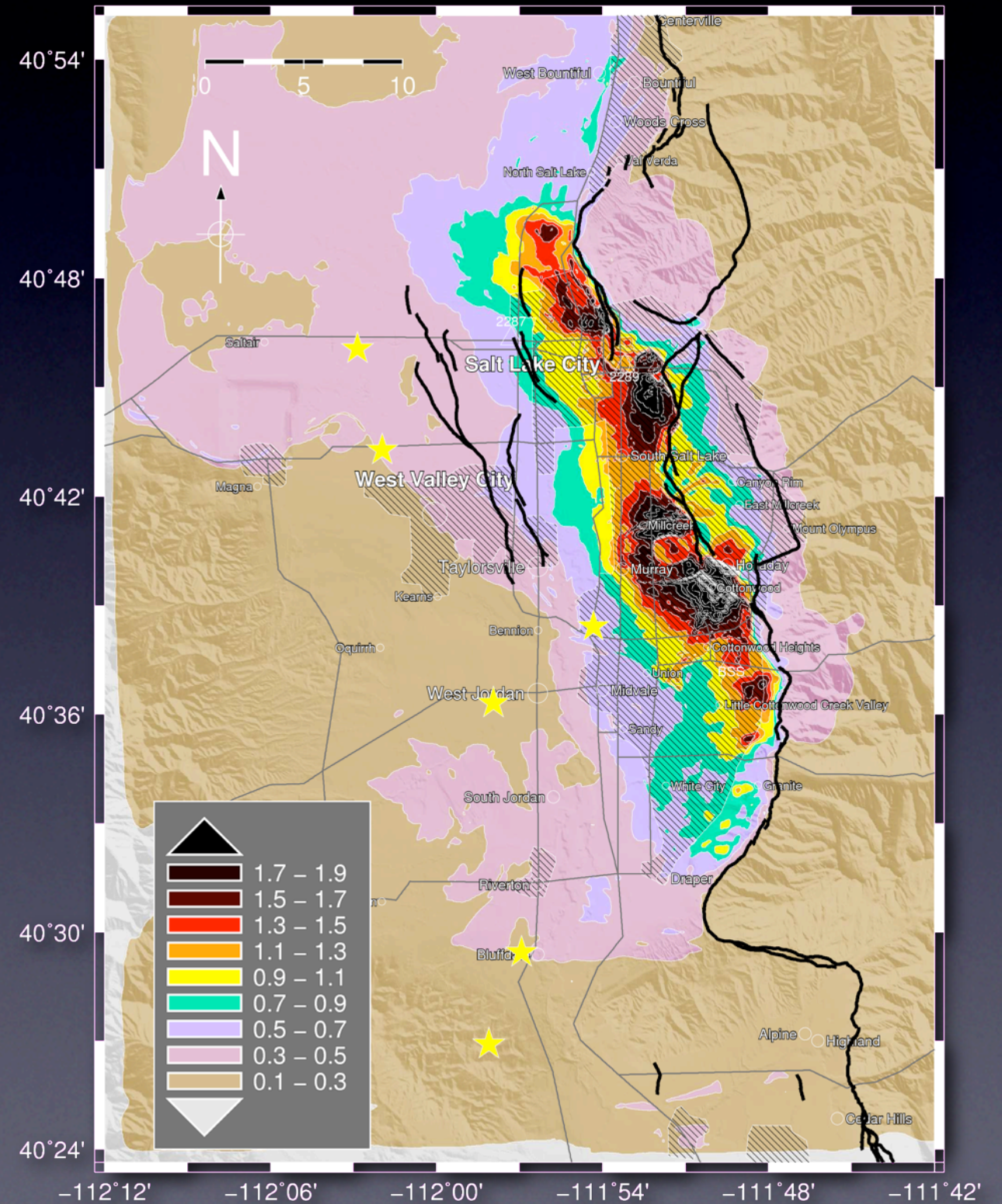
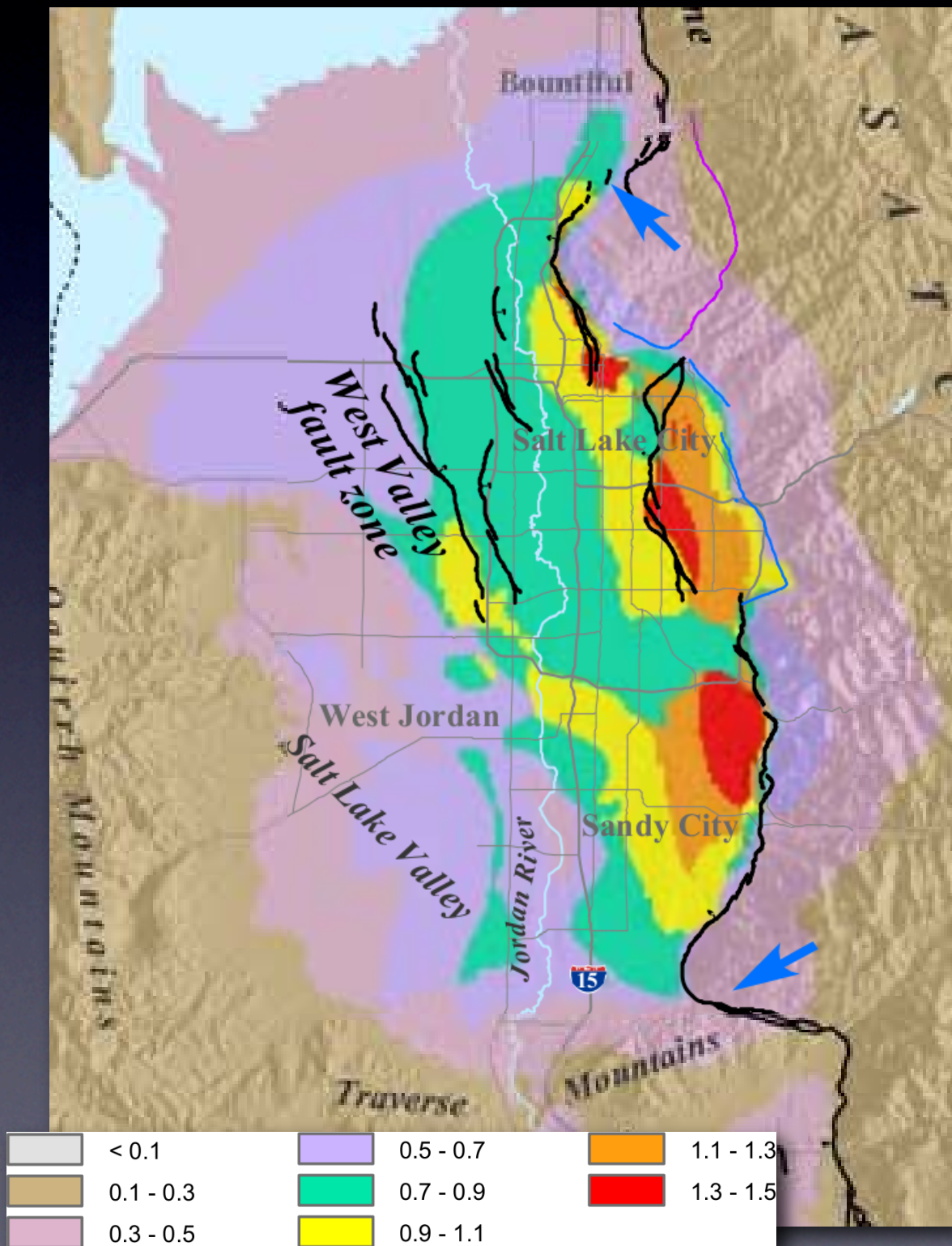
Average 1s-SAs



Average Is-SAs

Solomon et al. (2004)

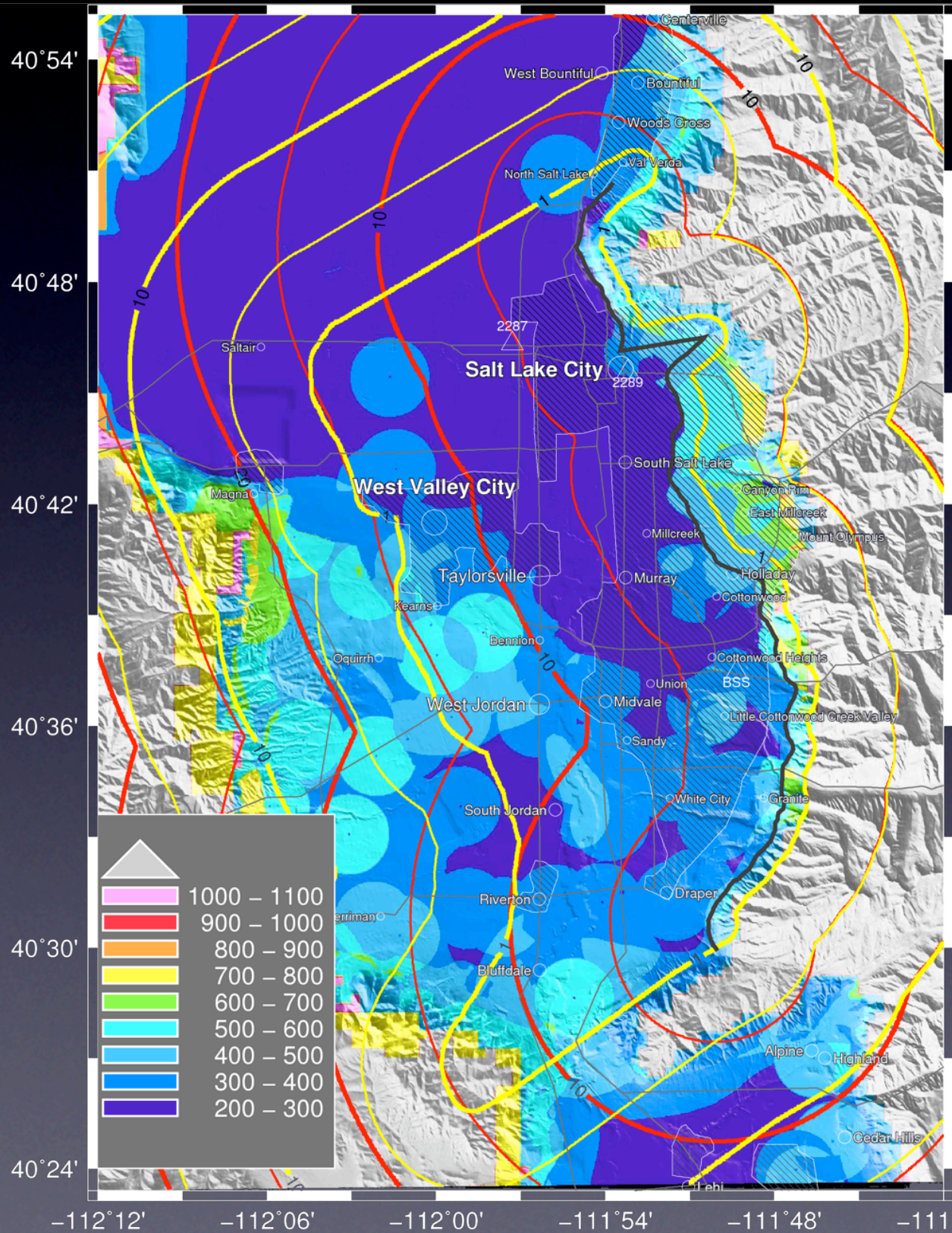
3-D FD simulations



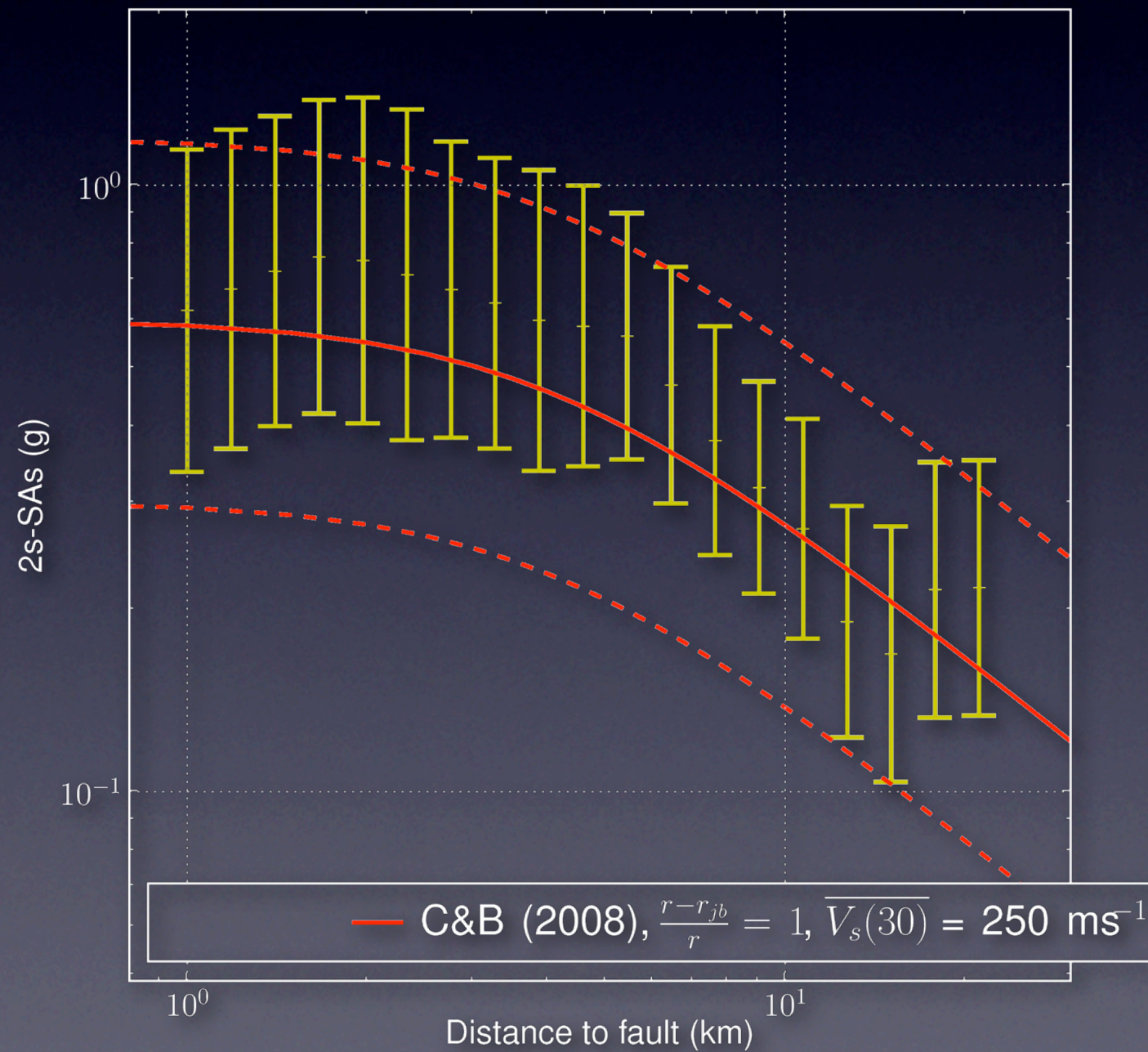
Comparison to NGA

$V_s(30)$ ms^{-1}

2s-SAs



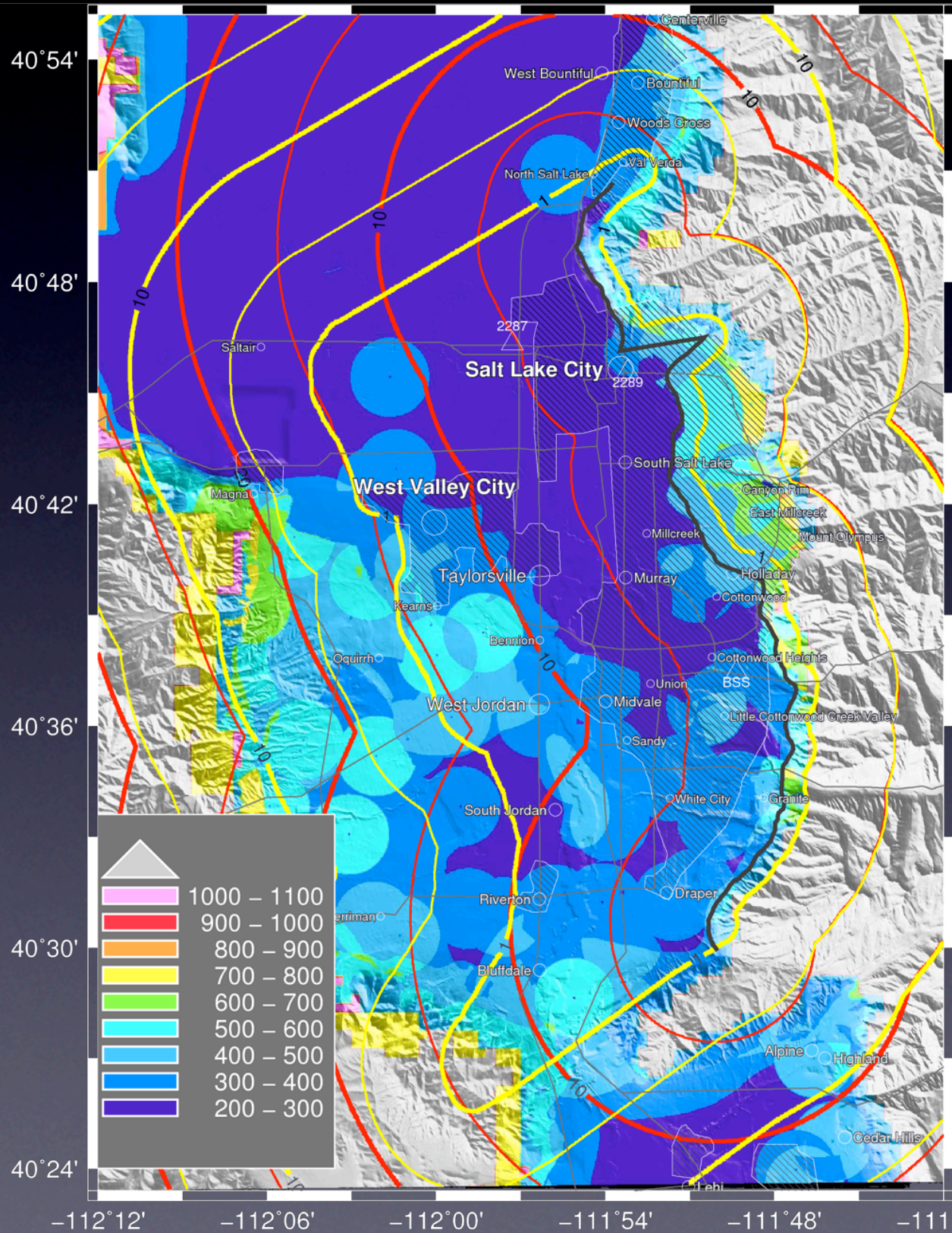
$200 \leq \overline{V_s(30)} \leq 300 \text{ ms}^{-1}$



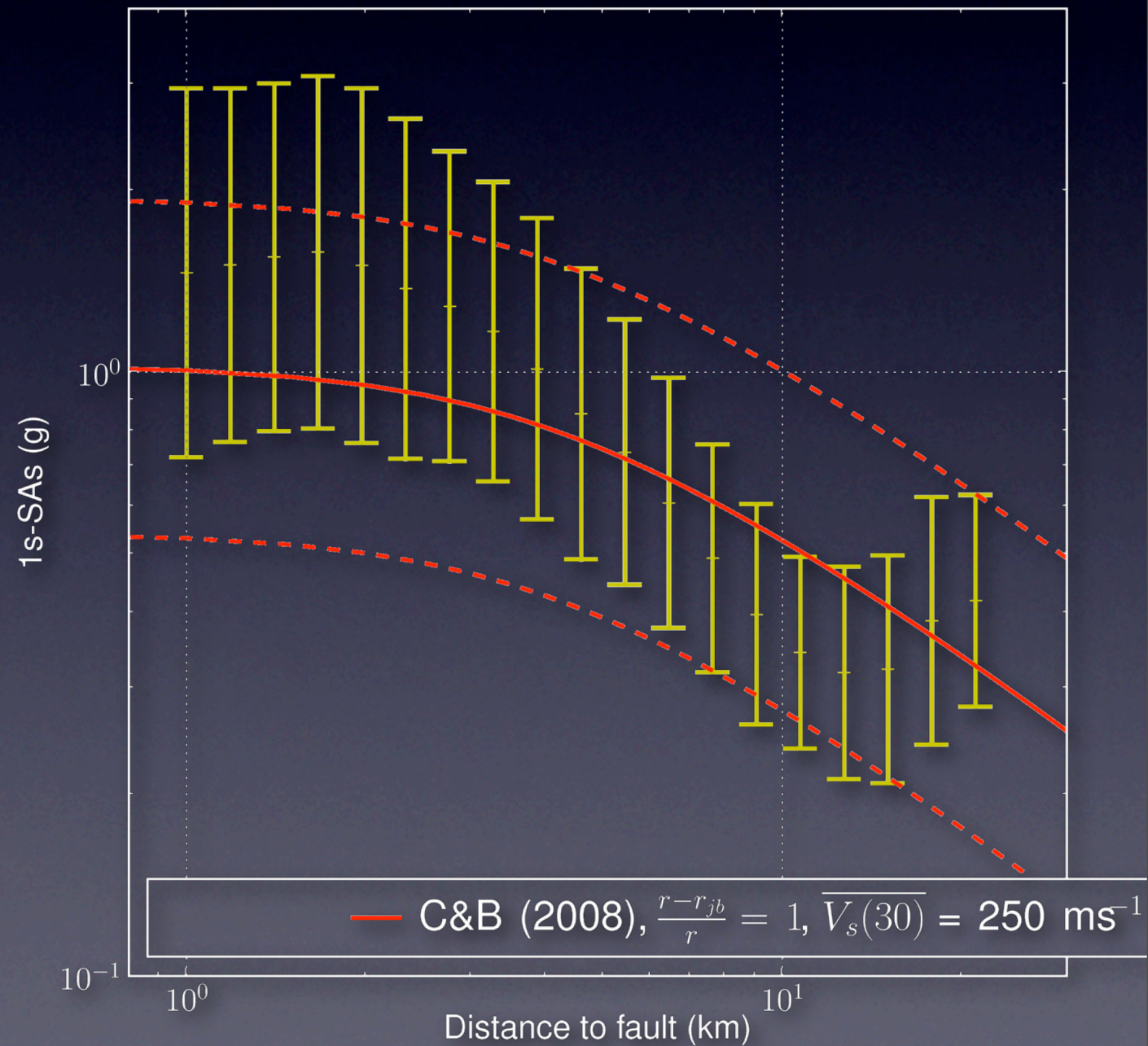
Comparison to NGA

$V_s(30)$ ms^{-1}

1s-SAs



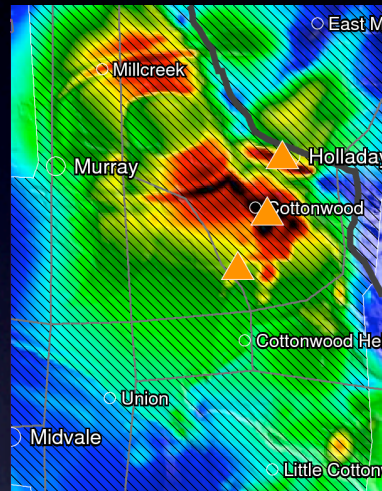
$200 \leq \overline{V_s(30)} \leq 300 \text{ ms}^{-1}$



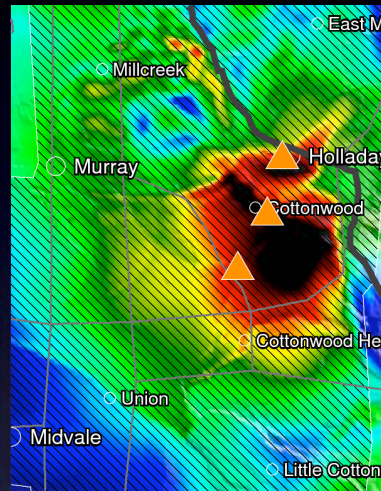
Is-SAs SW of Holladay stepover

What causes the up to 5g Is-SAs near Cottonwood?

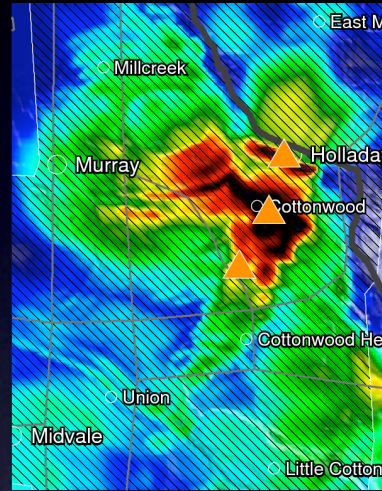
2a



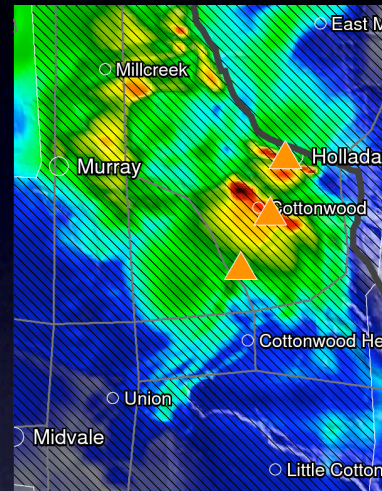
2aM



5a



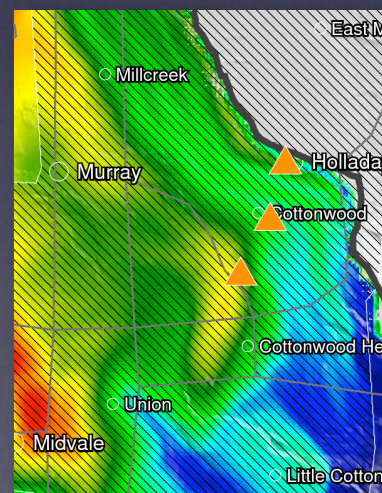
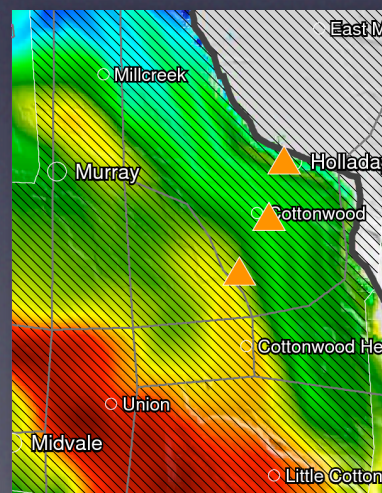
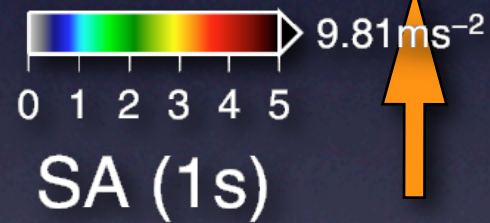
5aM



6c



3a

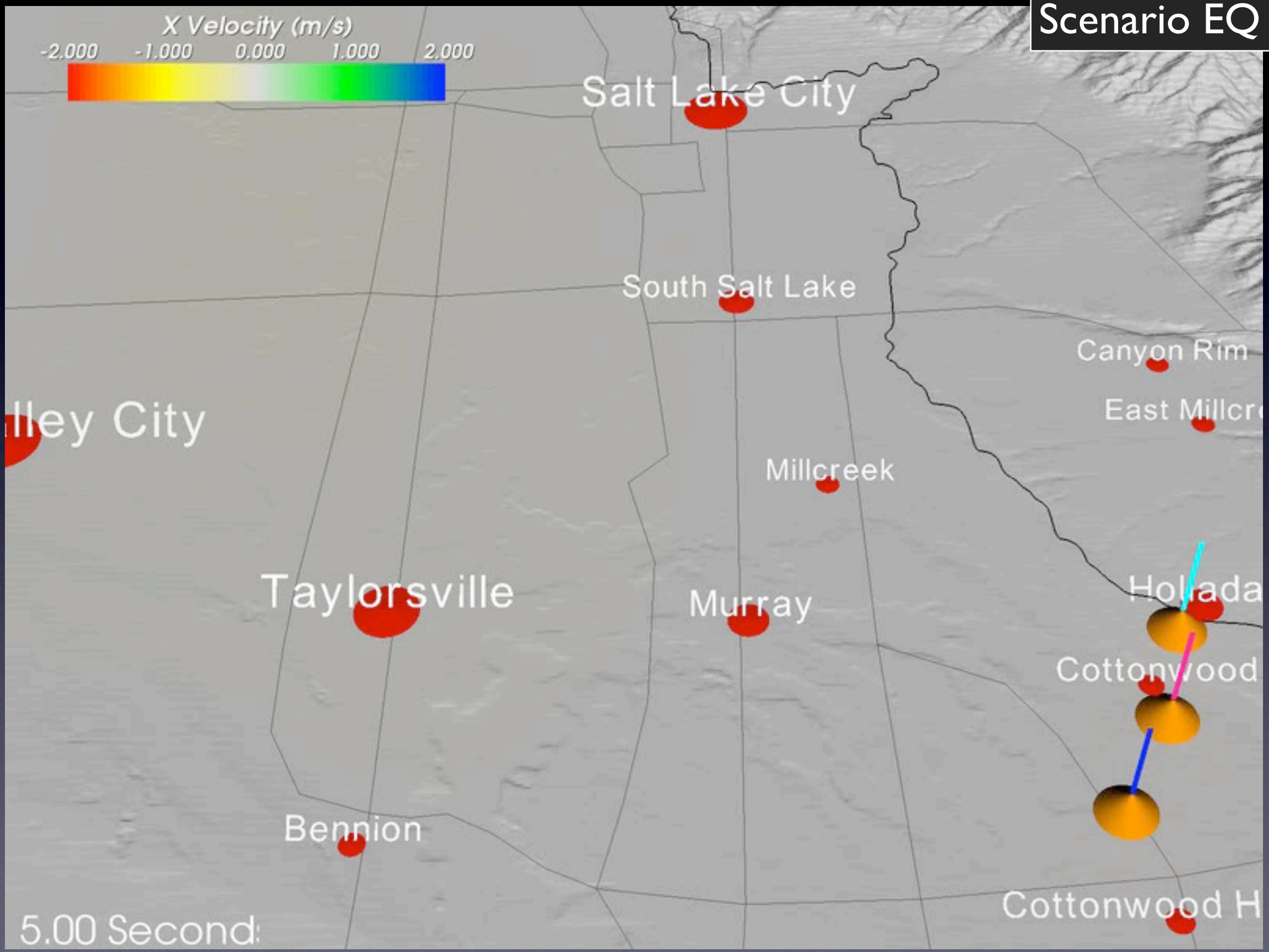


Is-SAs SW of Holladay stepover

Scenario EQ 5a:

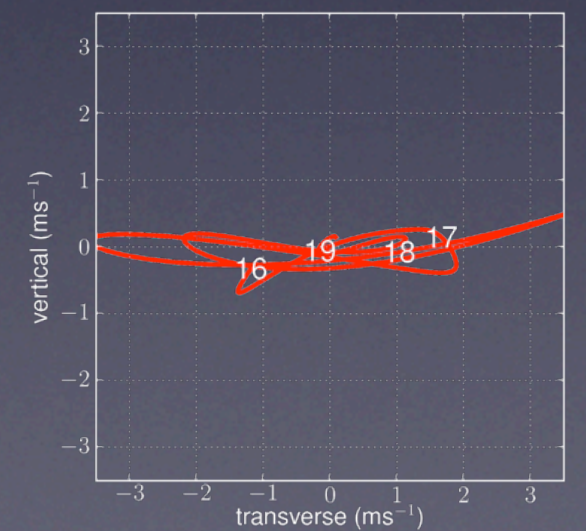
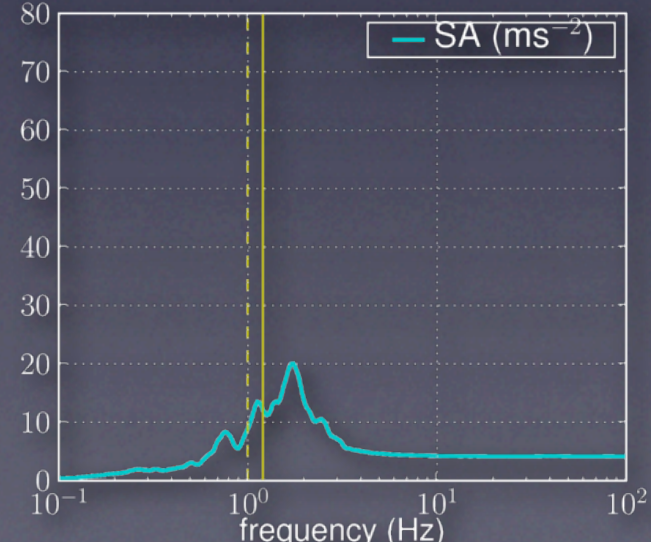
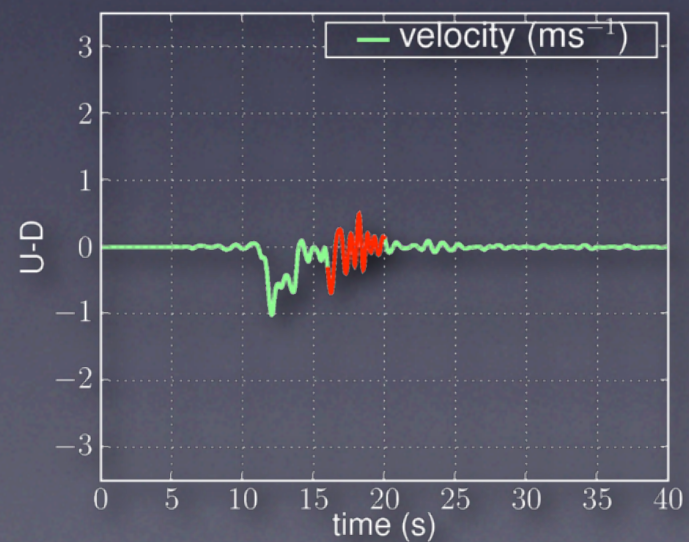
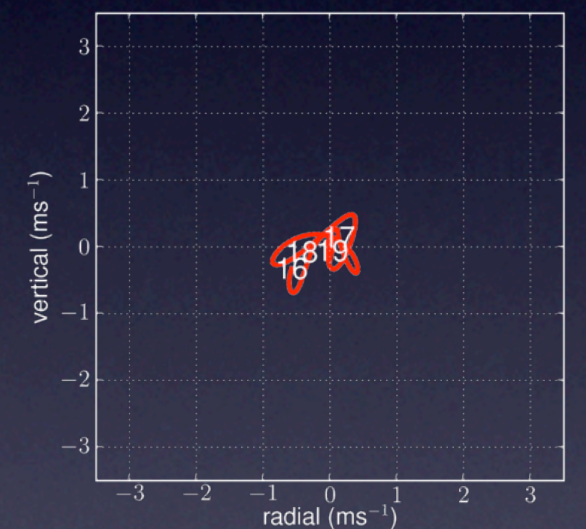
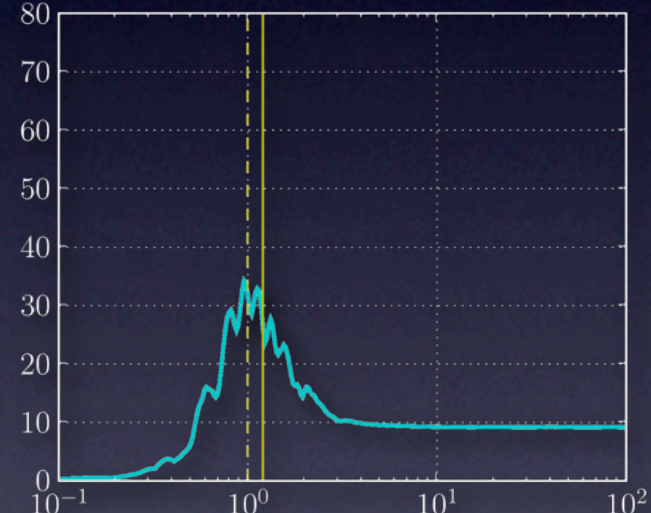
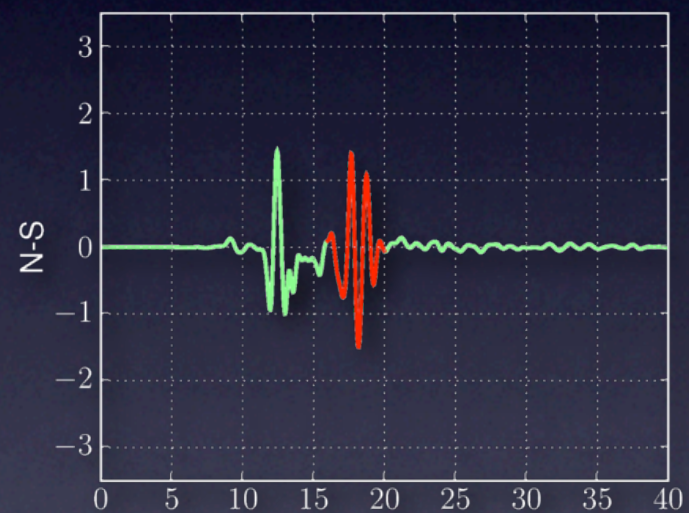
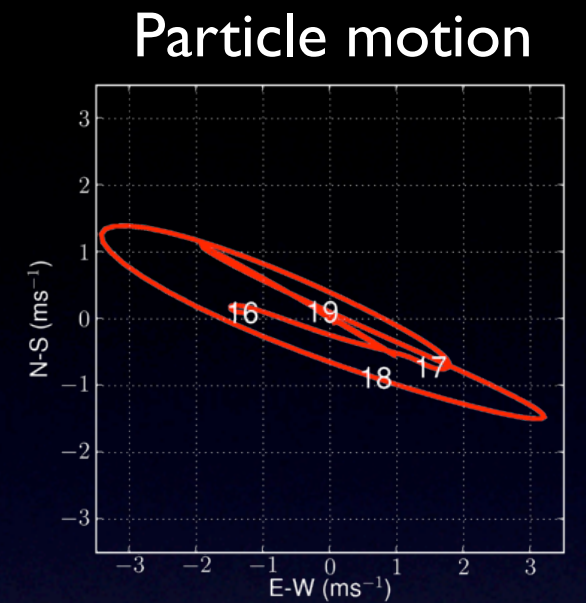
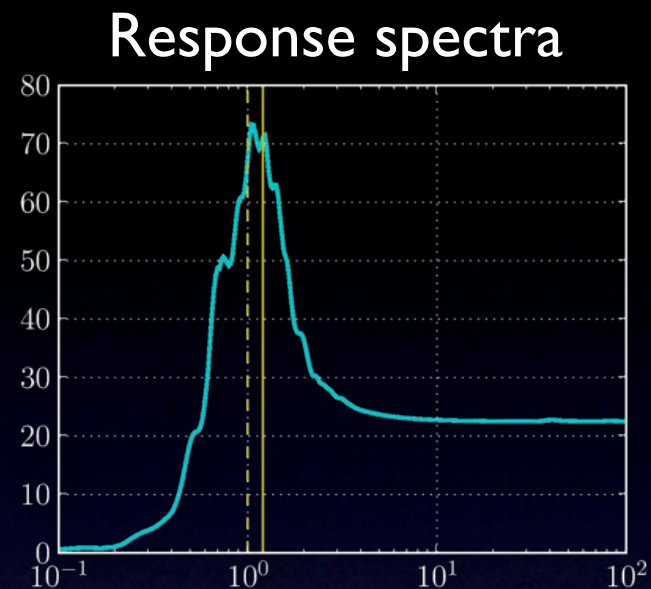
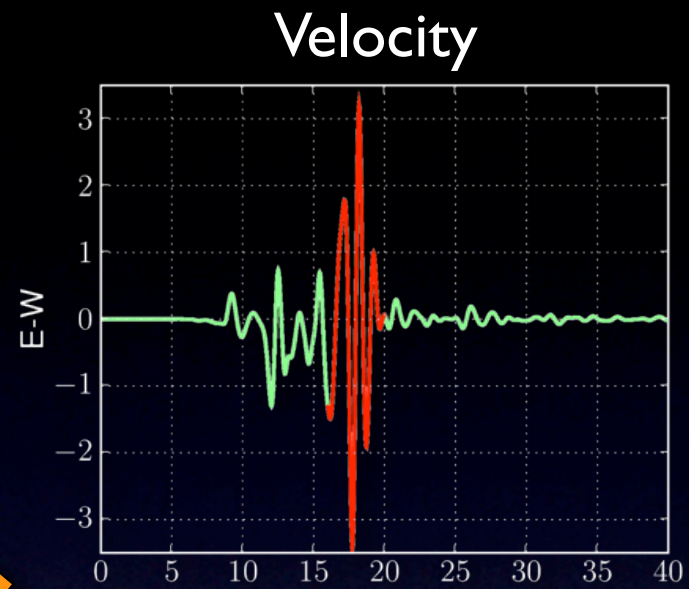
Is-SAs SW of Holladay stepover

Scenario EQ 5a:



Is-SAs SW of Holladay stepover

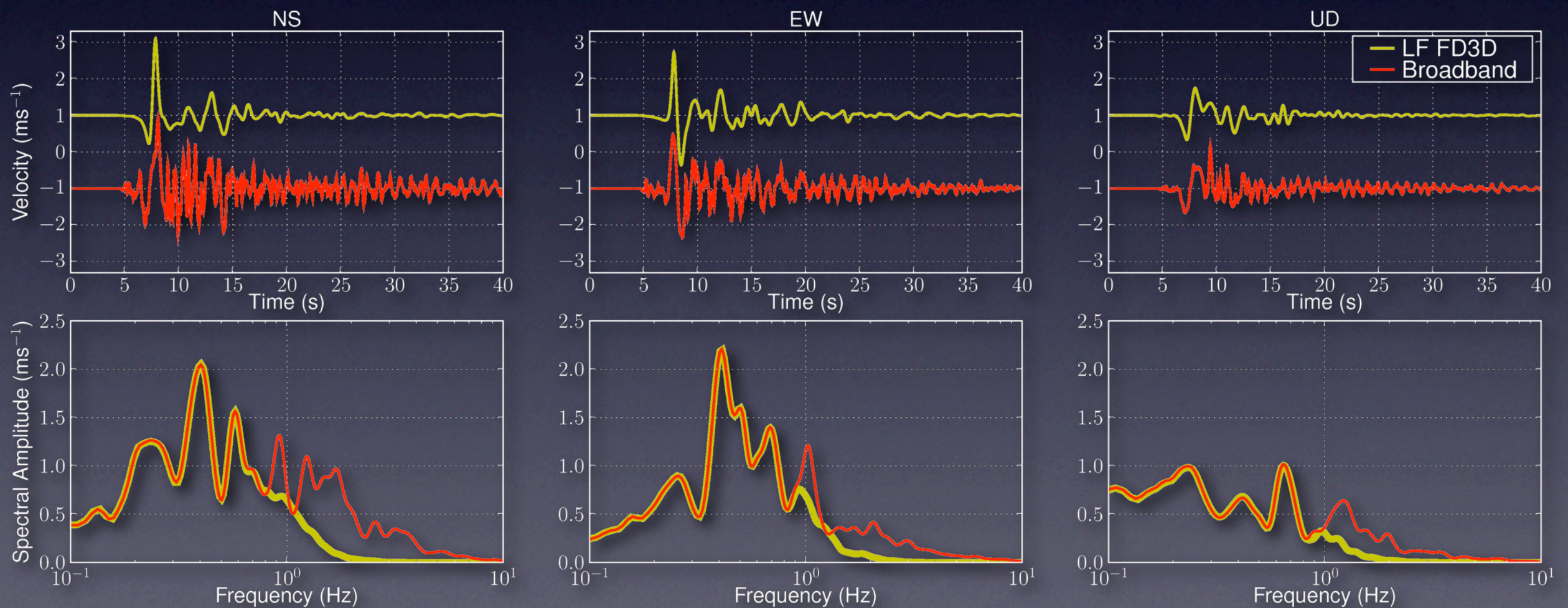
5a



Synthetic Broadband Seismograms

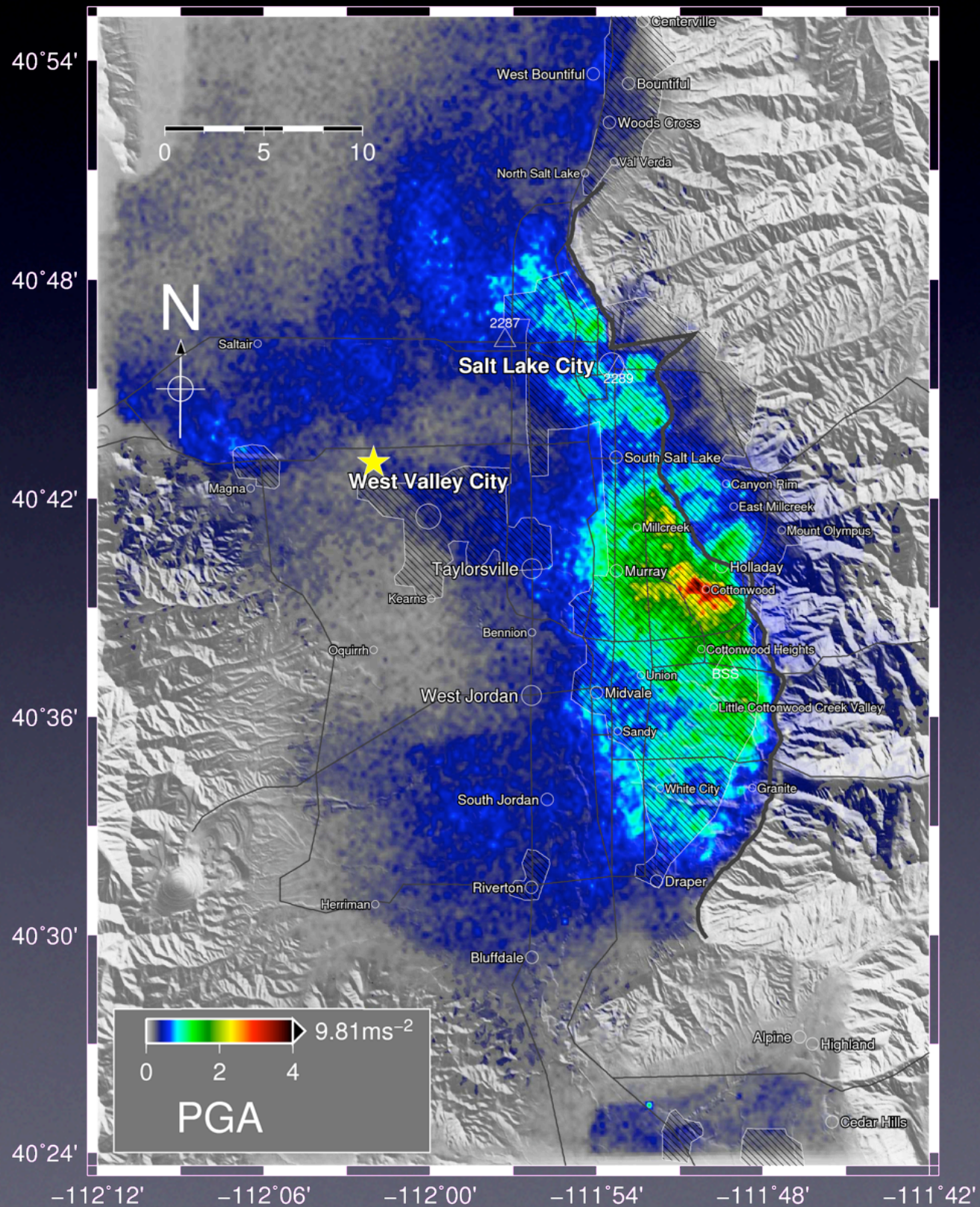
Combining low-frequency FD synthetics with high-frequency scattering operators:

- Scatterograms are computed using multiple scattering theory with scattering parameters based on site-specific velocity structure
- Scatterograms are convolved with dynamically consistent source time function
- LF and HF synthetics are combined into broadband seismograms in the frequency domain using a simultaneous amplitude and phase matching algorithm (Mai & Olsen, 2009)



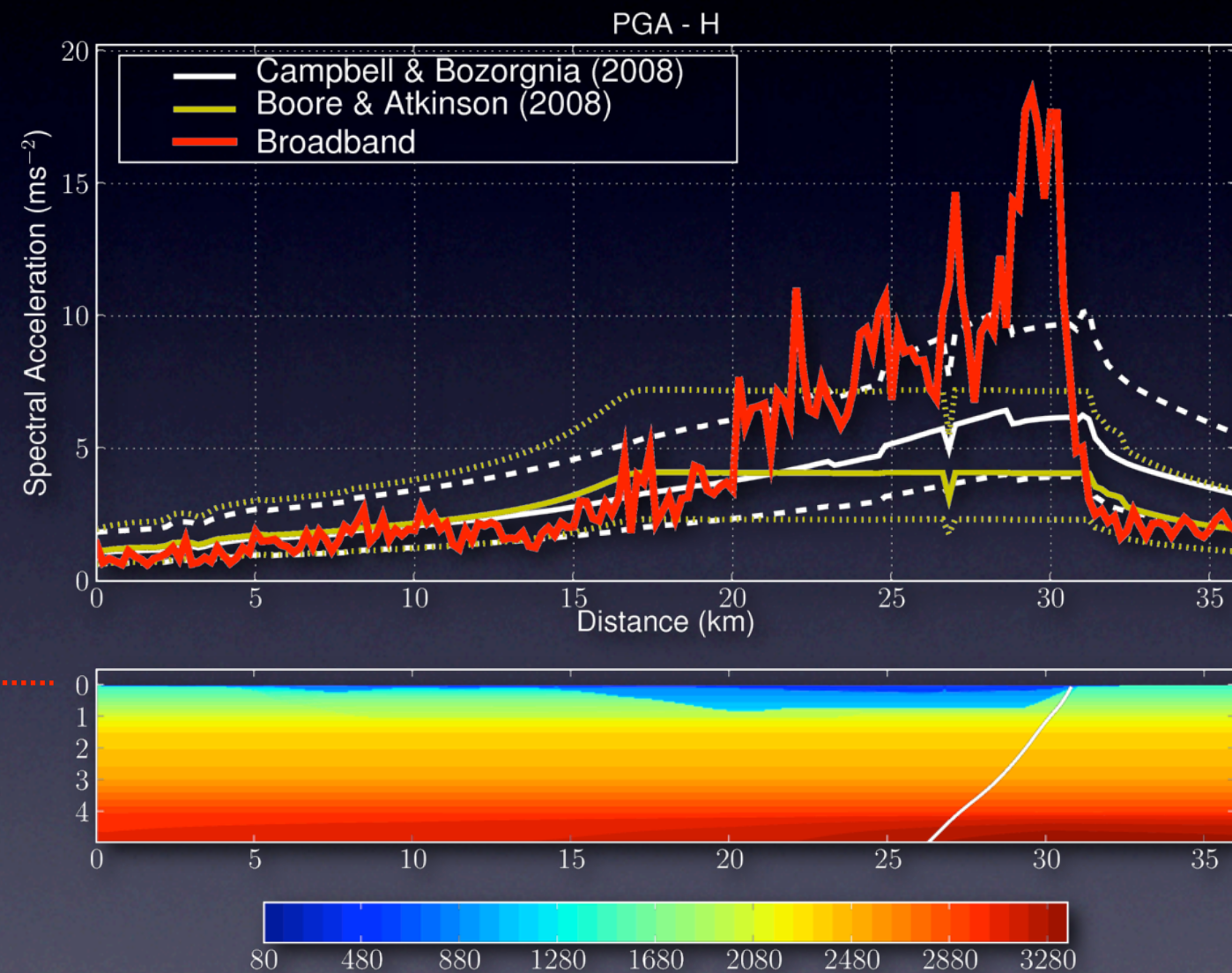
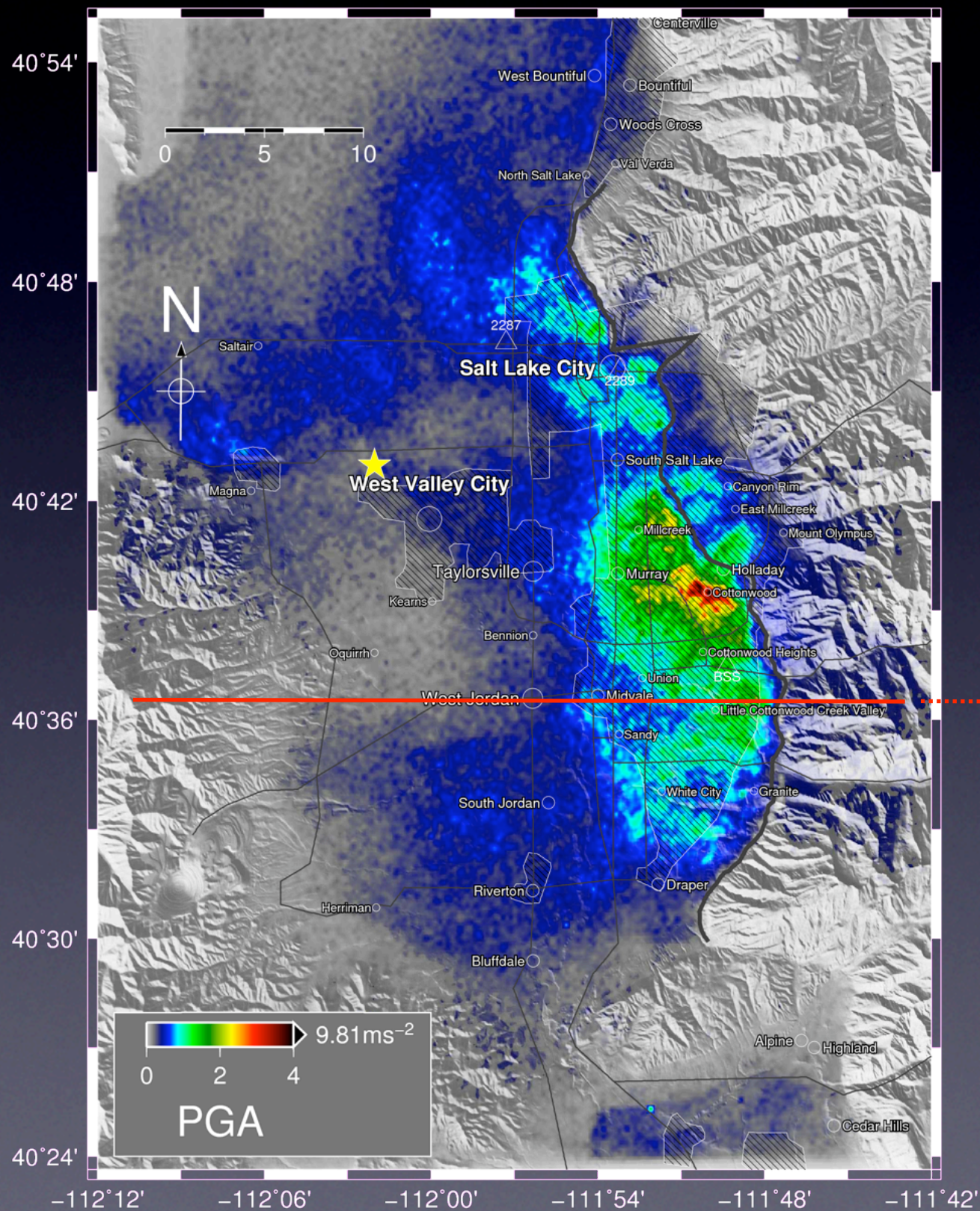
Synthetic Broadband Seismograms

Broadband PGA (Scenario 2a)



Synthetic Broadband Seismograms

Broadband PGA (Scenario 2a)



Simulation of Nonlinear Soil Response

- Nonlinear 1-D propagator *NOAH* (Bonilla et al., 2005) to model **SH** propagation in top 240m
- Not modeling pore water pressure or soil dilatancy (parameters are not available)
- Shear modulus reduction is controlled by **reference strain** γ_r :

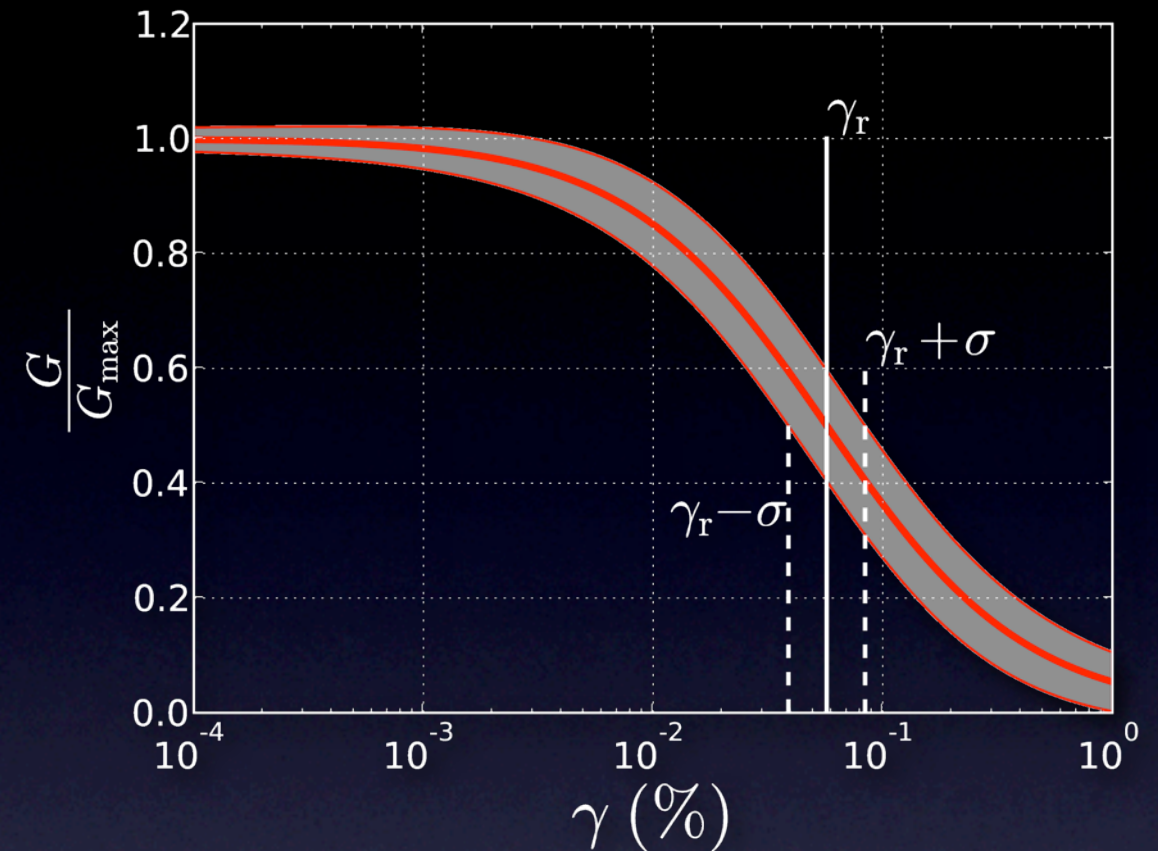
$$\frac{G}{G_{\max}} = \frac{1}{1 + \frac{\gamma}{\gamma_r}}$$

- Reference strain γ_r is derived from an **empirical relationship** (Darendelli, 2001), modified to take results of recent laboratory test of Bonneville clays into account (Bay & Sasanakul, 2005):

$$\gamma_r(\text{PI}, \text{OCR}, \sigma_v)$$

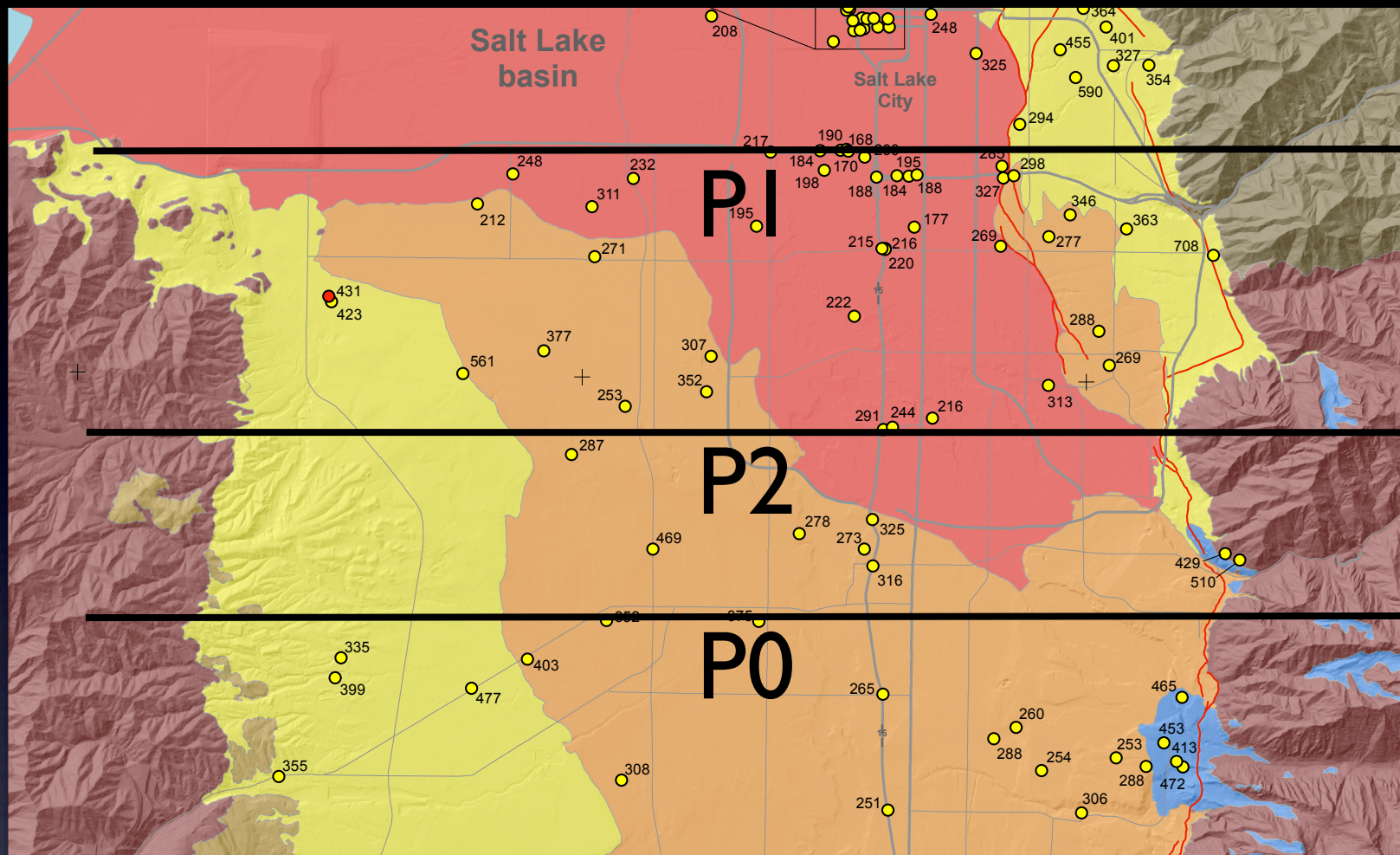
- Hysteresis dissipation is controlled by maximum damping ratio at large strains ξ_{\max} , which we also estimate from Darandelli (2001):

$$\xi_{\max}(\text{PI}, \text{OCR}, \sigma_v, N, f)$$



	Parameter	Value
PI	Plasticity Index	0 - 40
OCR	Overconsolidation ratio	1
σ_v	Confining pressure	$f(z)$
N	Number of cycles	10
f	Frequency	1 Hz

Nonlinear soil parameters



Q01 (PI=40%)

Q02 (PI=30%)

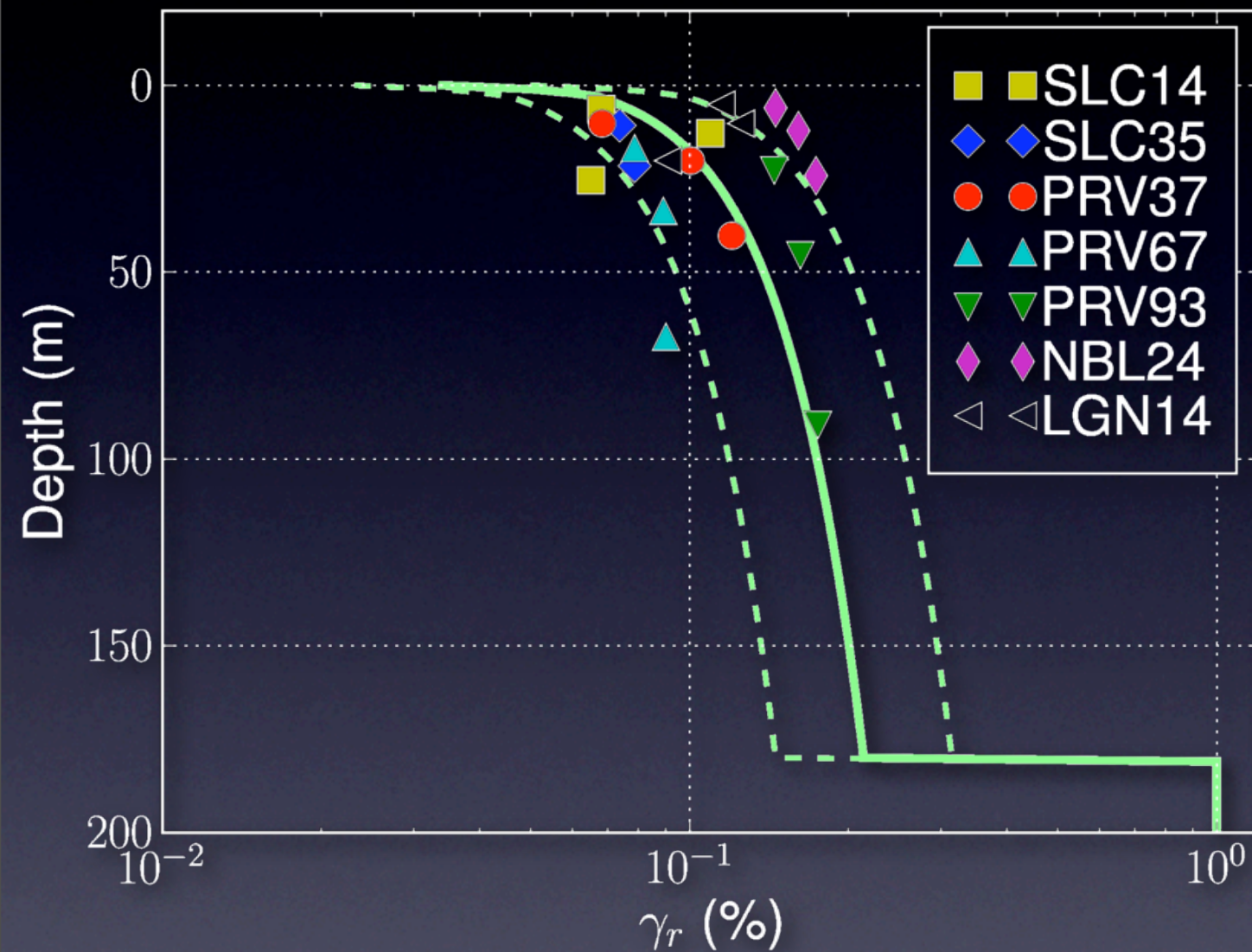
Q03 (PI=0%)

Rock (linear)

McDonald and Ashland (2008)

Nonlinear soil parameters

Example site on PI (5 km south of airport):



Three ID models for each site:

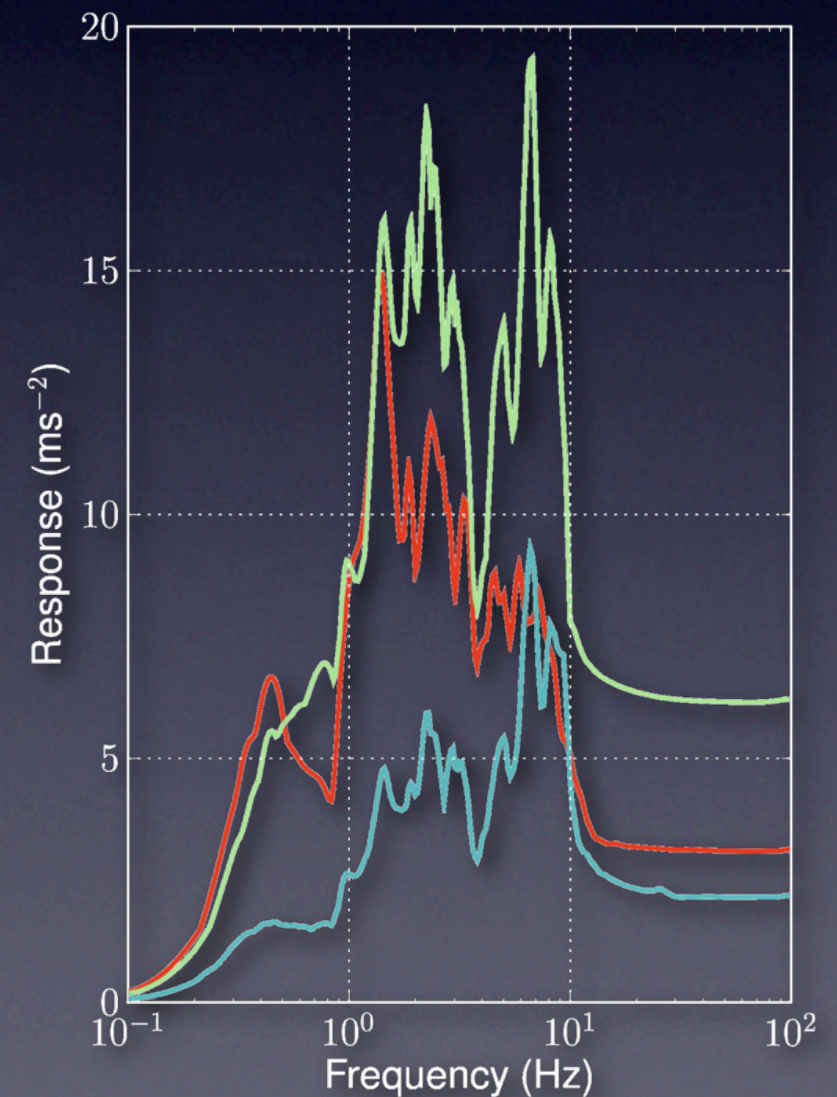
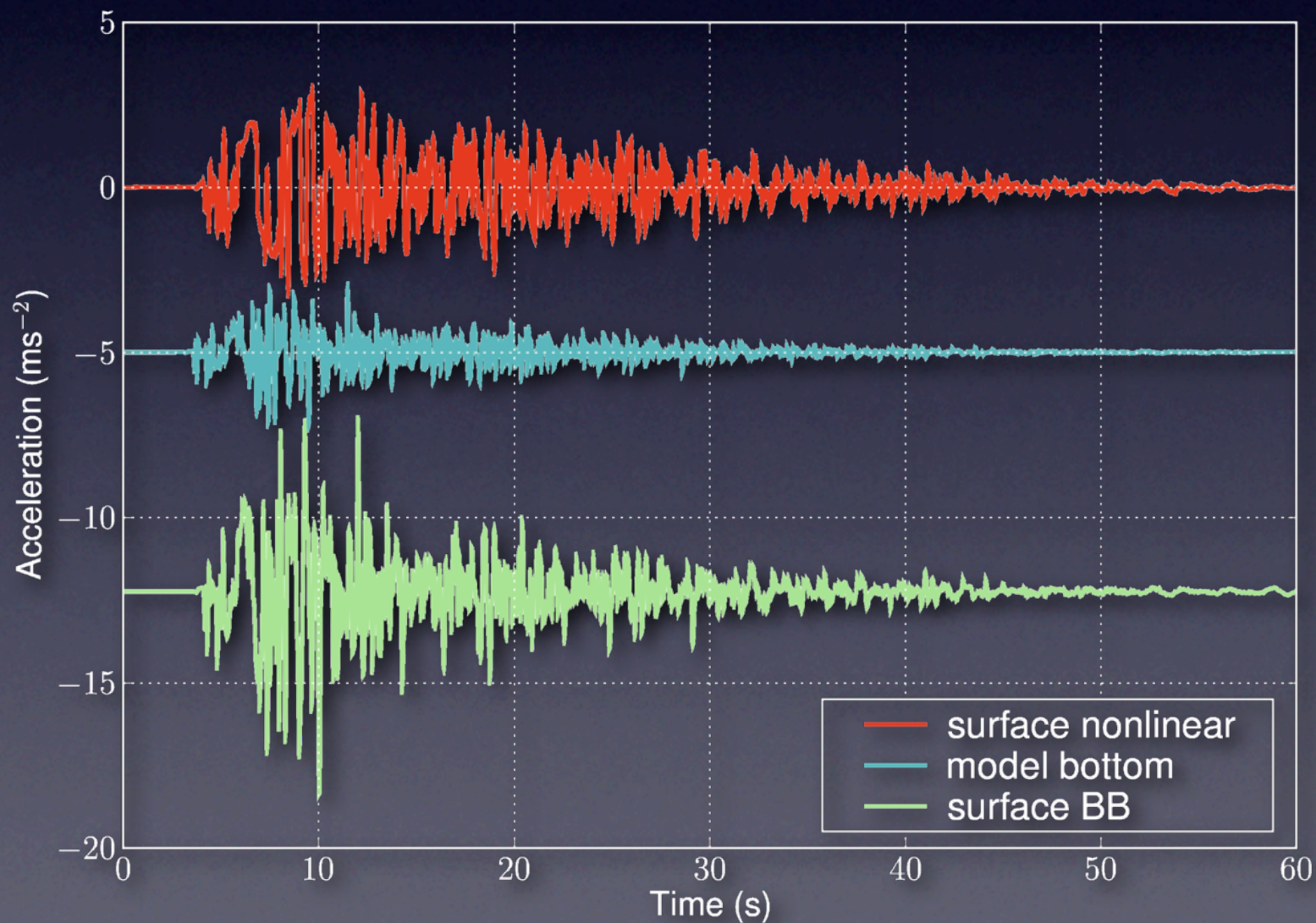
Model	Reference strain	Damping ratio
Nonlinear	γ_r	ξ
More nonlinear	$\gamma_r - \text{std}$	$\xi + \text{std}$
Less nonlinear	$\gamma_r + \text{std}$	$\xi - \text{std}$

— reference strain γ_r

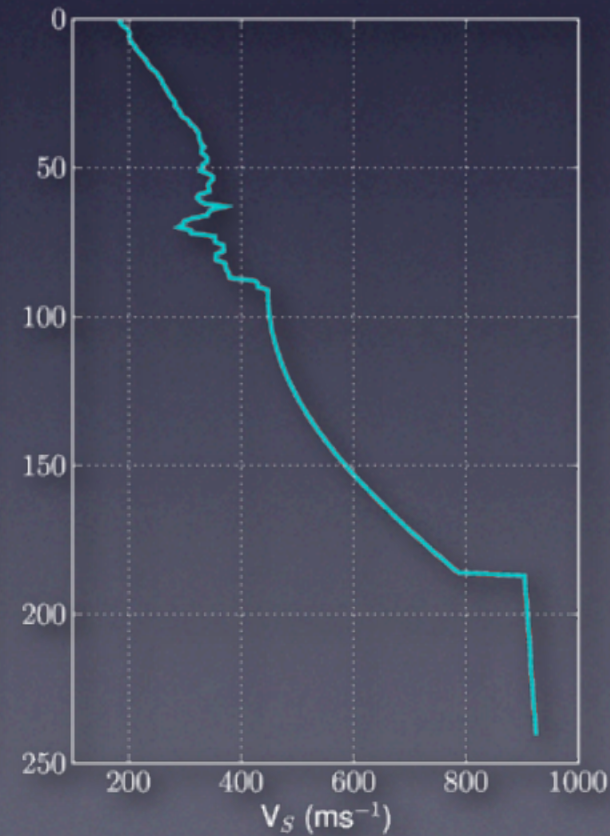
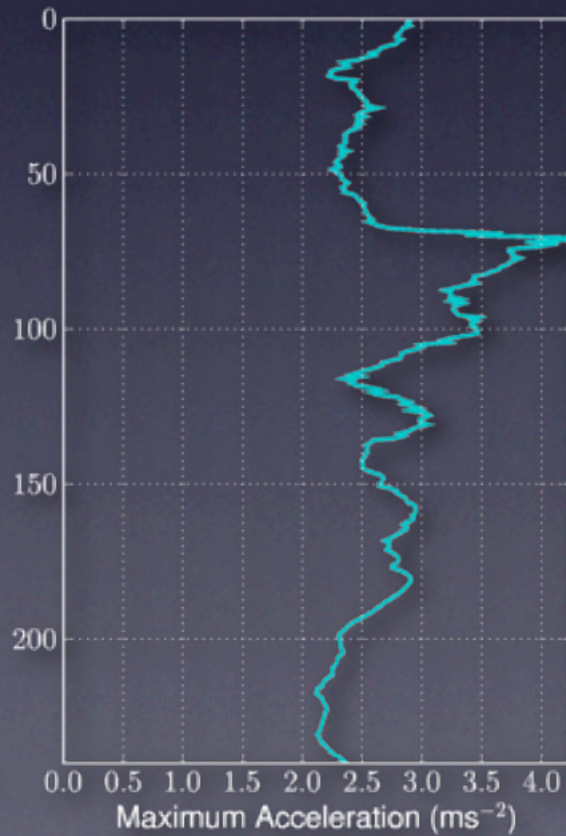
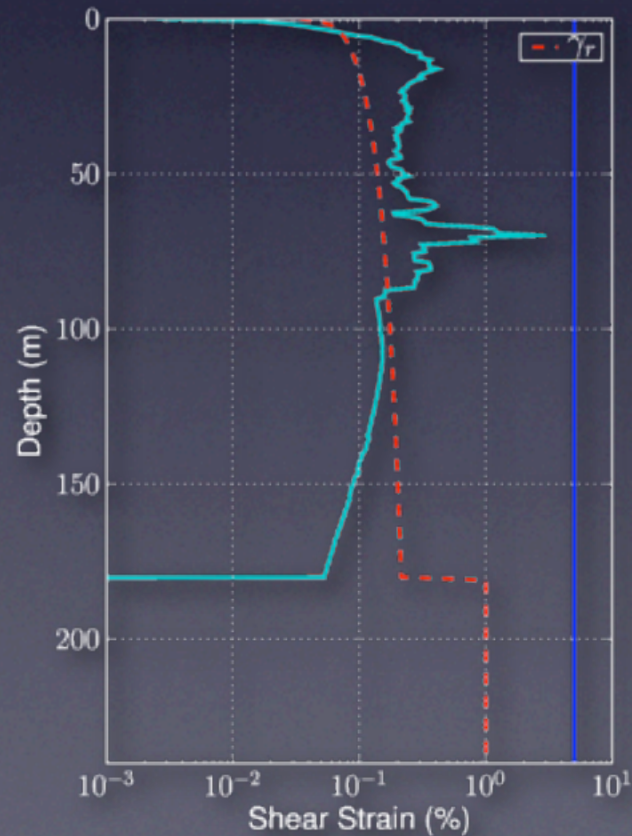
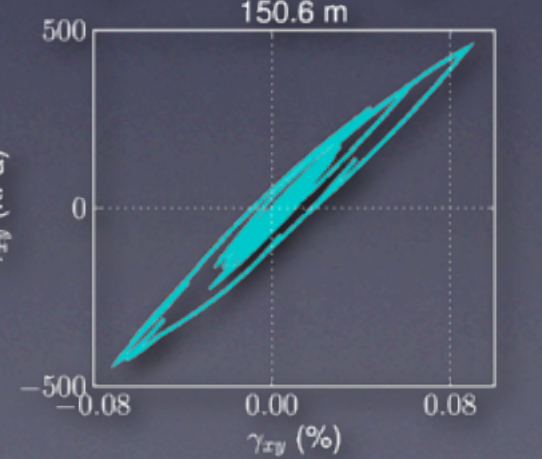
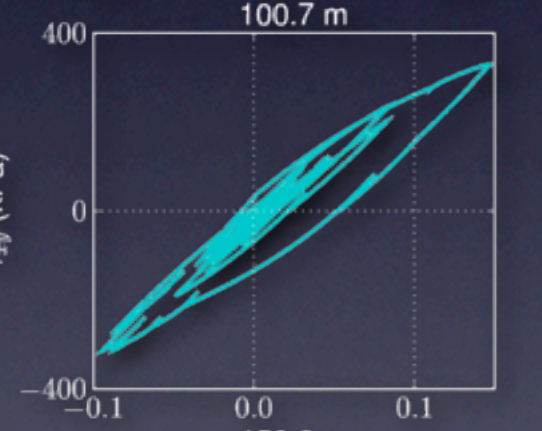
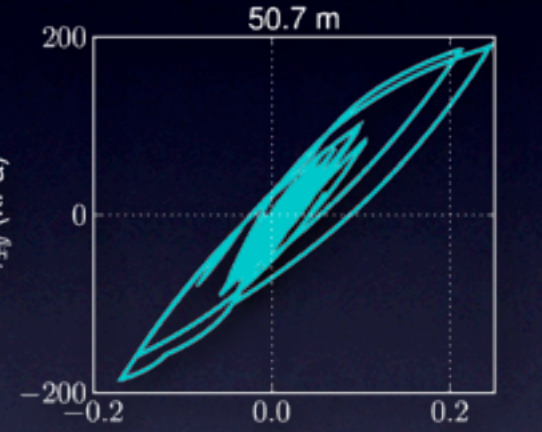
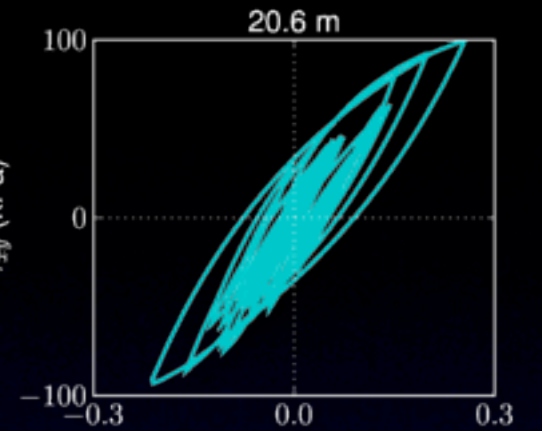
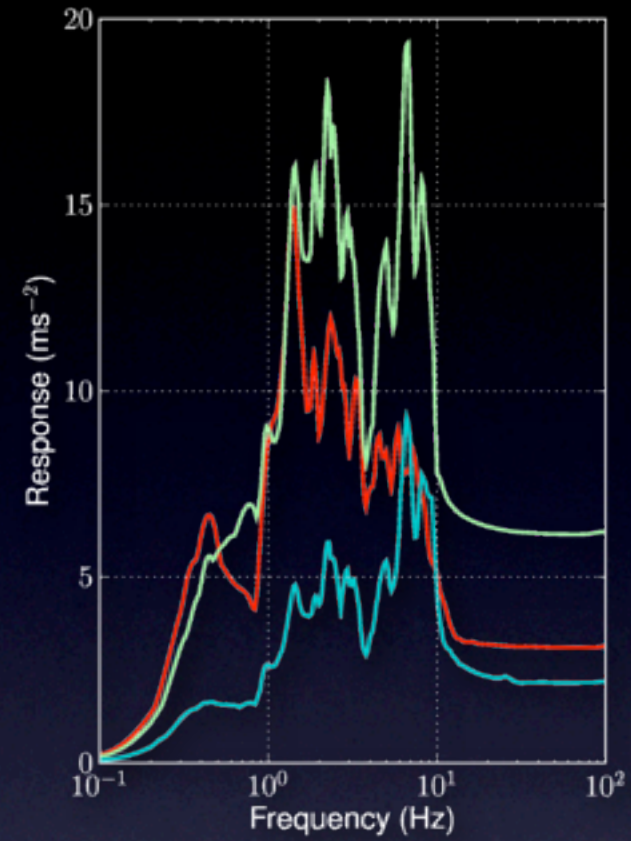
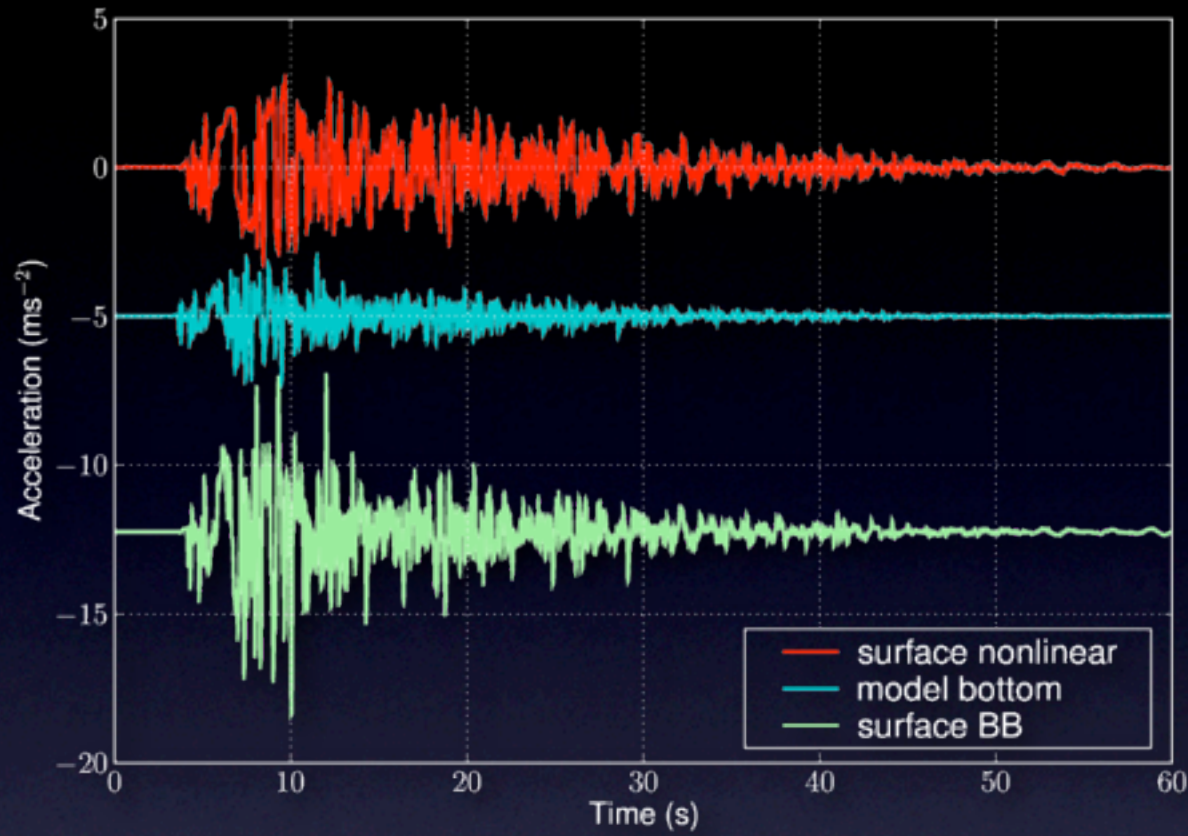
- - - $\gamma_r \pm \text{std}$

Simulation of Nonlinear Soil Response

- **Broadband synthetics at free surface** are deconvolved to remove response of upper 240m
- Resulting signal represents **incoming wavefield at depth** and serves as input for nonlinear simulation
- Nonlinear 1-D simulation yields ground motion on the **surface of the nonlinear layer**

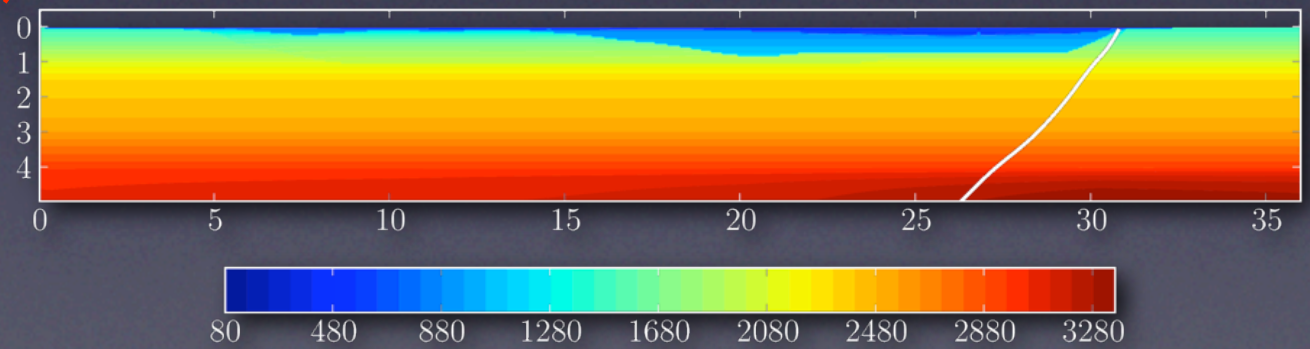
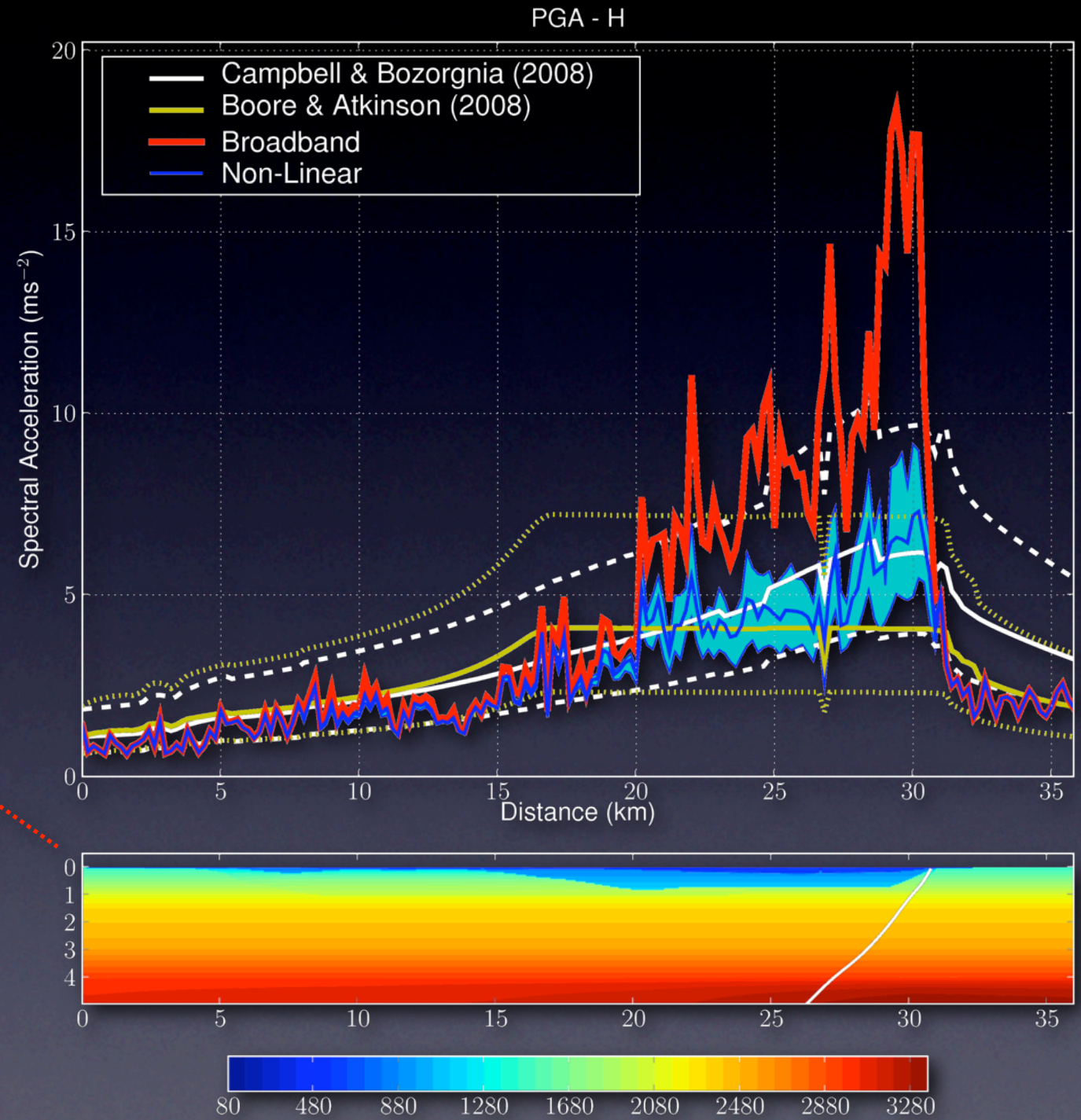
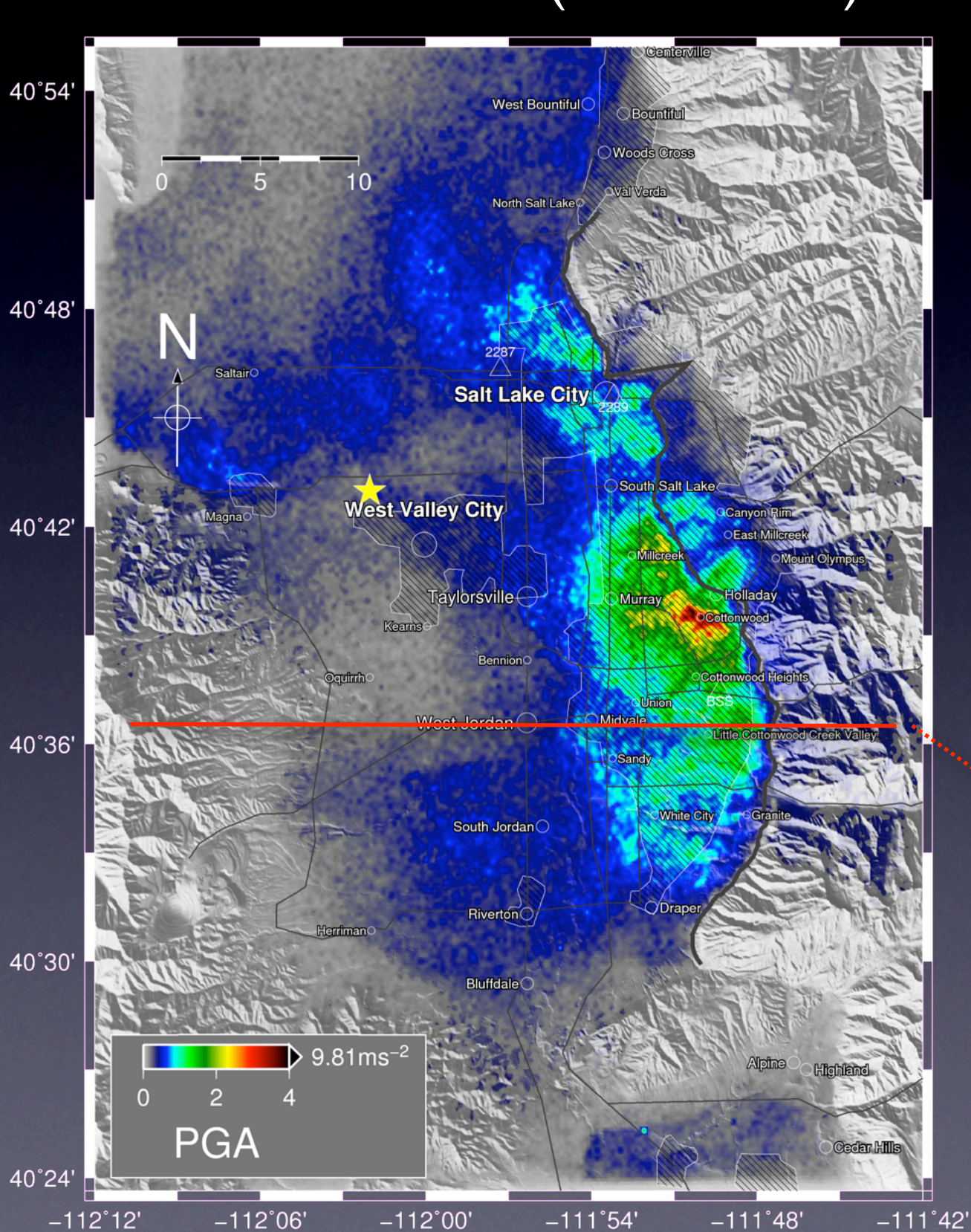


Simulation of Nonlinear Soil Response



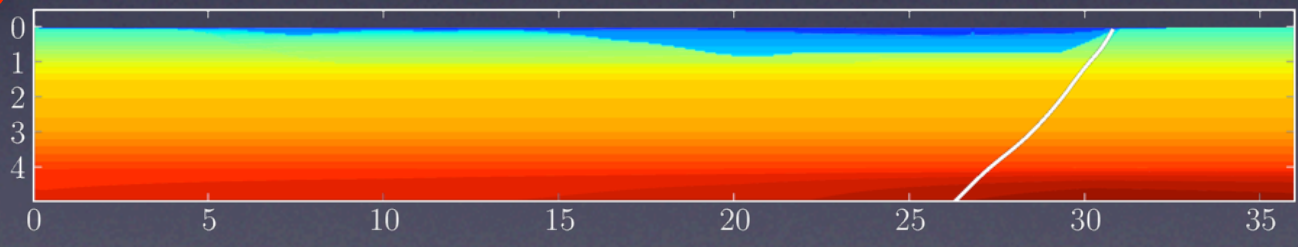
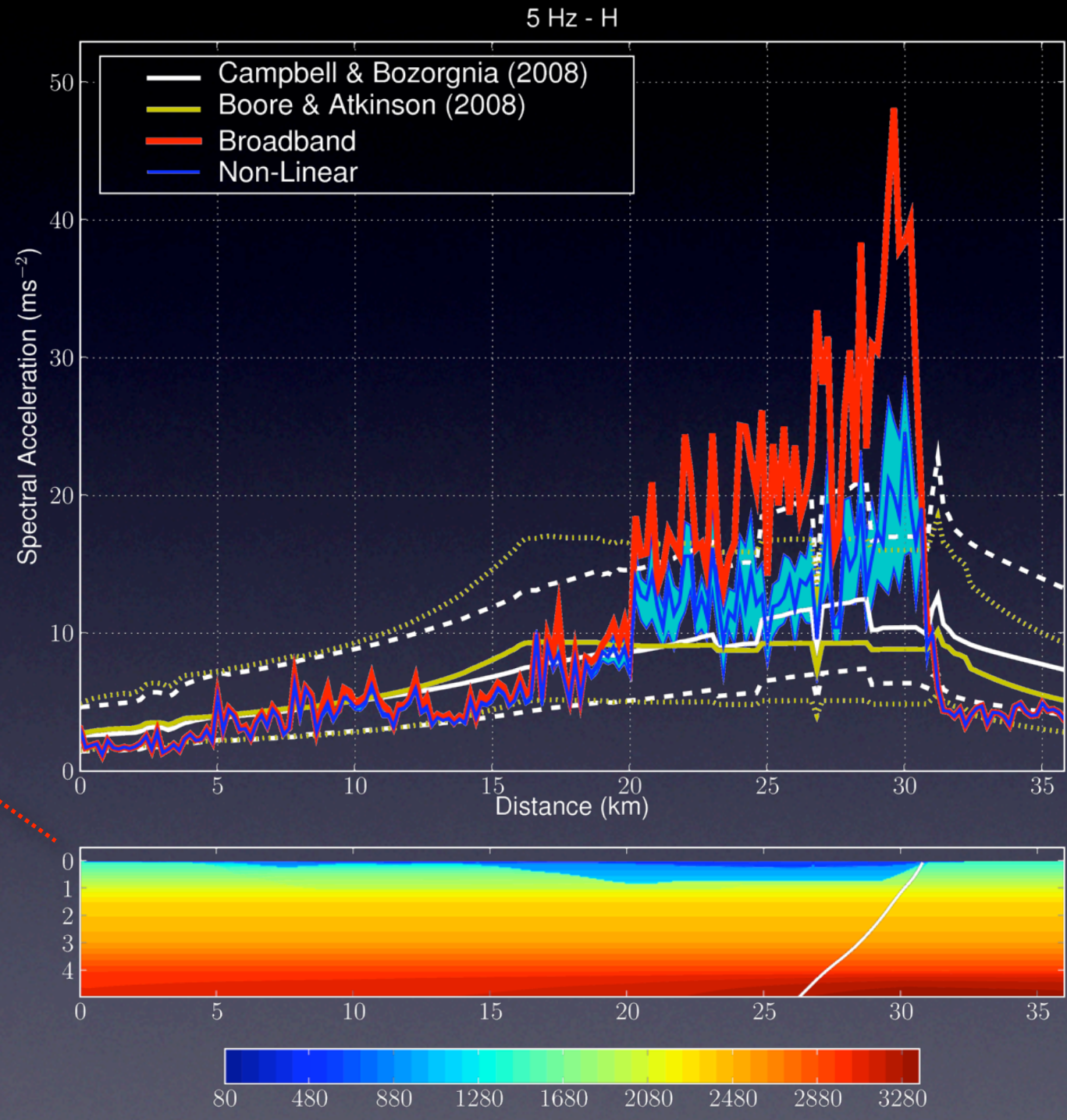
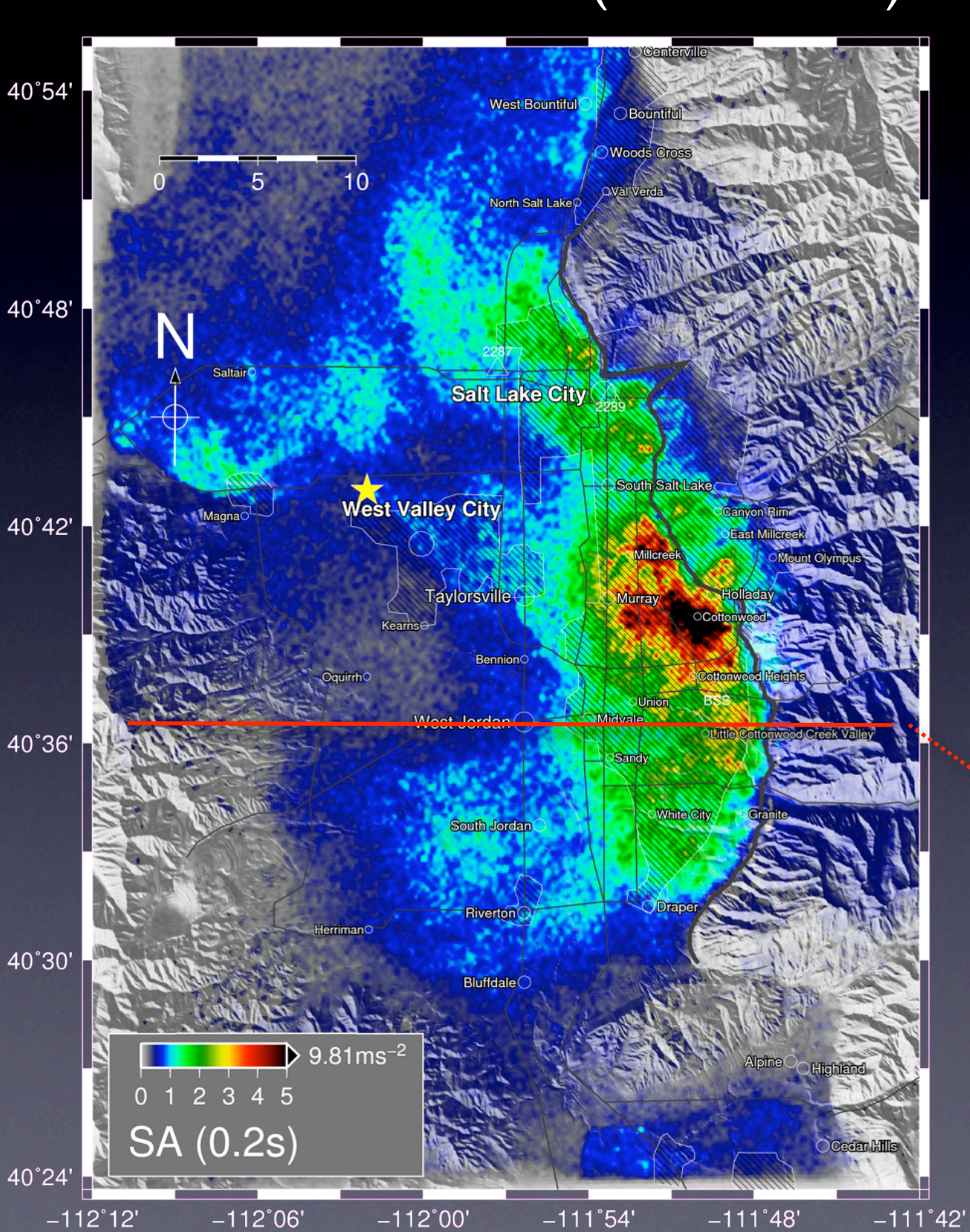
Linear (Broadband) vs. Nonlinear

Broadband PGA (Scenario 2a)



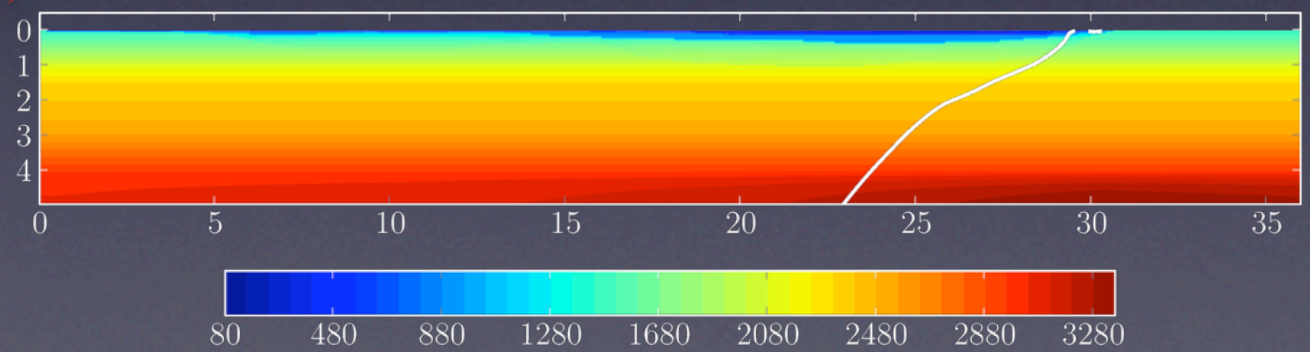
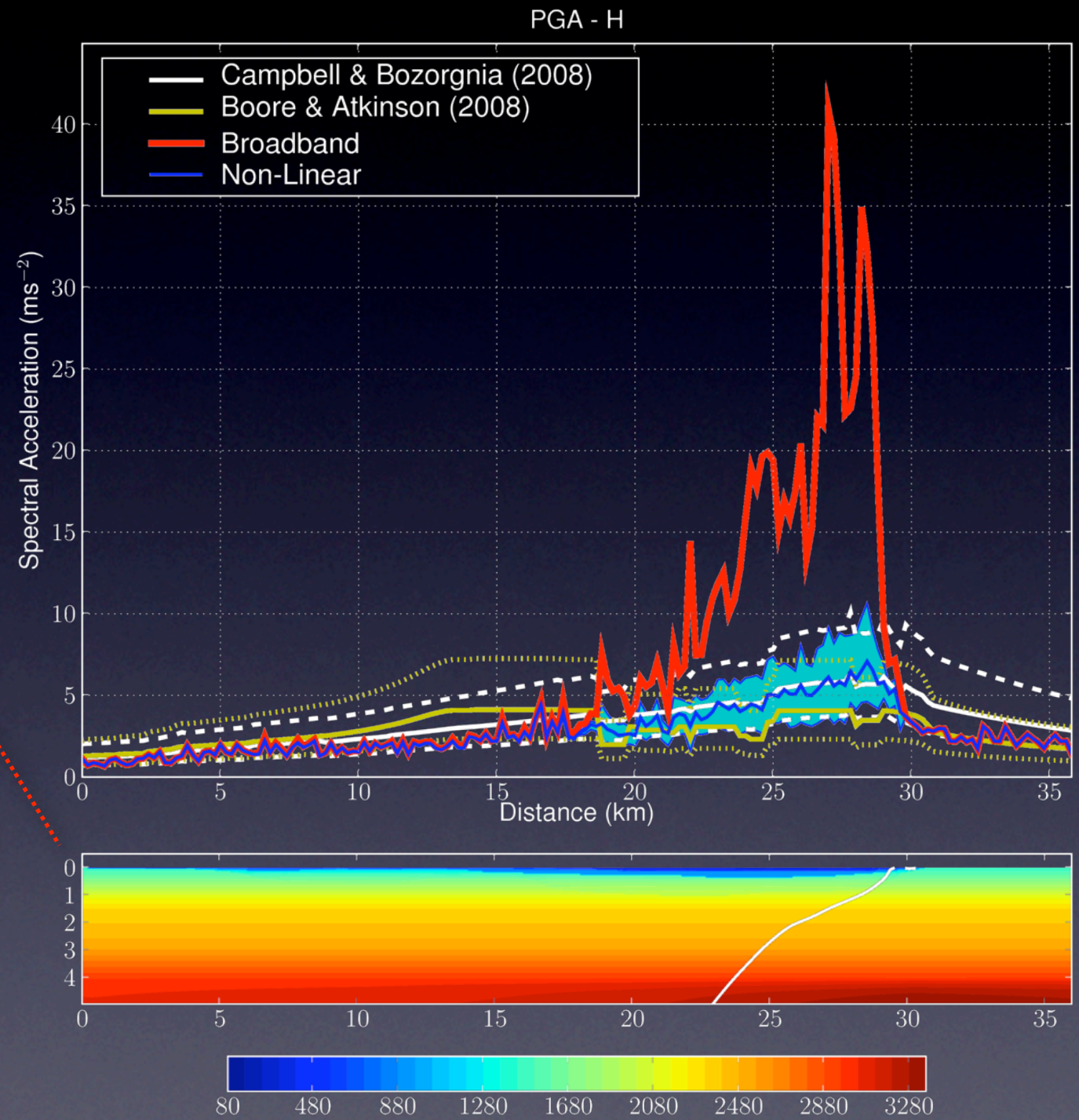
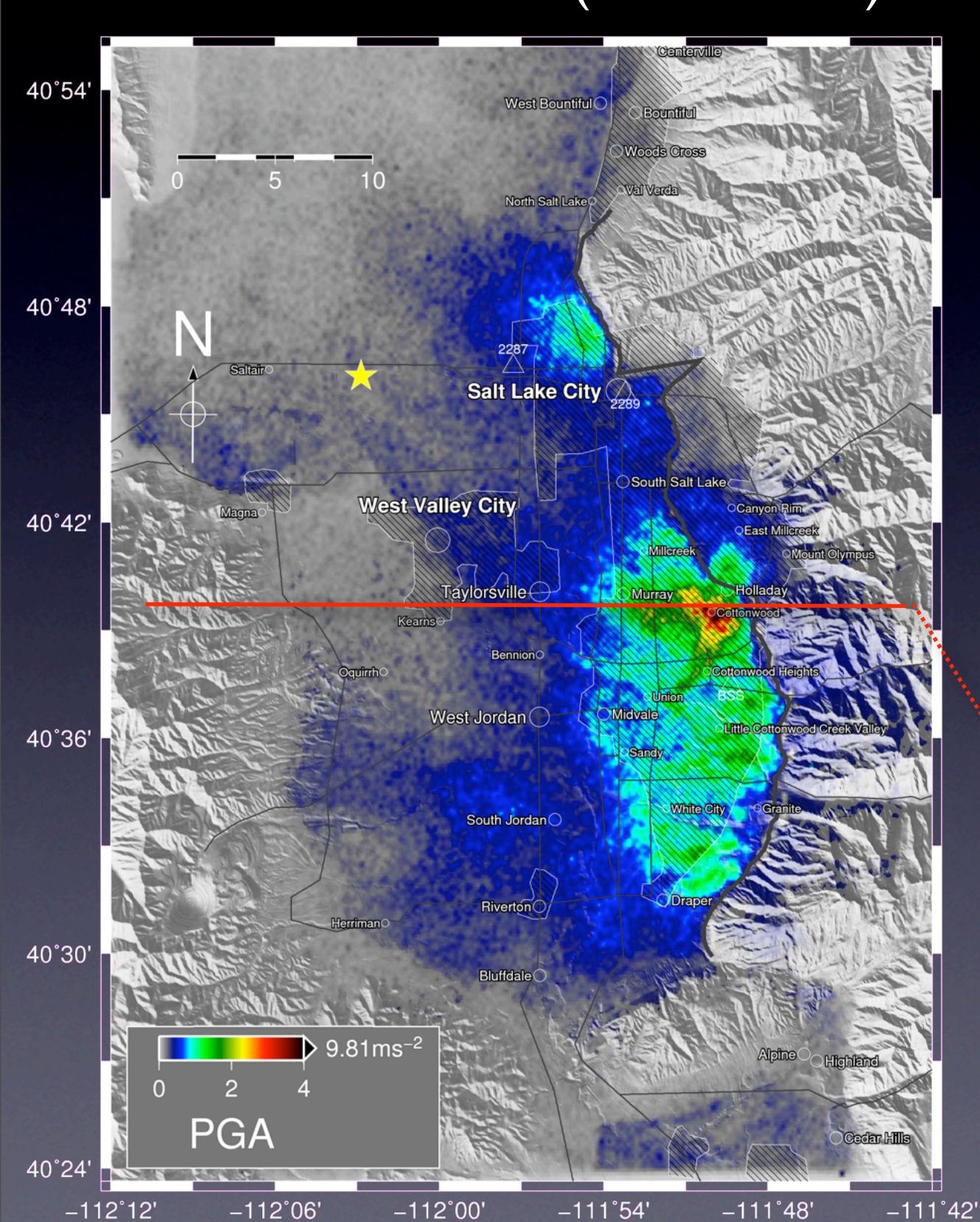
Linear (Broadband) vs. Nonlinear

Broadband 0.2s-SAs (Scenario 2a)



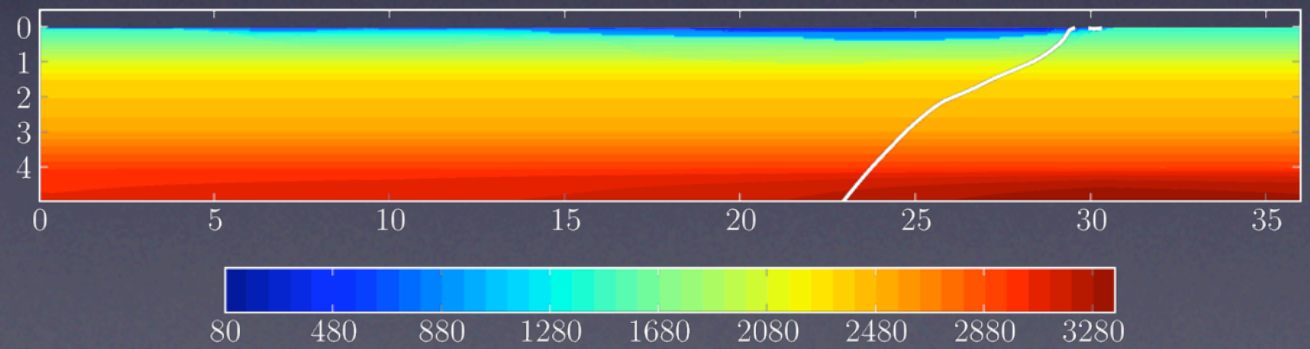
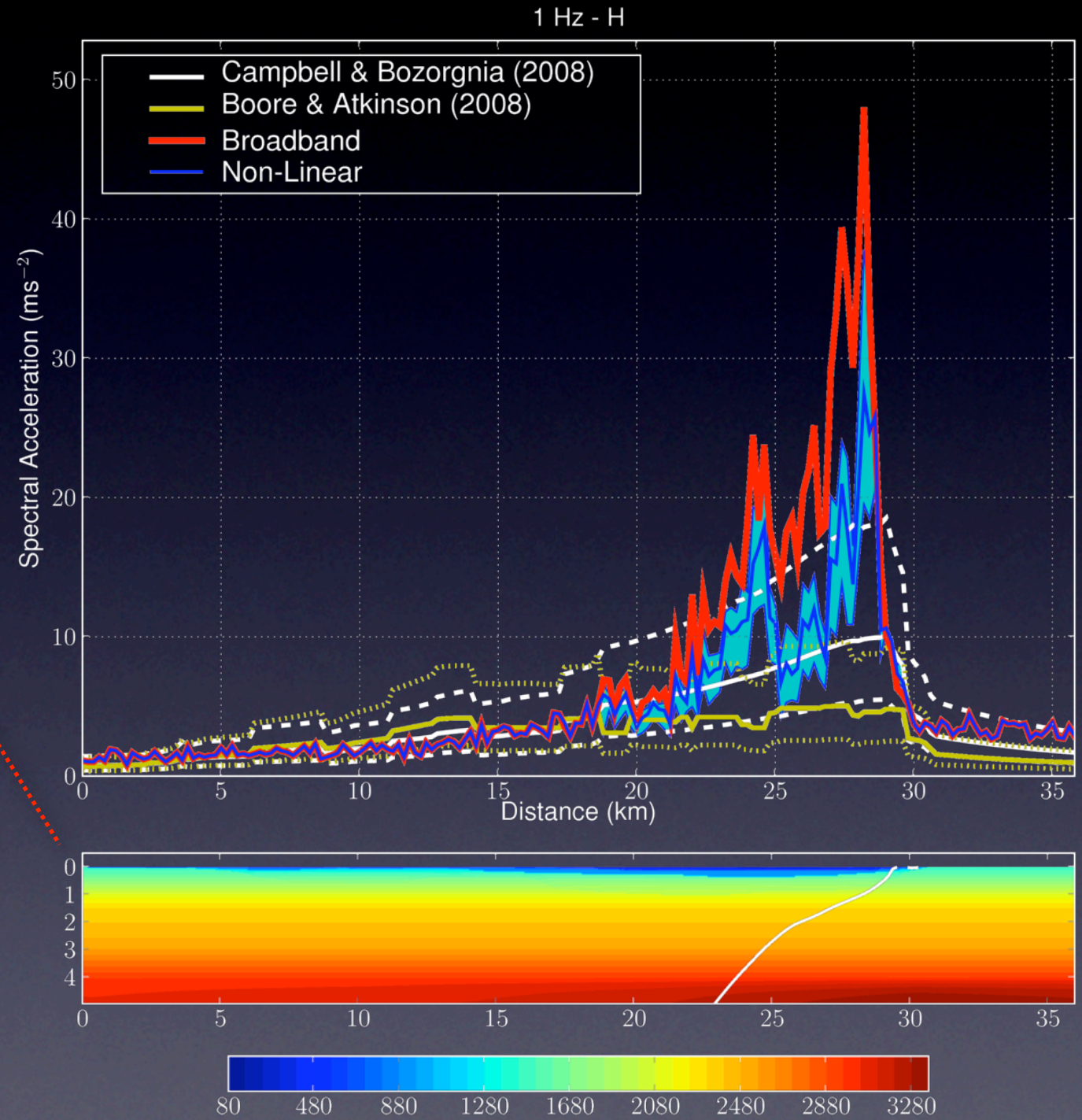
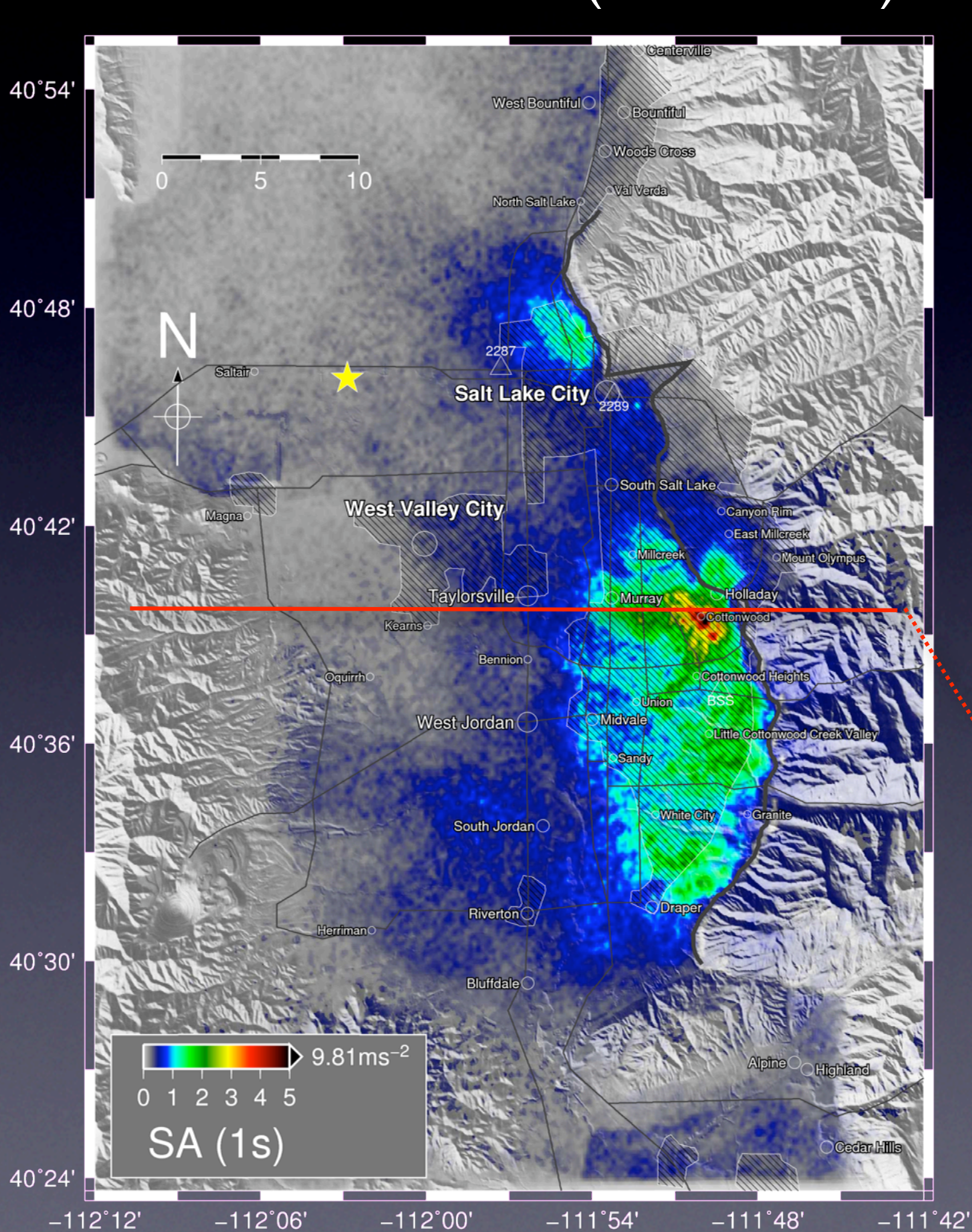
Linear (Broadband) vs. Nonlinear

Broadband PGA (Scenario 5a)



Linear (Broadband) vs. Nonlinear

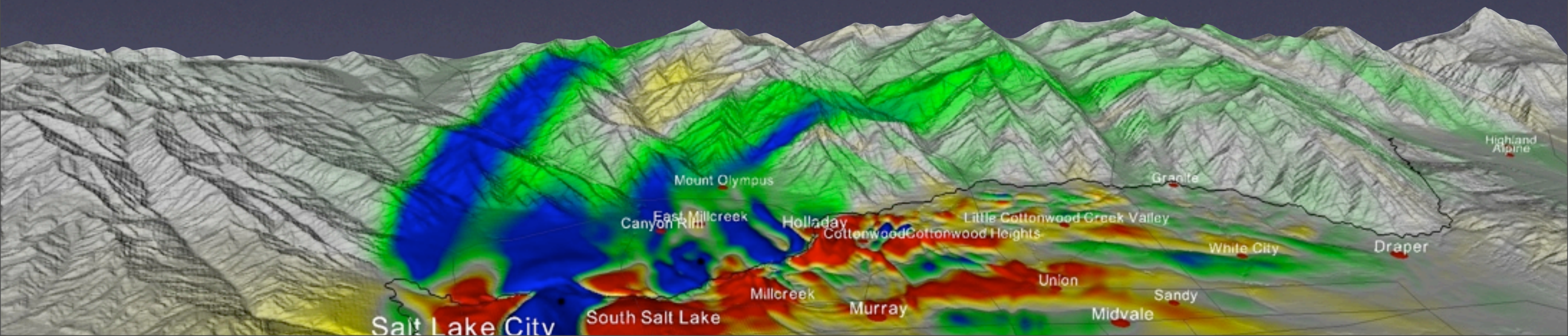
Broadband Is-SAs (Scenario 5a)



Conclusions I

0-1 Hz 3-D FD simulations of scenario earthquakes

- Ground motion tends to be larger on the low-velocity sediments on the hanging wall side of the fault than on outcropping rock on the footwall side, confirming results of previous studies on normal faulting EQs (O'Connell et al., 2007)
- The simulated ground motions reveal strong along-strike and along-dip directivity effects
- Compared to Solomon et al. (2004), our 3-D FD simulations predict larger ground motion on the hanging wall side of the fault, but lower values on the footwall side
- Our simulations suggest that the highest average 2s-SAs and 1s-SAs occur at ~2 km distance from the surface trace of the fault, where they exceed NGA predictions by up to 75%.
- Extreme 1s-SAs of up to 5g are caused by Love waves generated near the Holladay stepover



Conclusions II

Broadband (0-10Hz) synthetics:

- PGAs derived from broadband synthetic seismograms are exceeding those predicted by NGA models by more than one standard deviation at near-fault locations on the hanging wall side, but agree well at some distance from the fault

Nonlinear soil response:

- Synthetic ground motions obtained from a fully nonlinear 1-D propagator exhibit PGAs and SAs that are more consistent with values predicted by NGA models, even when taking into account the uncertainty in the nonlinear soil parameters

